DE LA RECHERCHE À L'INDUSTRIE

Mesurer l'infiniment petit et observer l'infiniment grand

Basé sur le cours de Stefano Panebianco

Maxence Vandenbroucke
06/2017

université PARIS-SACLAY

Plan des cours

Cours 1 : Généralités

-Introduction générale sur l'importance de la mesure
-Qu'est-ce qu'une expérience de physique subatomique ?
-Que veut-on observer à propos d'une particule?
-Architecture générale d'une expérience en physique subatomique

Cours 2 : Les détecteurs à ionisation

- Interaction particule-matière
- Les Détecteurs à ionisations
- L'exemple des détecteurs gazeux

Cours 3 : Exemples d'expériences ?

PLAN DES COURS

Cours 1 : Généralités

-Introduction générale sur l'importance de la mesure

-Qu'est-ce qu'une expérience de physique subatomique ?

-Que veut-on observer à propos d'une particule?

-Architecture générale d'une expérience en physique subatomique

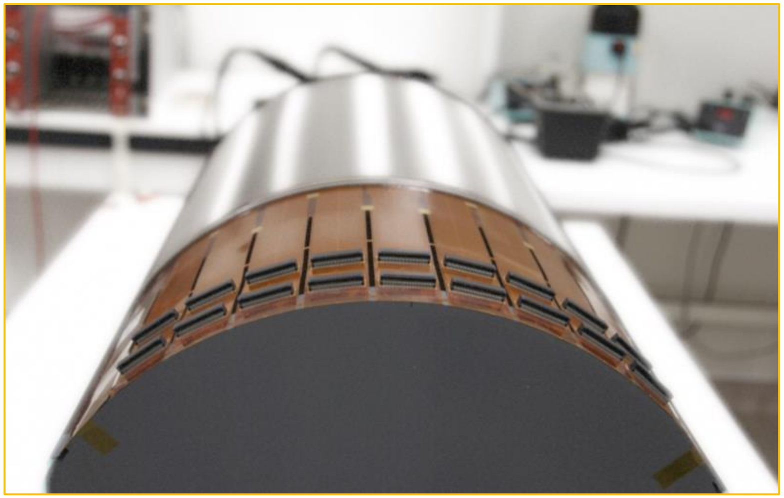

La theorie et la Pratique

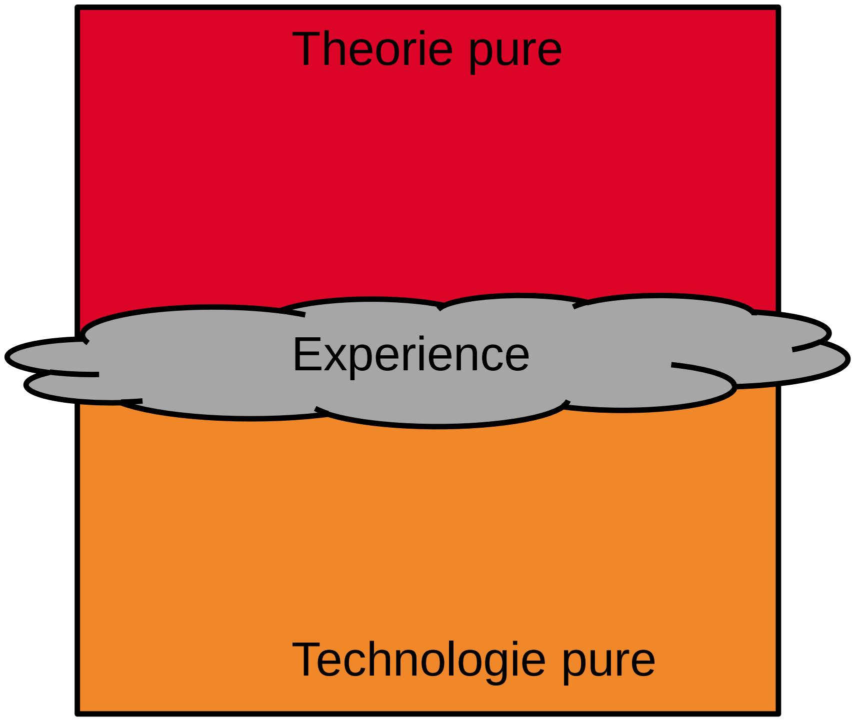

- Théorie
- Construction des Modèles
- Prédiction avec des Modèles
- Simulation d’expérience MC

- Design d’expérience
- Recherche sur les détecteurs
- Electronique/acquisition
- Reconstruction des évènements
- Comparaison avec le MC
- Papier !

Le physicien complet est à la fois proche des interrogations fondamentales, mais aussi des avancés technologiques pour trouver un espace de découverte potentielle

(vision un peu naïve)

MESURER C'EST QUOI ?

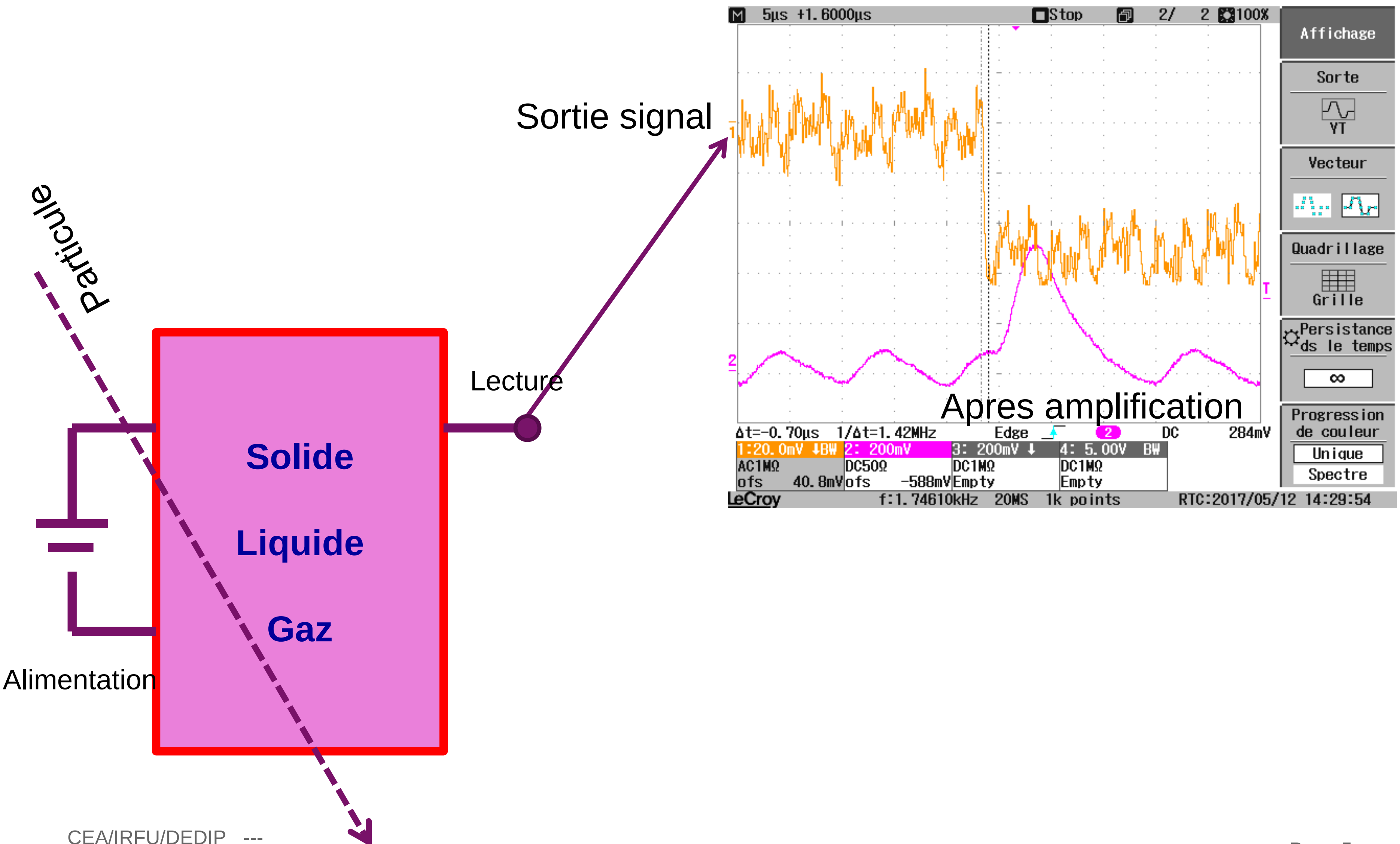

INTERACTIONS PARTICULE-MATIERE

Passage dans la matière d'une particule avec charge électrique

Ex.: un muon ou un proton du rayonnement cosmique

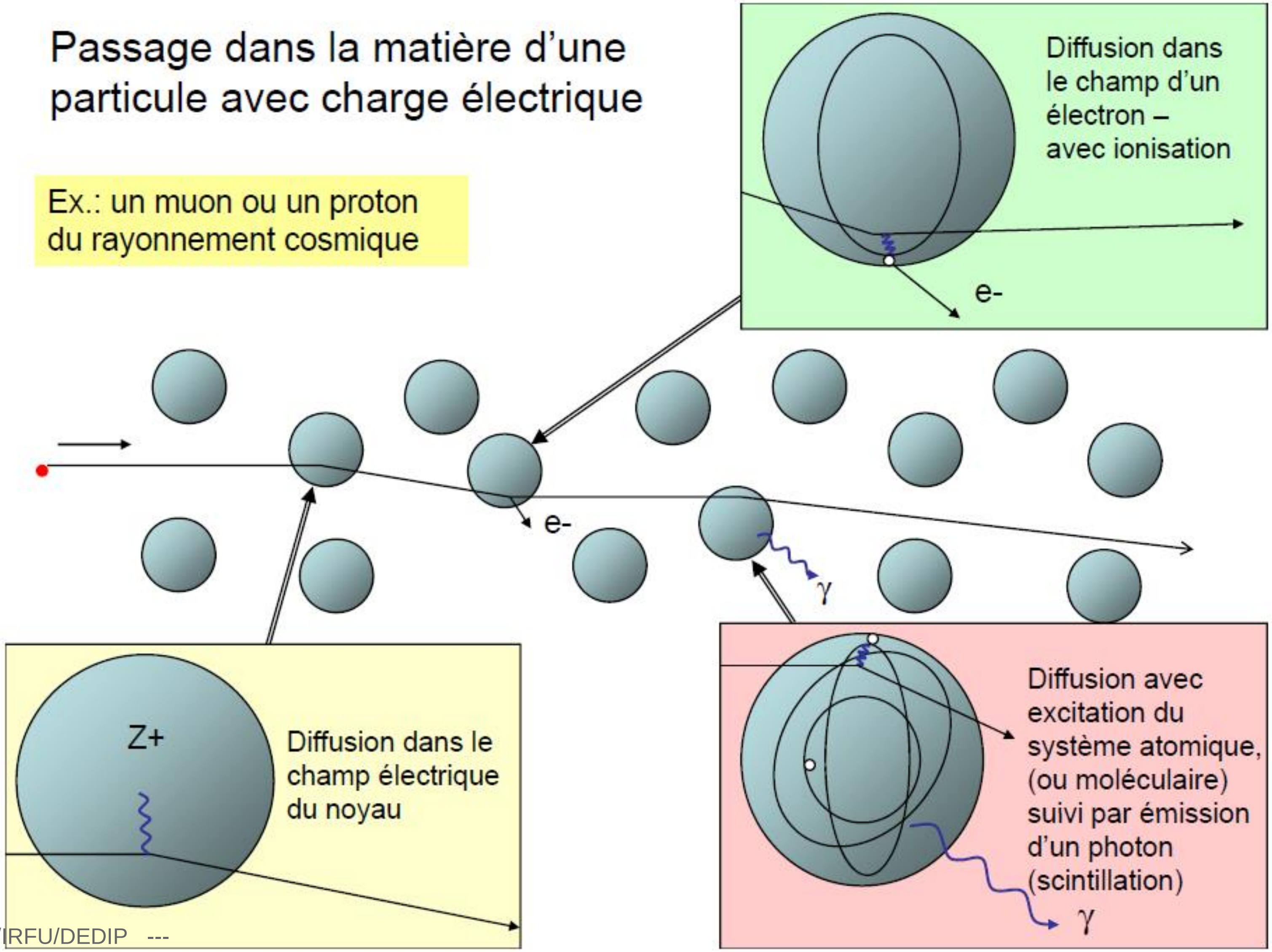

DÉTECTION : TRACKER SILICIUM

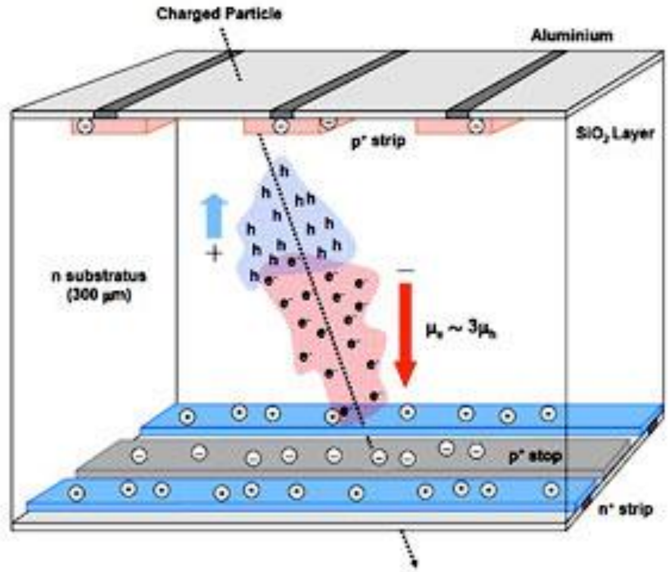

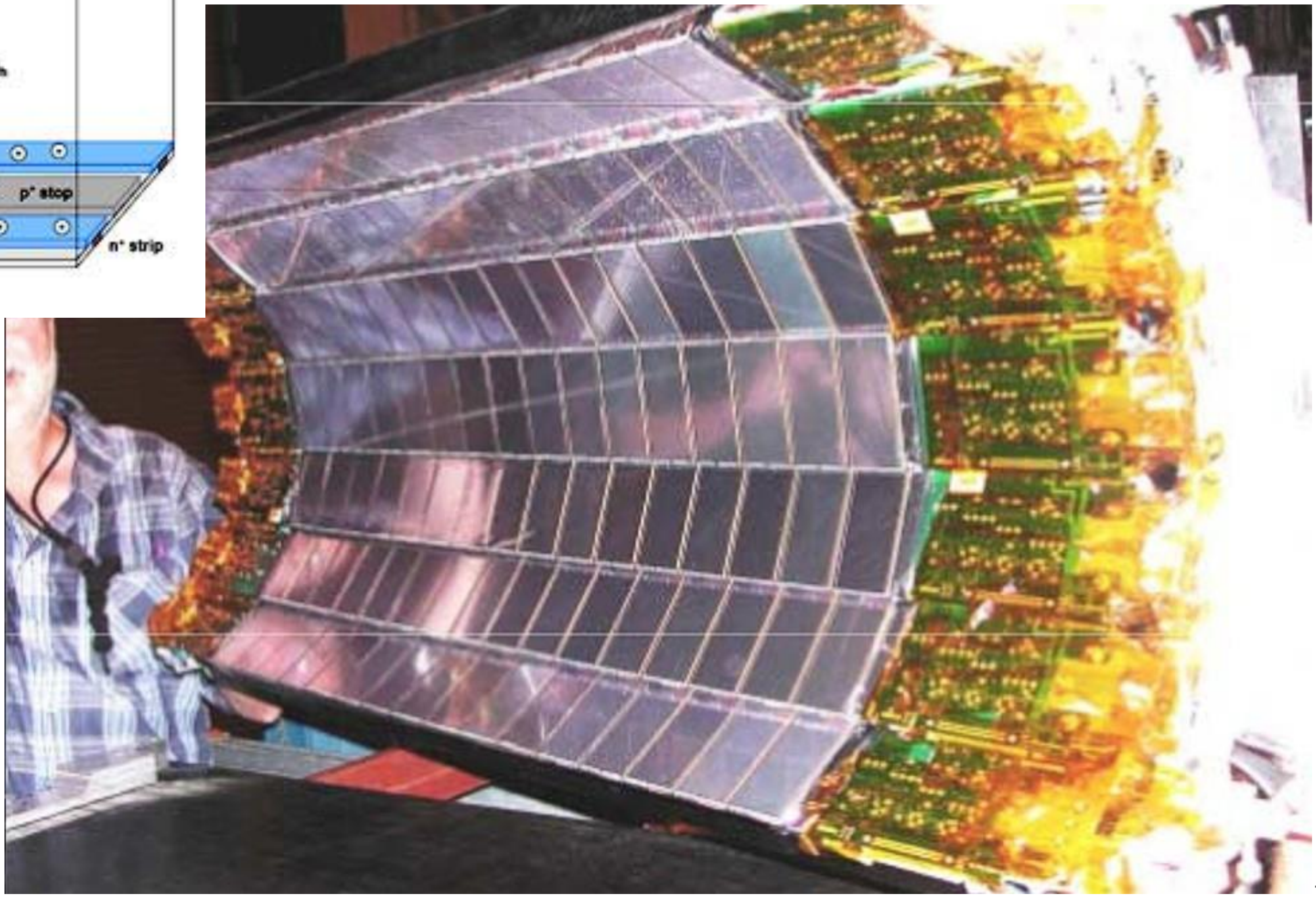

Mesurer quoi ?

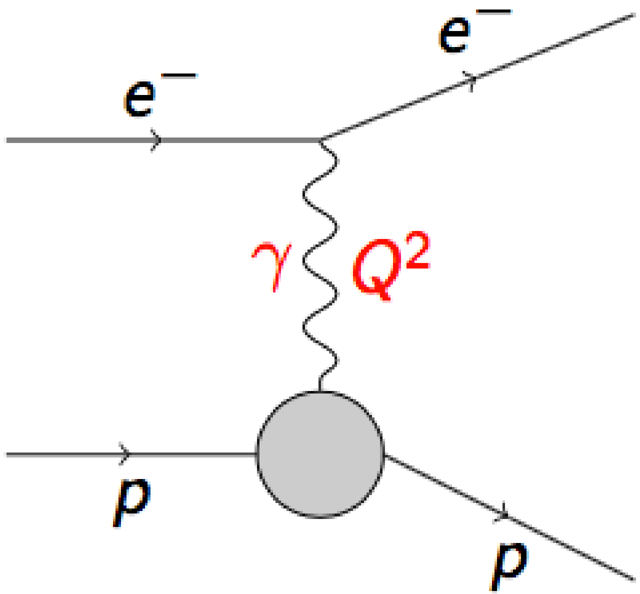

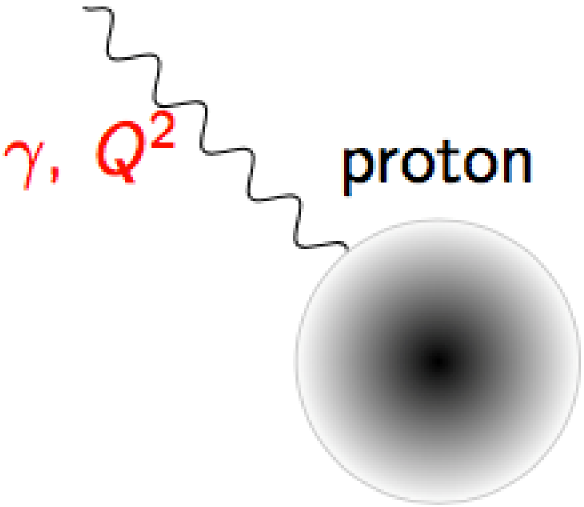

Diffusion élastique.

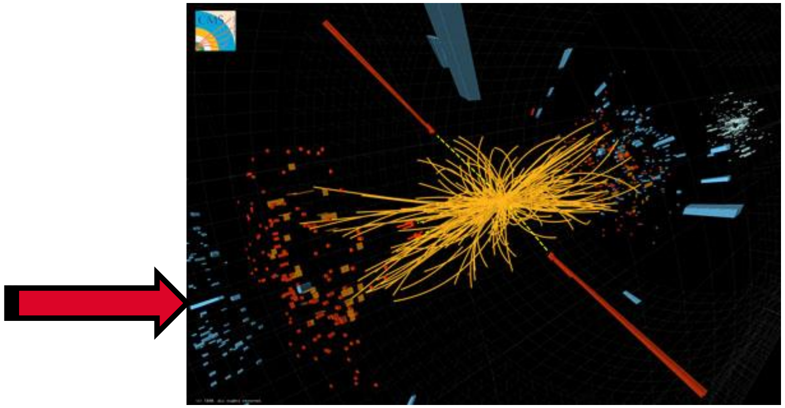

MESURER QUOI ?

Déterminer la carte d'identité d'une particule :

- QUADRIVECTEUR IMPULSION-ÉNERGIE
- MASSE ET CHARGE (QU'ON REGROUPE SOUVENT SOUS LE NOM DE PID POUR PARTICLE IDENTIFICATION)
- SPIN/PARITÉ (ÉVENTUELLEMENT...)

Mesure de l’impulsion

Mesure de l'impulsion

- Technique de spectrométrie magnétique (ou du B-rho)

$$qvB=mv^2/\rho \quad \rightarrow \quad p_\perp=p\cos\vartheta=qB\rho$$

- Technique de temps de vol (TOF pour Time Of Flight)

$$L=v\tau=\beta c\tau=\beta c\gamma\tau_0=p\tau_0/m$$

Mesure de l'impulsion

- Technique de spectrométrie magnétique (ou du B-rho)
- Technique de temps de vol (TOF pour Time Of Flight)

Mesure de l'énergie

- Calorimétrie
- Perte d'energie dE/dx

CEA/IRFU/DEDIP --- maxence.vandenbroucke@cea.fr

DES OBSERVABLES A LA TECHNIQUE DE MESURE

Mesure de l'impulsion

- Technique de spectrométrie magnétique (ou du B-rho)
- Technique de temps de vol (TOF pour Time Of Flight)

Mesure de l'énergie

- Calorimétrie
- Perte d'energie dE/dx

Mesure de spin et de la parité

- (Pas traitée ici)
- Avec un polarimetre indirectement
- Par selection

Mesure de la masse et de la charge (PID)

- Combinaison B-rho et TOF
- Combinaison B-rho et dE/dx
- Masse manquante …
- Direction de la courbure dans un spectromètre magnétique
- Mesure de la perte d'énergie dE/dx qui dépend de la charge
- L'electrometre

UN EXEMPLE

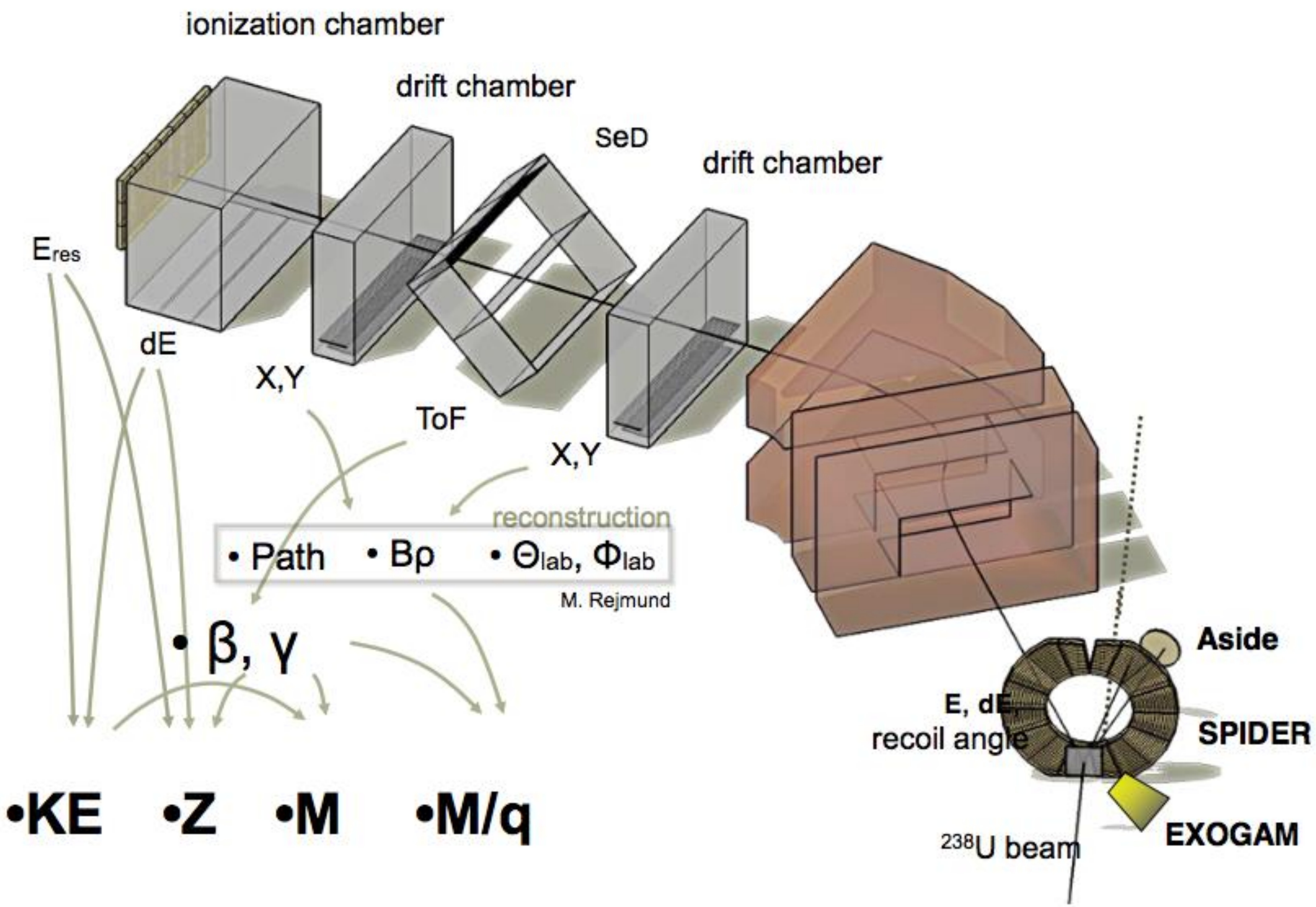

ionization chamber
drift chamber
SeD
drift chamber
Eres
dE
X,Y
ToF
X,Y
reconstruction
• Path • Bρ • Θlab, Φlab
M. Rejmund
• β, γ
•KE •Z •M •M/q
Aside
E, dE,
recoil angle
SPIDER
EXOGAM
238U beam

UN PLUS GROS

Compact Muon Solenoïd

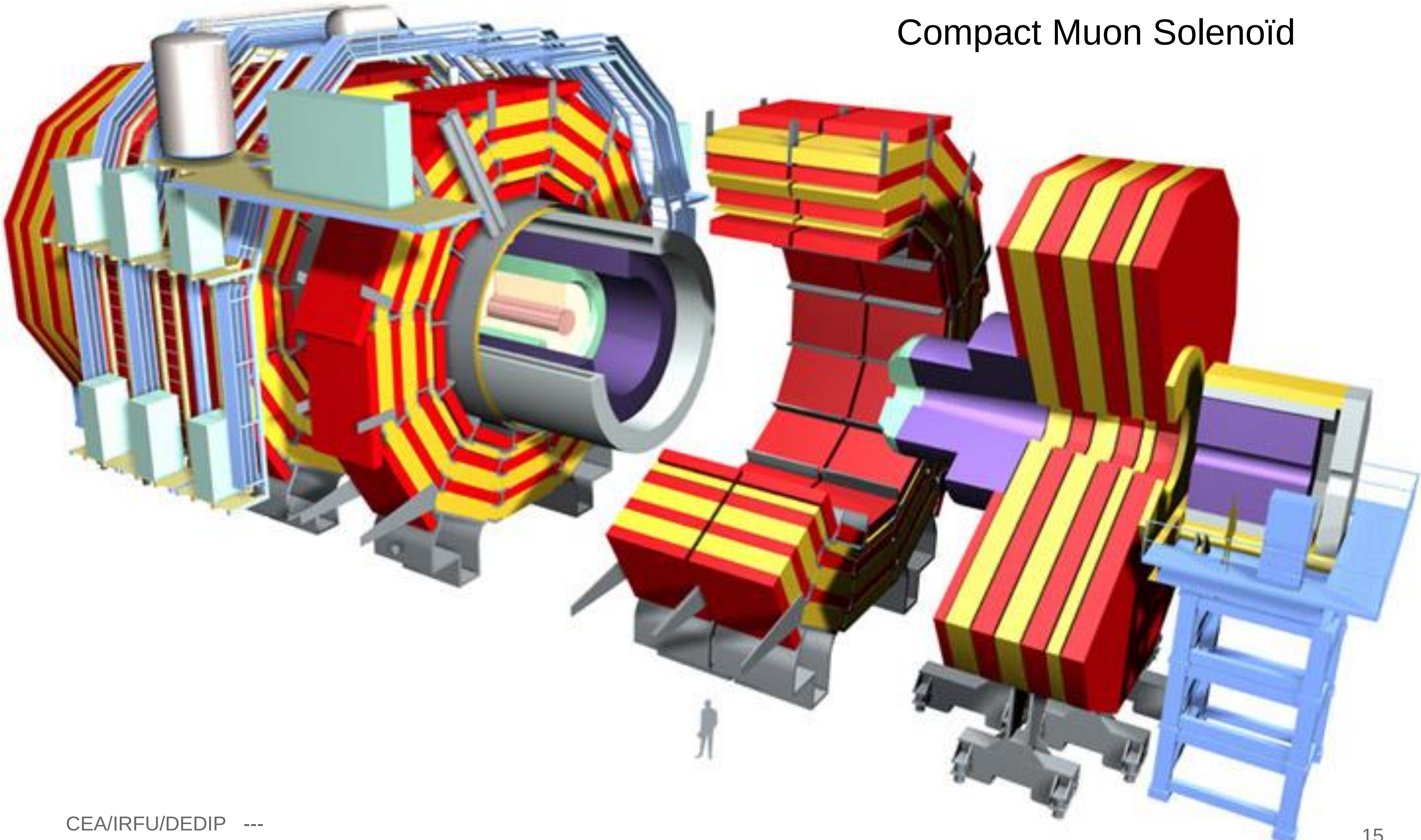

CMS

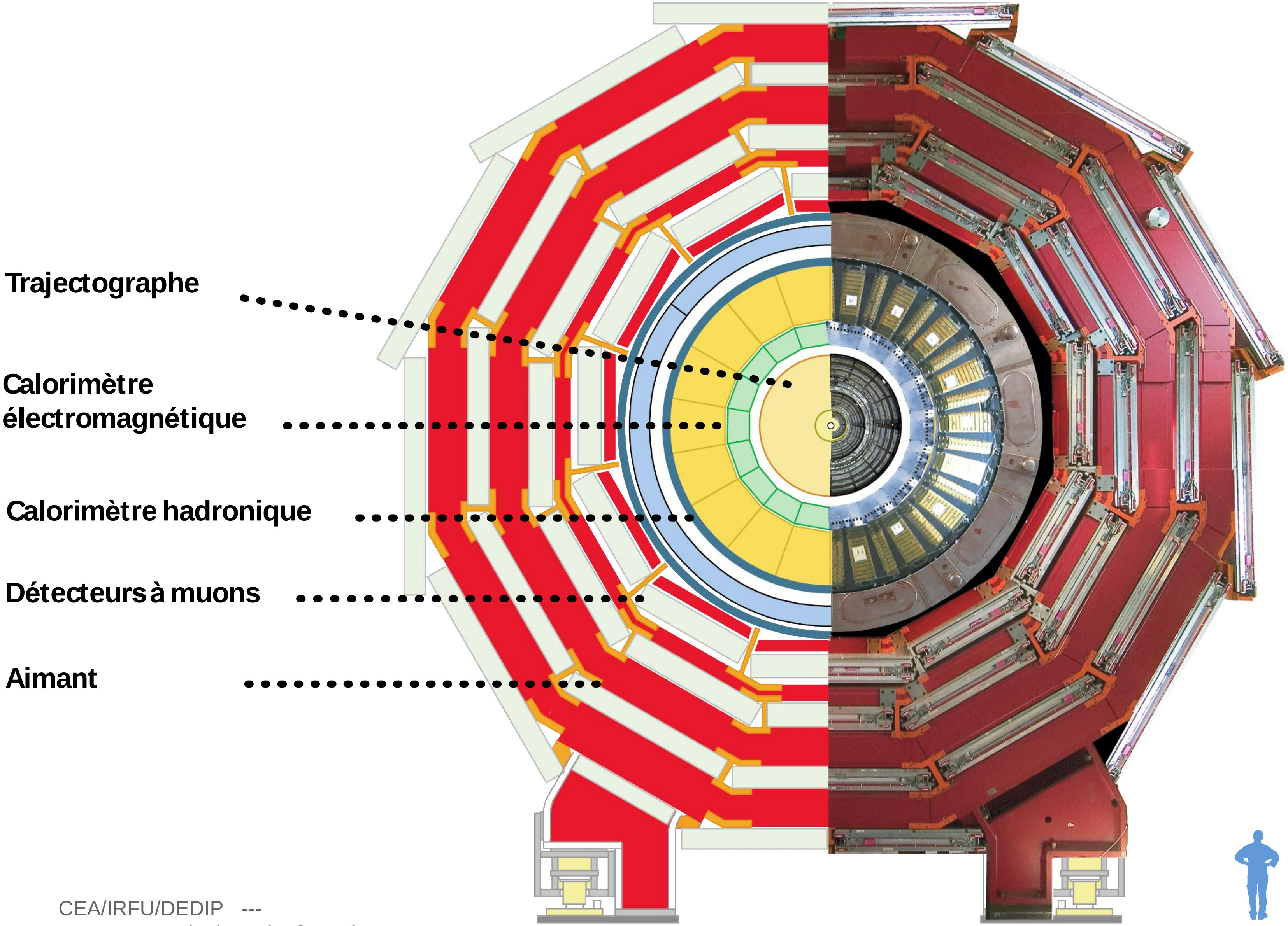

Trajectographe
Calorimètre électromagnétique
Calorimètre hadronique
Détecteurs à muons
Aimant

CMS EVENT

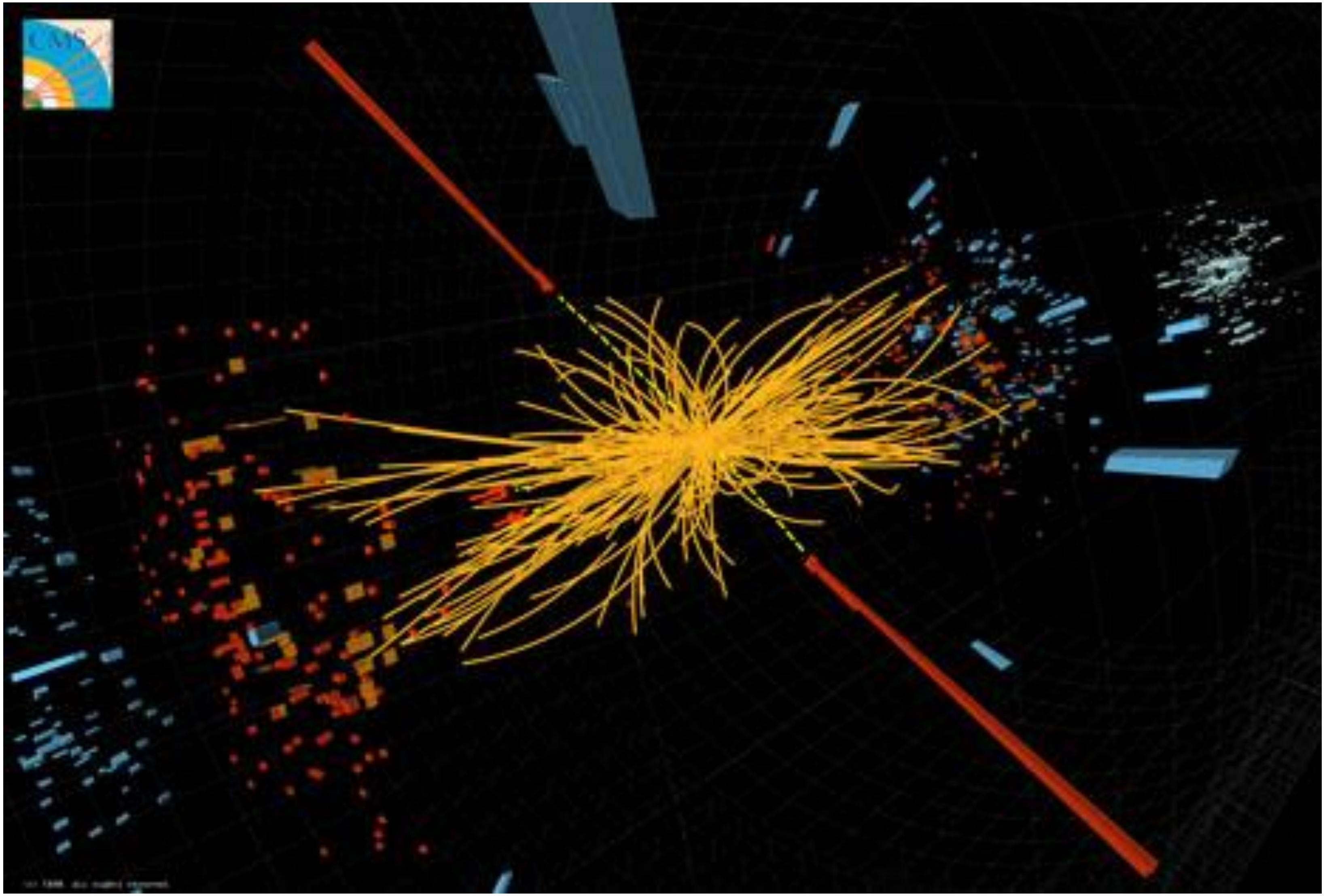

Courbes = trajectoire mesurée par les trajectographes

CMS 3

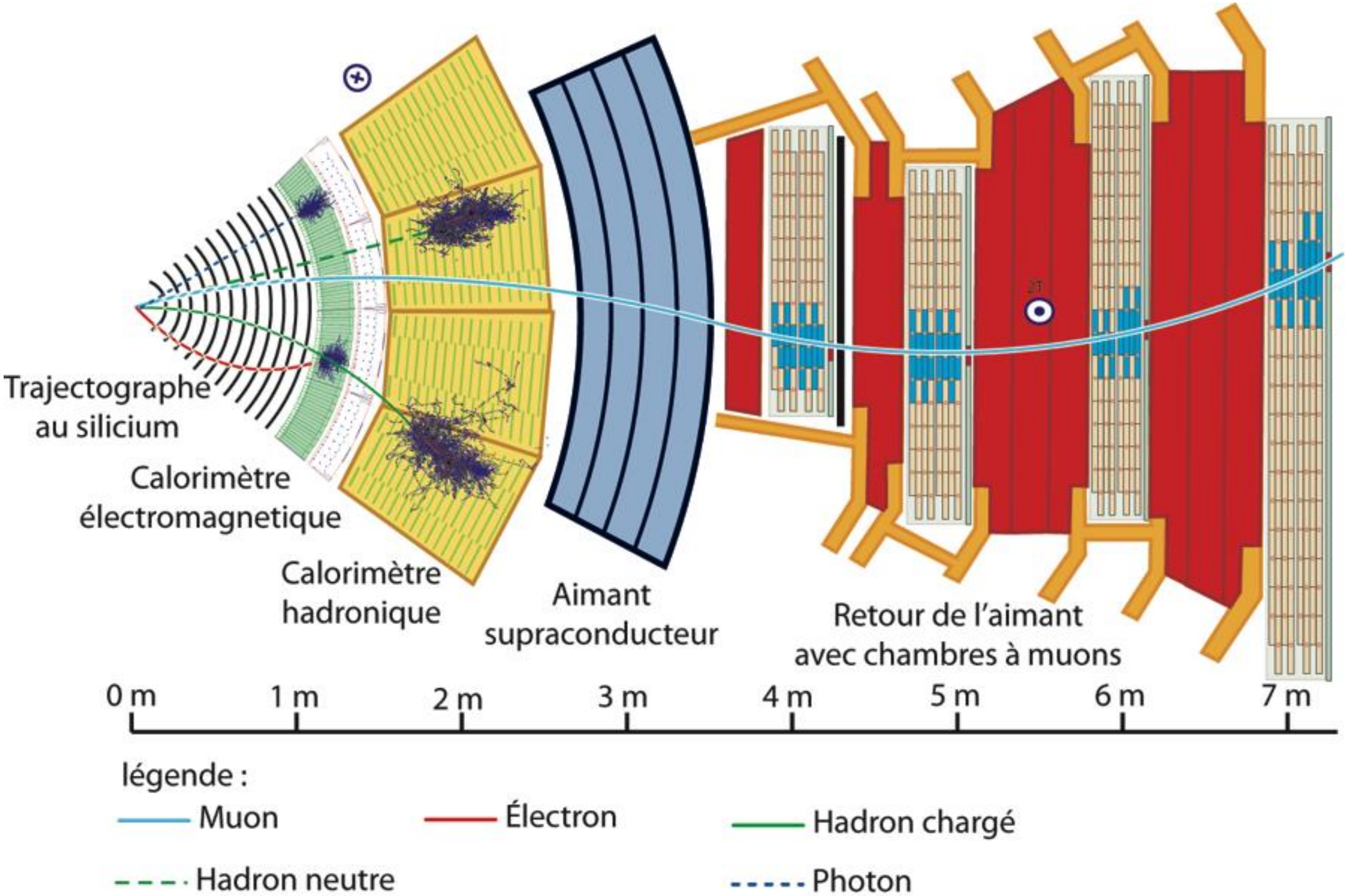

Trajectographe au silicium
Calorimètre électromagnetique
Calorimètre hadronique
Aimant supraconducteur
Retour de l'aimant avec chambres à muons
0 m
1 m
2 m
3 m
4 m
5 m
6 m
7 m
légende :
Muon
Électron
Hadron chargé
Hadron neutre
Photon

W EVENT -> ISOLATED LEPTON

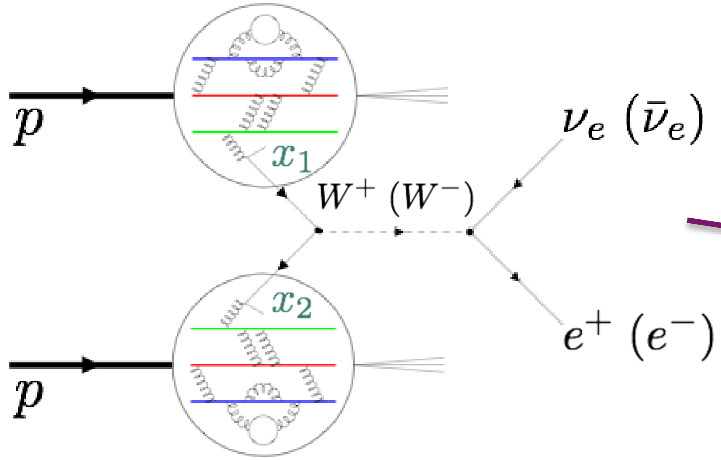

W+/W-

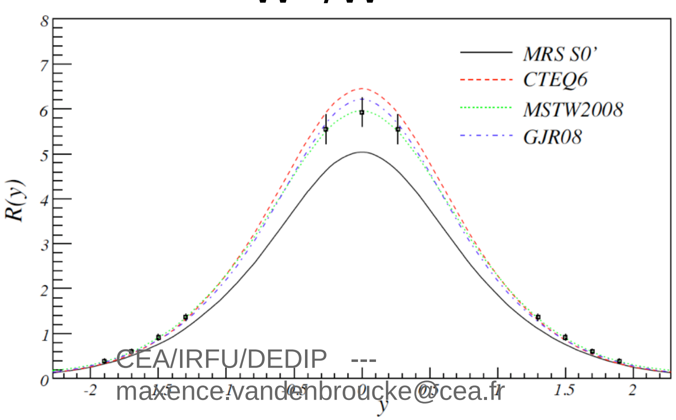

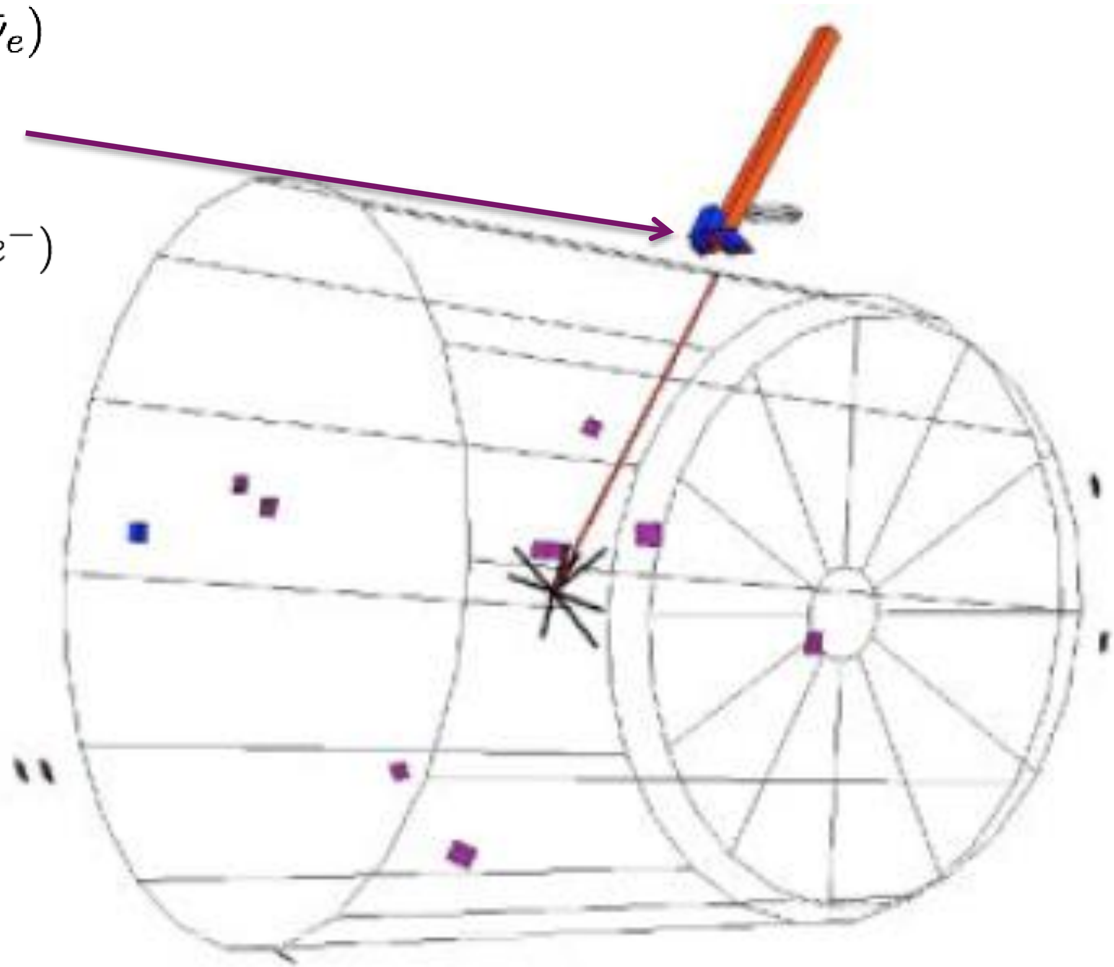

STAR experiment at BNL

Mesurer l'infiniment petit et observer l'infiniment grand

Cours 2 : Les détecteurs de particules

- **Trajectographie :**
  - **-Détecteurs Gazeux**
  - **-Détecteurs au Silicium**
- **Calorimétrie**
- **Scintillation**

Basé sur les cours de Stefano Panebianco (CEA/IRFU),
et le cours de Werner Riegler (CERN),
Particle Detectors , Second Edition, C. Grupen & B. Shwartz

Trajectographes Semi-Conducteur

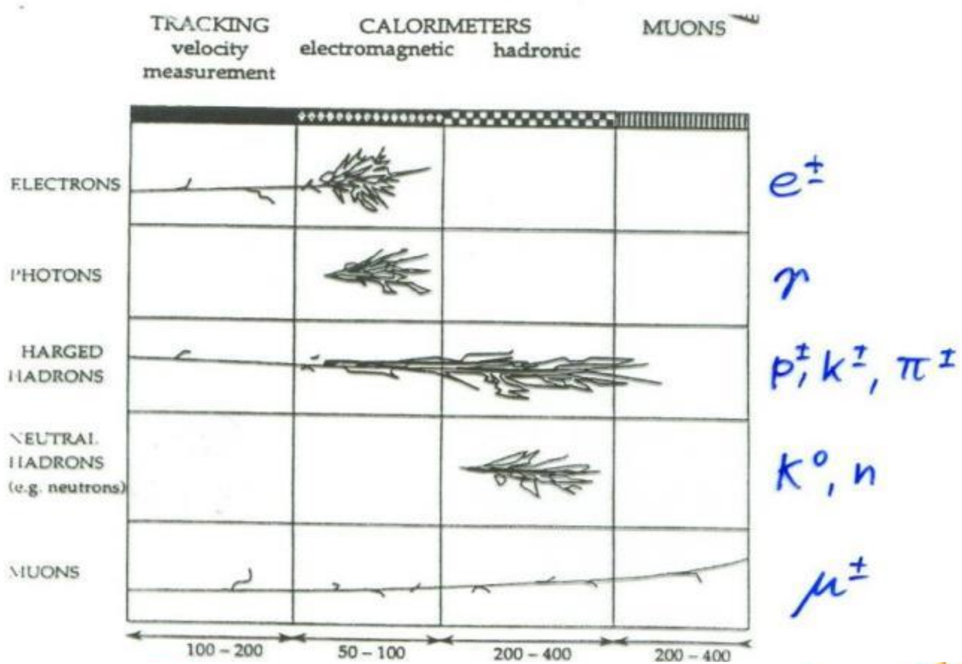

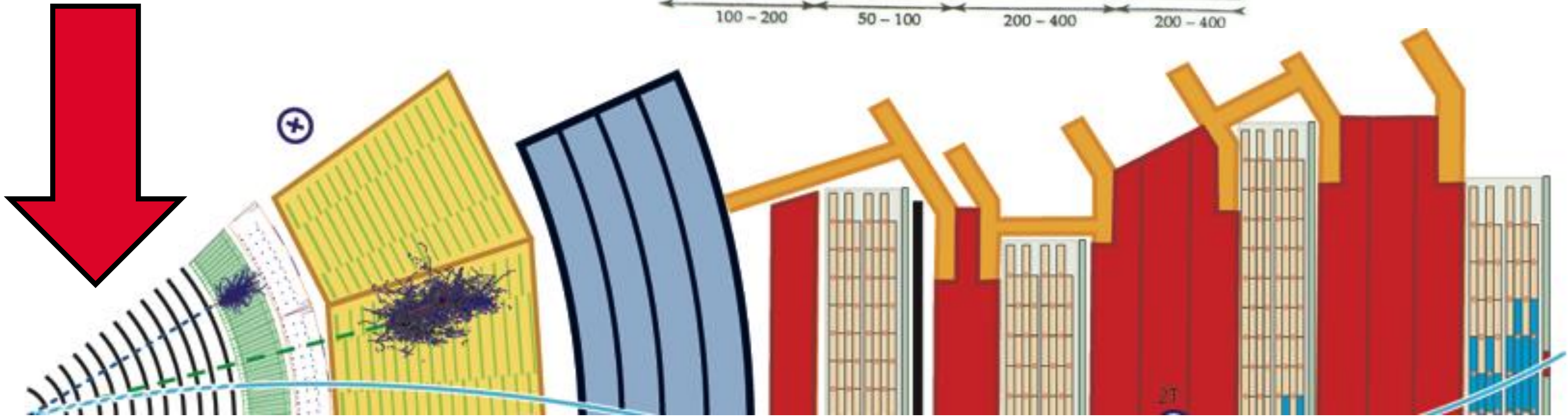

Les Détecteurs à base de Semi-Conducteur

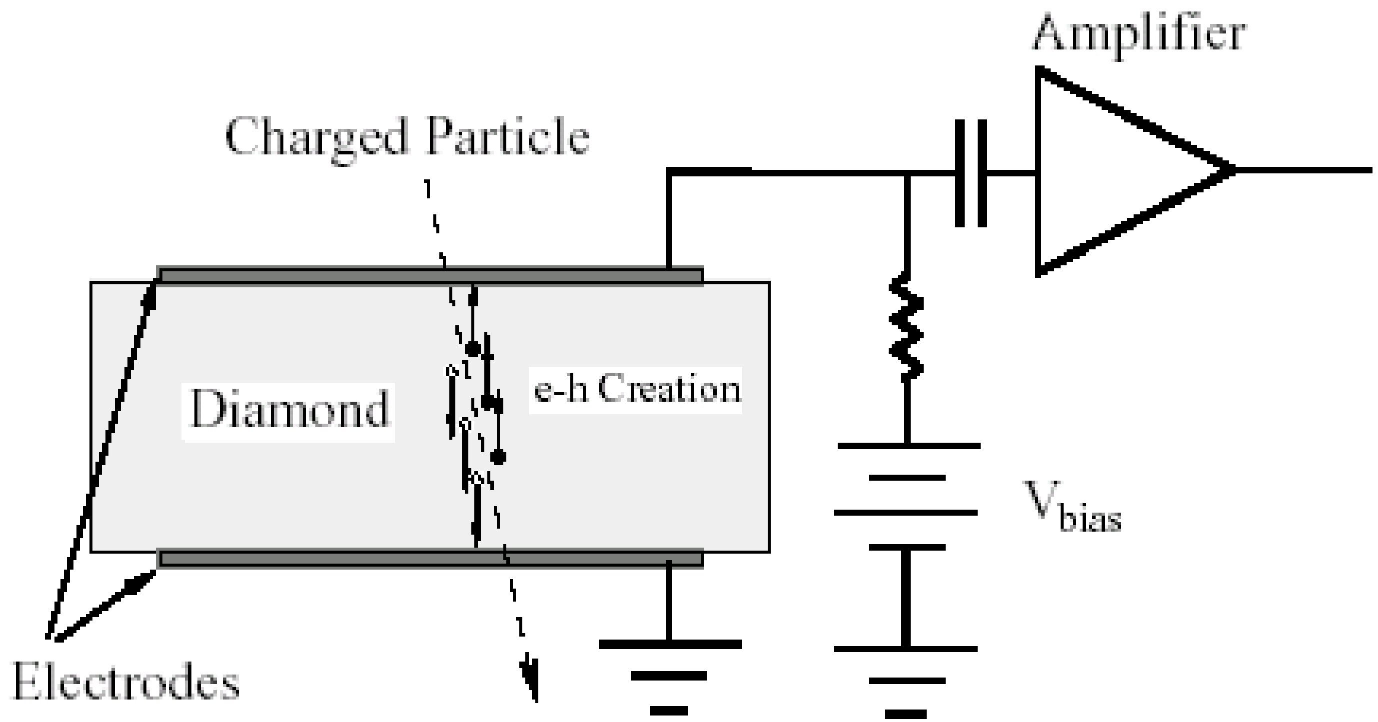

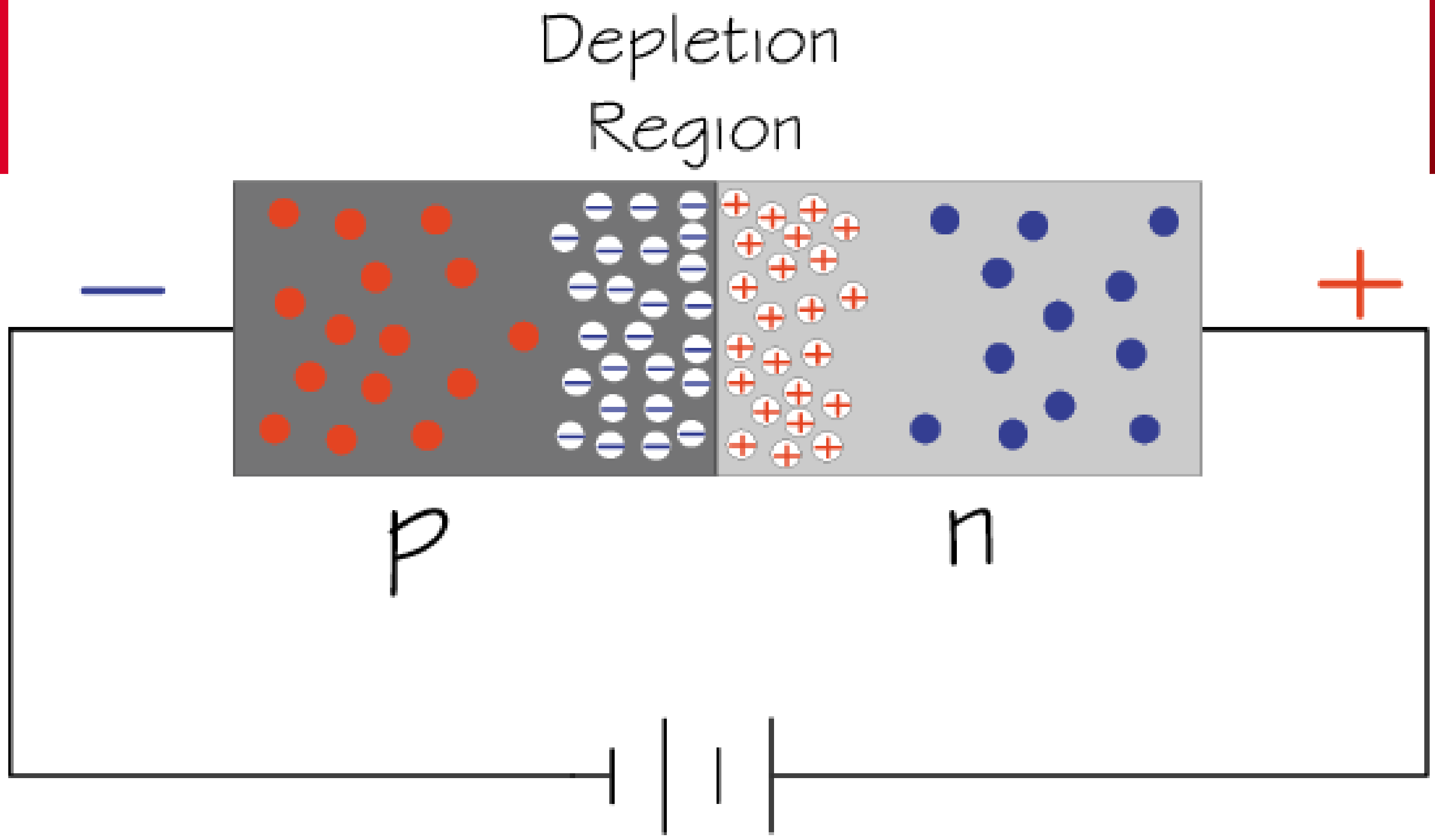

- Electron
- Positive ion from removal of electron in n-type impurity
- Negative ion from filling in p-type vacancy
- Hole

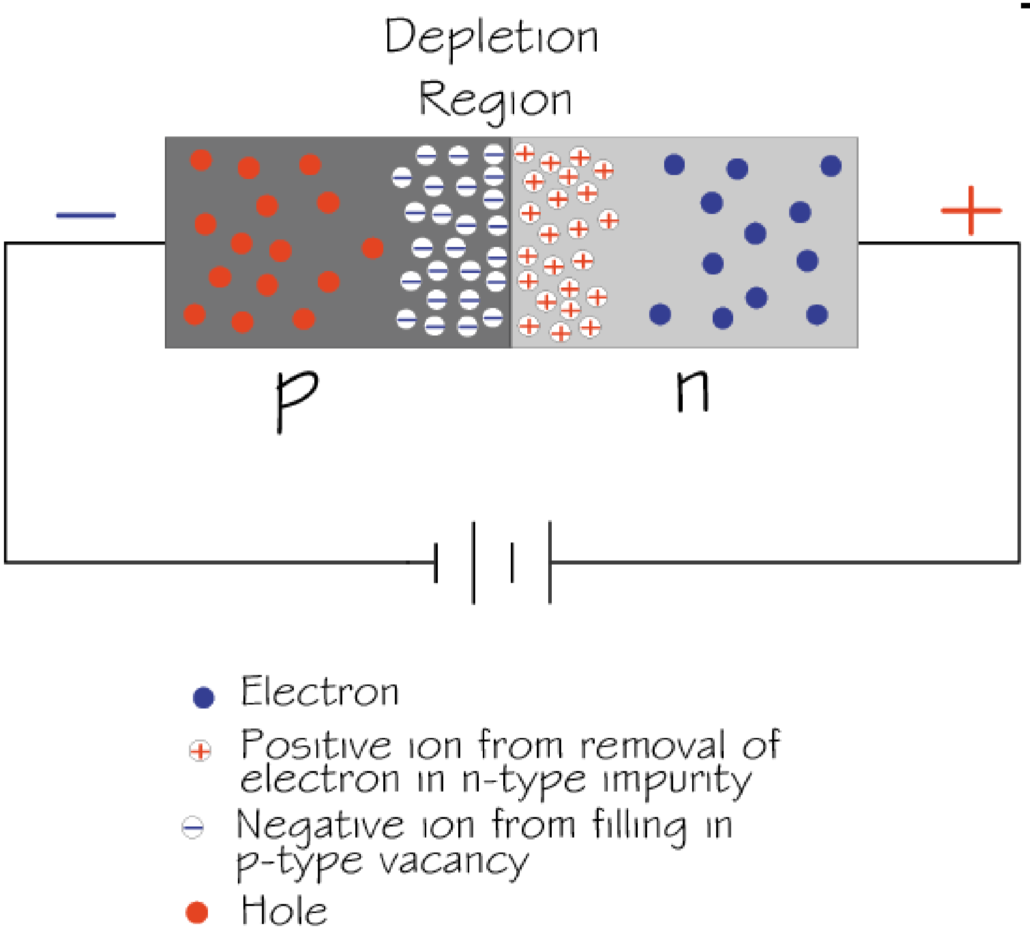

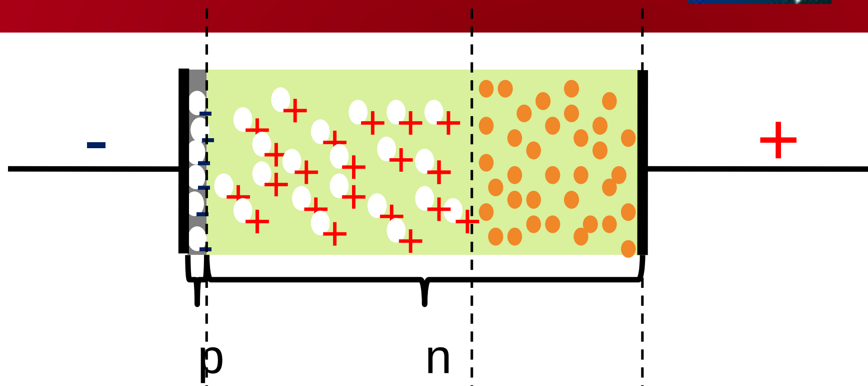

Zone without free charge carriers positively charged. Sensitive Detector Volume.

Zone with free electrons. Conductive. Insensitive to particles.

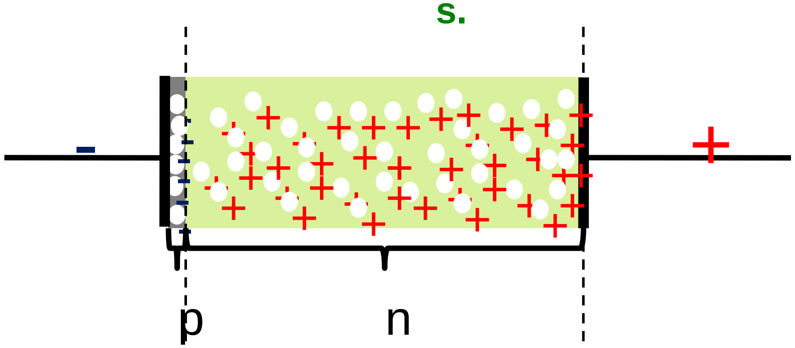

Fully depleted

Silicon Drift Detector

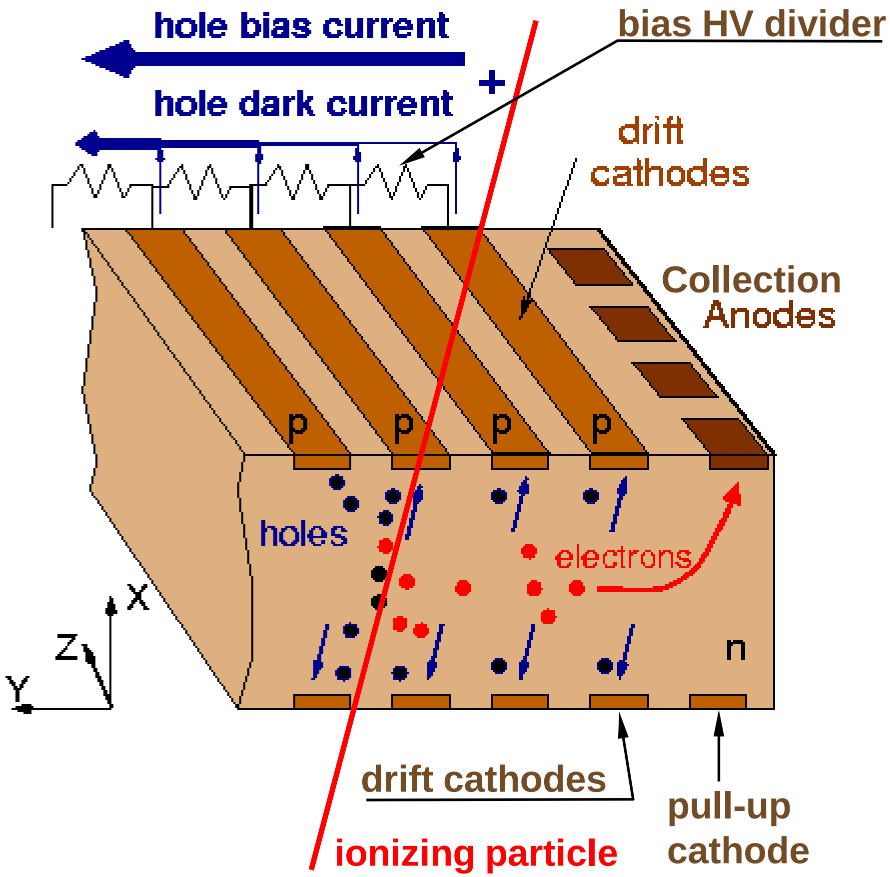

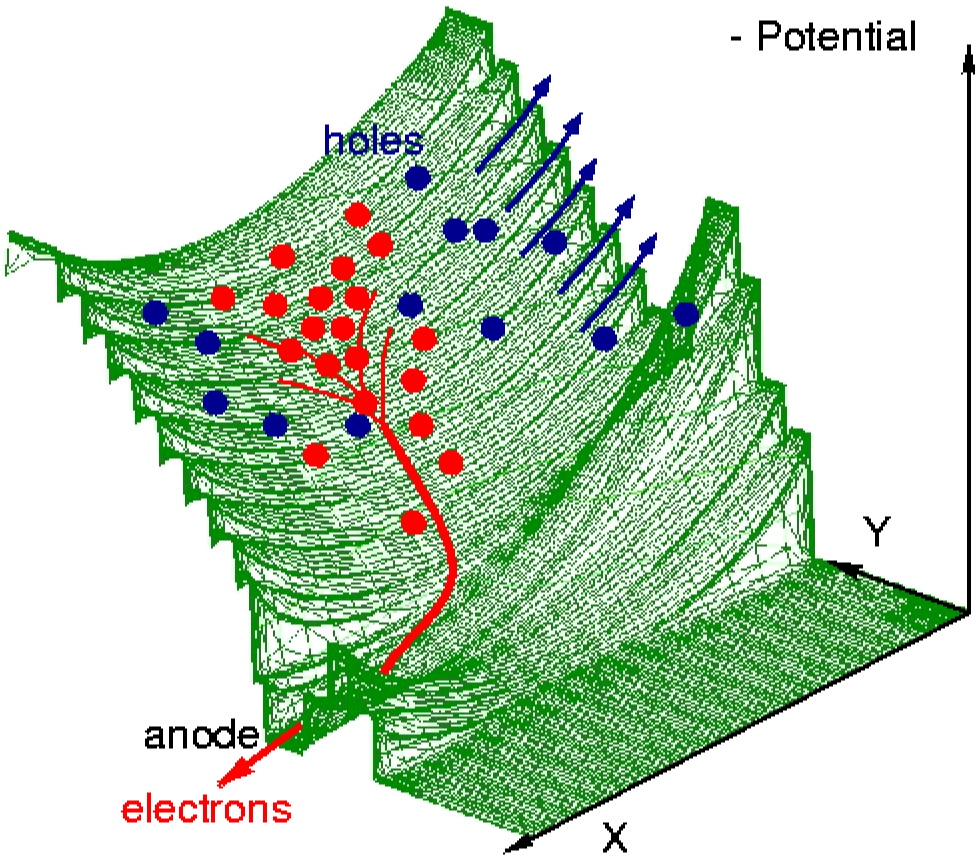

CMS Tracker

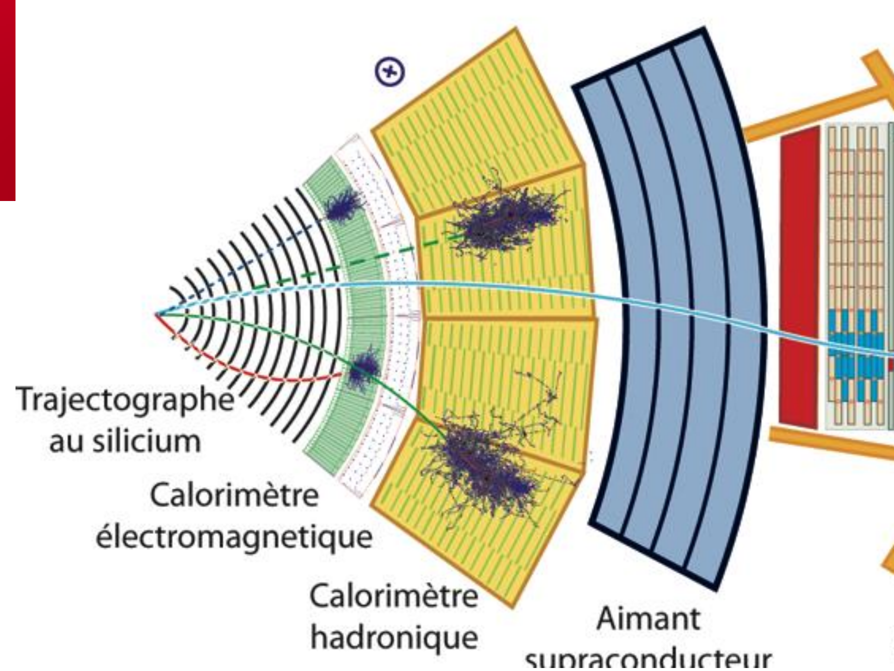
Trajectographe au silicium
Calorimètre électromagnetique
Calorimètre hadronique
Aimant supraconducteur

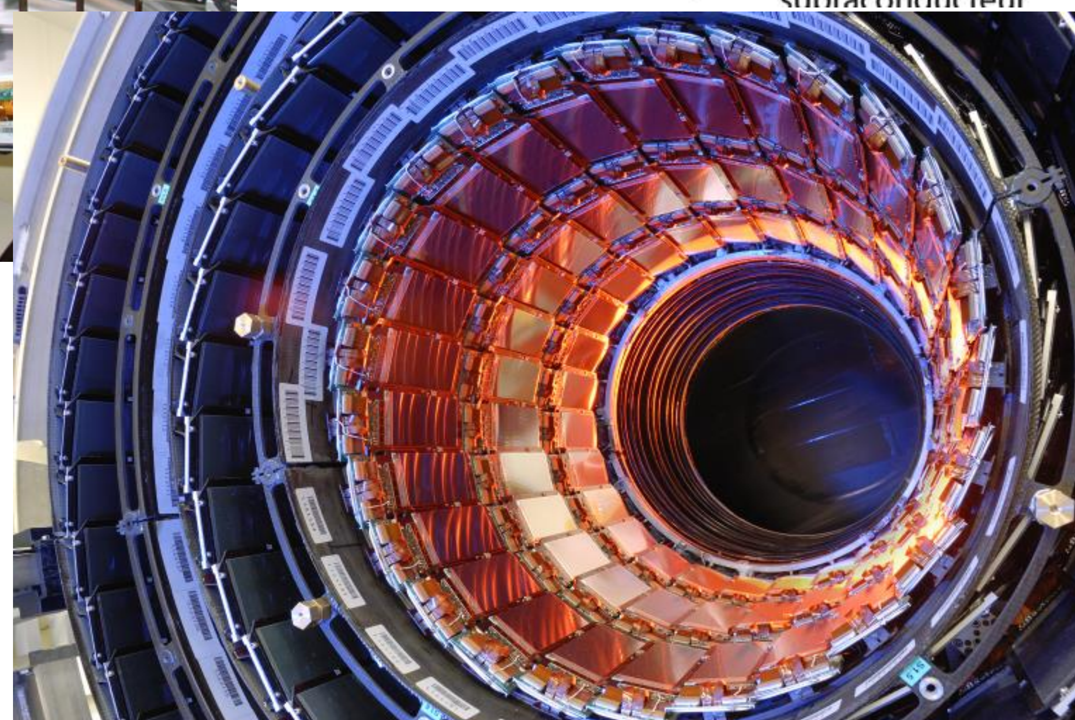

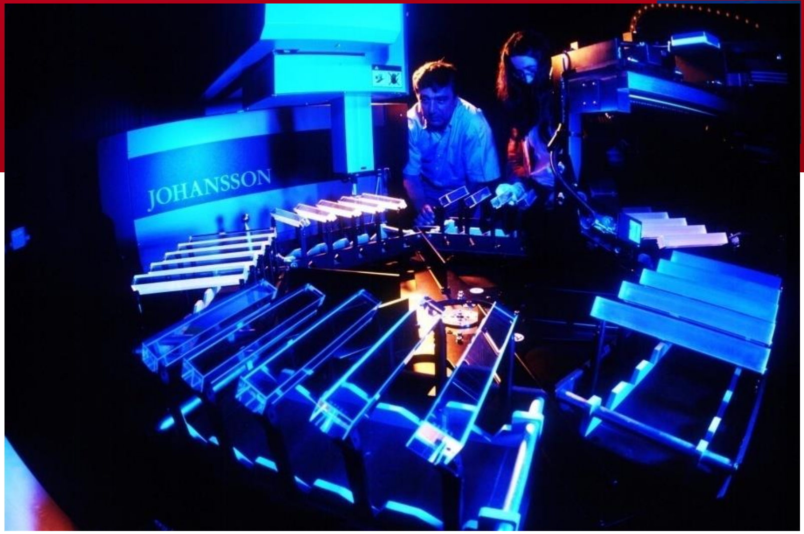

Les Détecteur à base de scintillation

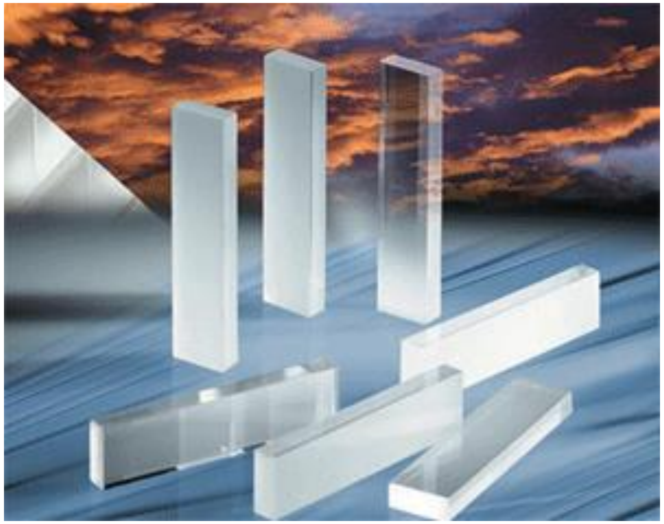

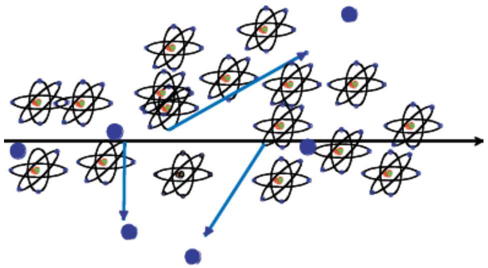

Detectors based on Registration of excited Atoms → Scintillators

Emission of photons of by excited Atoms, typically UV to visible light.

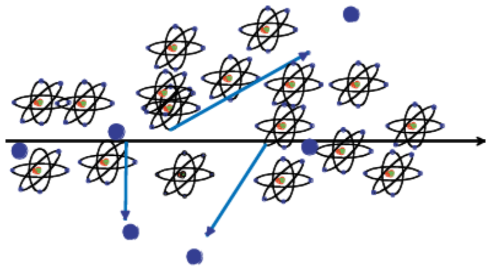

Detectors based on Registration of excited Atoms → Scintillators

Emission of photons of by excited Atoms, typically UV to visible light.

a) Observed in Noble Gases (even liquid !)

b) Inorganic Crystals

→ Substances with largest light yield. Used for precision measurement of energetic Photons. Used in Nuclear Medicine.

c) Polyzyclic Hydrocarbons (Naphtalen, Anthrazen, organic Scintillators)

→ Most important category. Large scale industrial production, mechanically and chemically quite robust. Characteristic are one or two decay times of the light emission.

Organic ('Plastic') Scintillators

Inorganic (Crystal) Scintillators

Low Light Yield **Fast: 1-3ns**

Large Light Yield **Slow: few 100ns**

Type	Light[a] output	λ_{max}[b] (nm)	Attenuation[c] length (cm)	Risetime (ns)	Decay[d] time (ns)	Pulse FWHM (ns)
NE 102A	58–70	423	250	0.9	2.2–2.5	2.7–3.2
NE 104	68	406	120	0.6–0.7	1.7–2.0	2.2–2.5
NE 104B	59	406	120	1	3.0	3
NE 110	60	434	400	1.0	2.9–3.3	4.2
NE 111	40–55	375	8	0.13–0.4	1.3–1.7	1.2–1.6
NE 114	42–50	434	350–400	~1.0	4.0	5.3
Pilot B	60–68	408	125	0.7	1.6–1.9	2.4–2.7
Pilot F	64	425	300	0.9	2.1	3.0–3.3
Pilot U	58–67	391	100–140	0.5	1.4–1.5	1.2–1.9
BC 404	68	408	—	0.7	1.8	2.2
BC 408	64	425	—	0.9	2.1	~2.5
BC 420	64	391	—	0.5	1.5	1.3
ND 100	60	434	400	—	3.3	3.3
ND 120	65	423	250	—	2.4	2.7
ND 160	68	408	125	—	1.8	2.7

	Relative light output	λ_{max} emission (nm)	Decay time (ns)	Density (g/cm^3)
Inorganic crystals				
NaI(Tl)	230	415	230	3.67
CsI(Tl)	250	560	900	4.51
$Bi_4Ge_3O_{12}$ (BGO)	23–86	480	300	7.13
Organic crystals				
Anthracene	100	448	22	1.25
Trans-stilbene	75	384	4.5	1.16
Naphthalene	32	330–348	76–96	1.03
p,p'-Quarterphenyl	94	437	7.5	1.20
Primary activators				
2,5-Diphenyl-oxazole (PPO)	75	360–416	5[a]	
2-Phenyl-5-(4-biphenylyl)-1,3,4-oxadiazole (PBD)	96	360–5		
4,4''-Bis(2-butyloctyloxy)-p-quaterphenyl (BIBUQ)	60	365,393	1.30[b]	

LHC bunchcrossing 25ns

LEP bunchcrossing 25μs

Typical Geometries:

- Light guides: transfer by total internal reflection (+outer reflector)

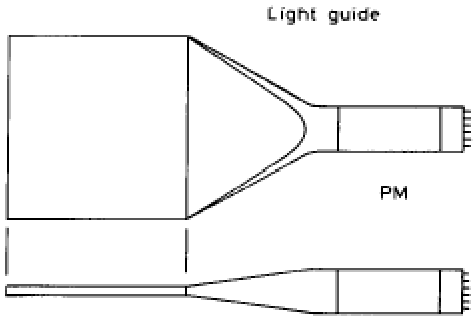

“fish tail”

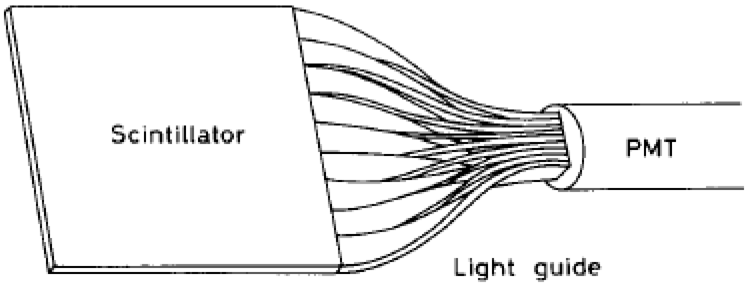

adiabatic

- wavelength shifter (WLS) bars

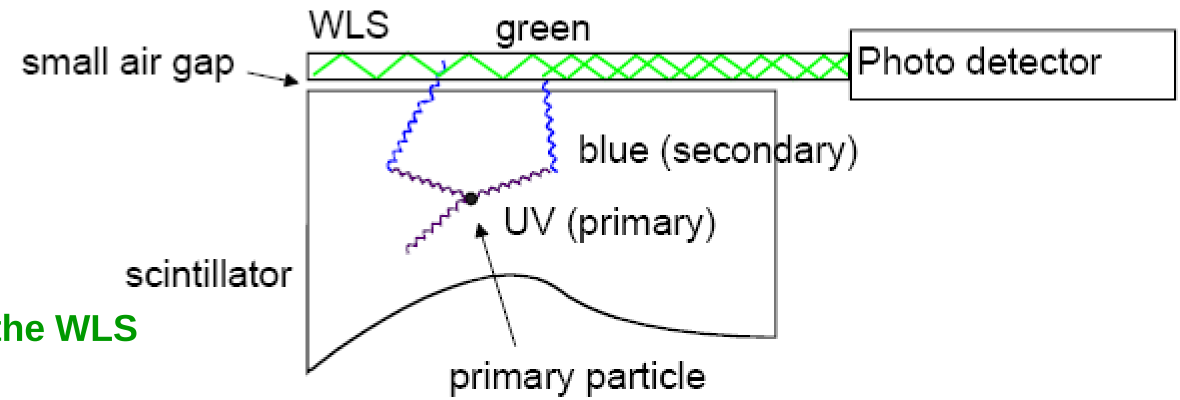

UV light enters the WLS material
Light is transformed into longer wavelength
→Total internal reflection inside the WLS material
→ ‘transport’ of the light to the photo detector

From C. Joram

Fiber Tracking

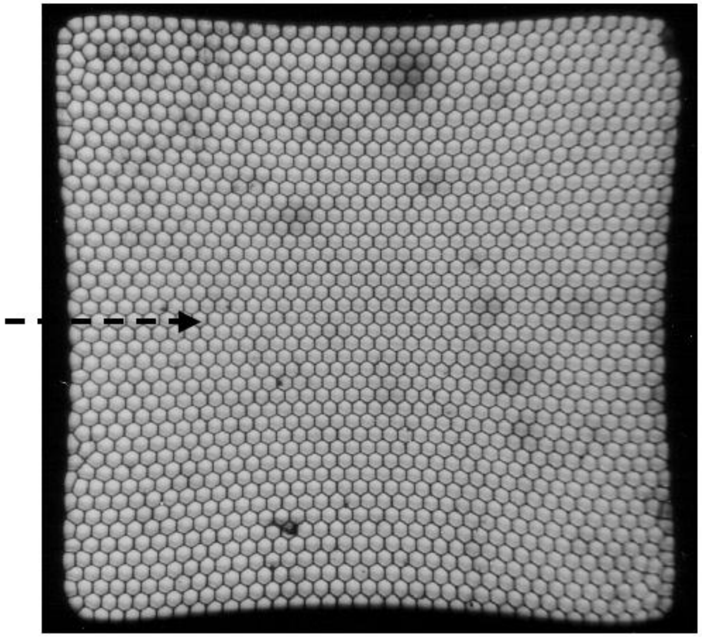

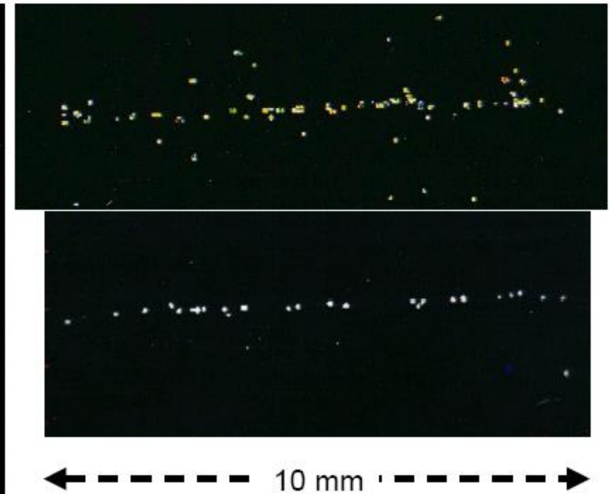

Images of tracks from 5 GeV/c pions (1989)

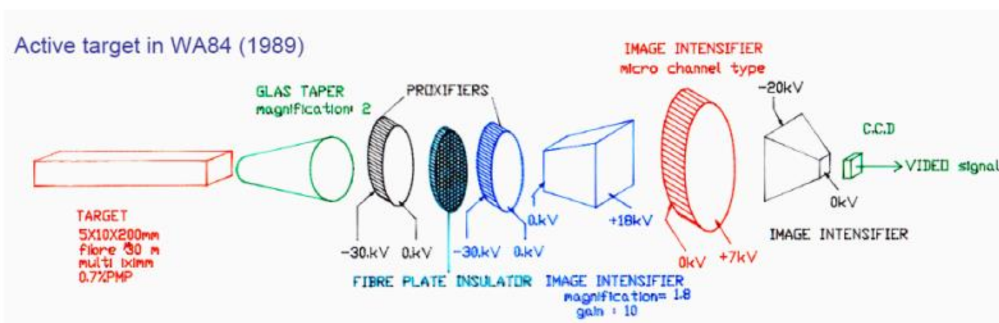

Readout of photons in a cost effective way is rather challenging.

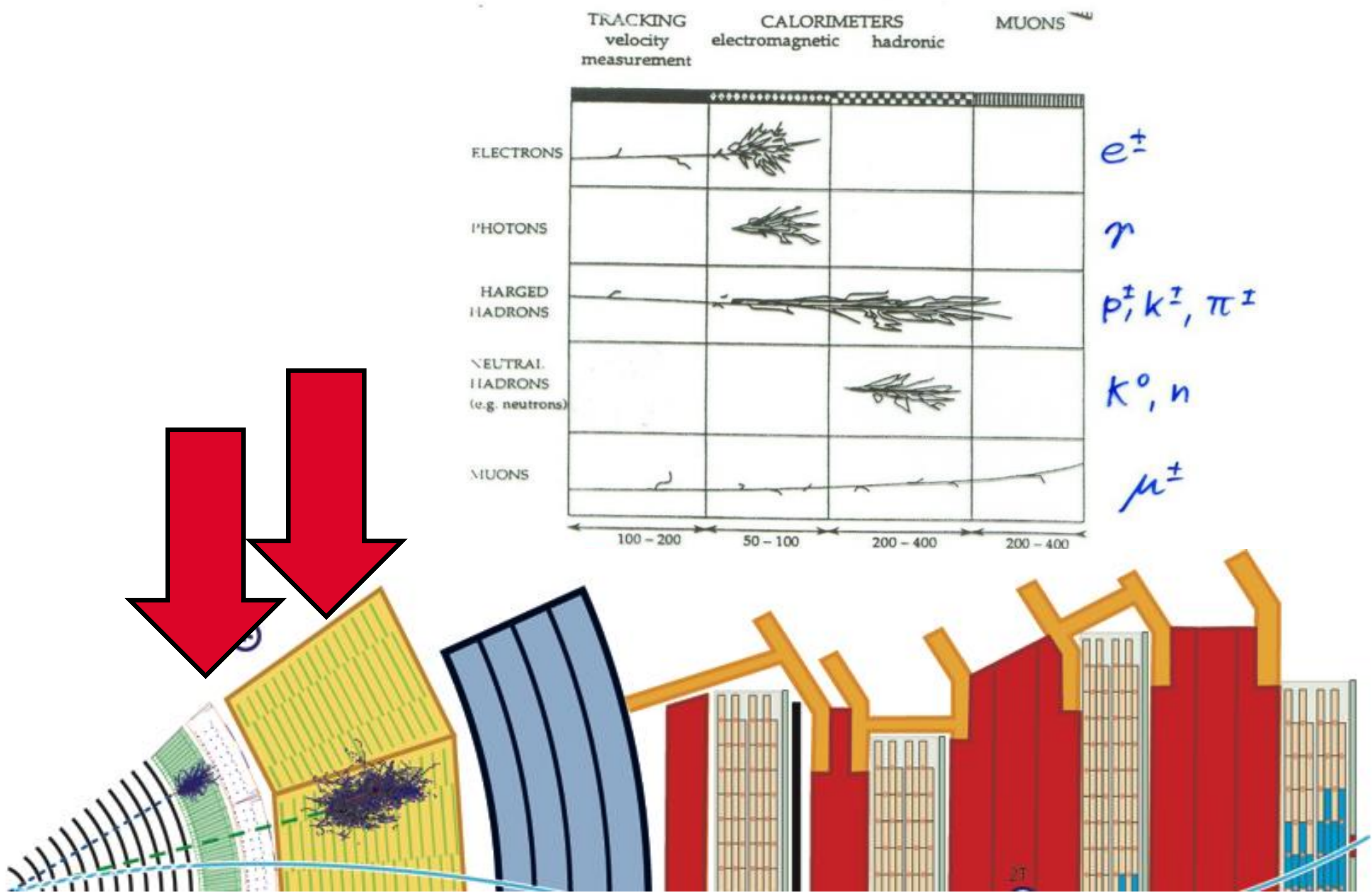
TRACKING
velocity measurement
CALORIMETERS
electromagnetic
hadronic
MUONS
ELECTRONS
PHOTONS
HARGED HADRONS
NEUTRAL HADRONS (e.g. neutrons)
MUONS
100 – 200
50 – 100
200 – 400
200 – 400
$e^{\pm}$
γ
$p^{\pm}, k^{\pm}, \pi^{\pm}$
k^0, n
$\mu^{\pm}$

Calorimetry

Calorimeters can be classified into:

Electromagnetic Calorimeters,
to measure electrons and photons through their EM interactions.

Hadron Calorimeters,
Used to measure hadrons through their strong and EM interactions.

The construction can be classified into:

Homogeneous Calorimeters,
that are built of only one type of material that performs both tasks, energy degradation and signal generation.

Sampling Calorimeters,
that consist of alternating layers of an absorber, a dense material used to degrade the energy of the incident particle, and an active medium that provides the detectable signal.

C.W. Fabjan and F. Gianotti, Rev. Mod. Phys., Vol. 75, N0. 4, October 2003

EM Calorimetry

At high energies (higher than 100 MeV) electrons lose their energy almost exclusively by bremsstrahlung while photons lose their energy by electron–positron pair production

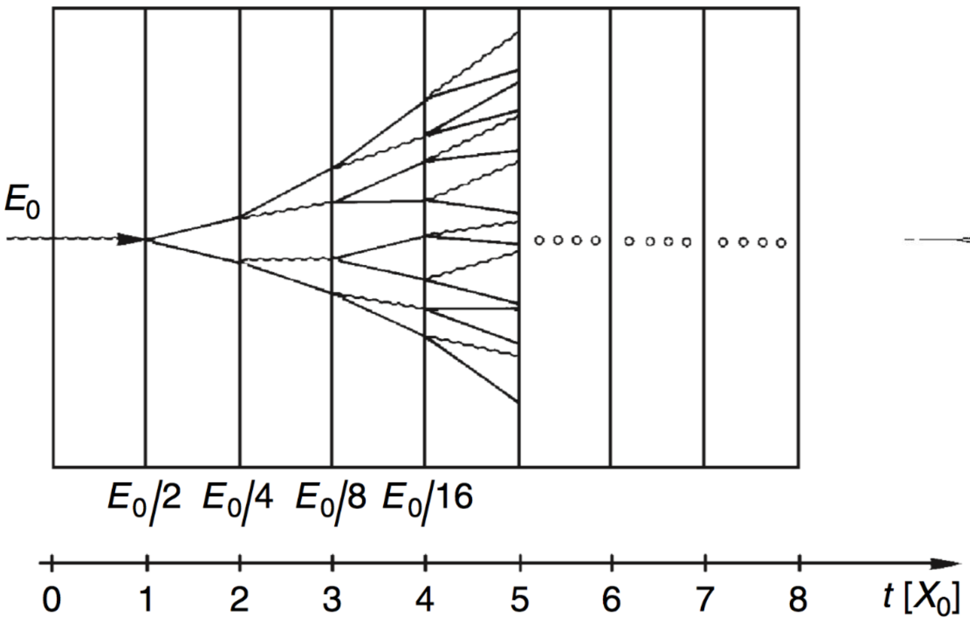

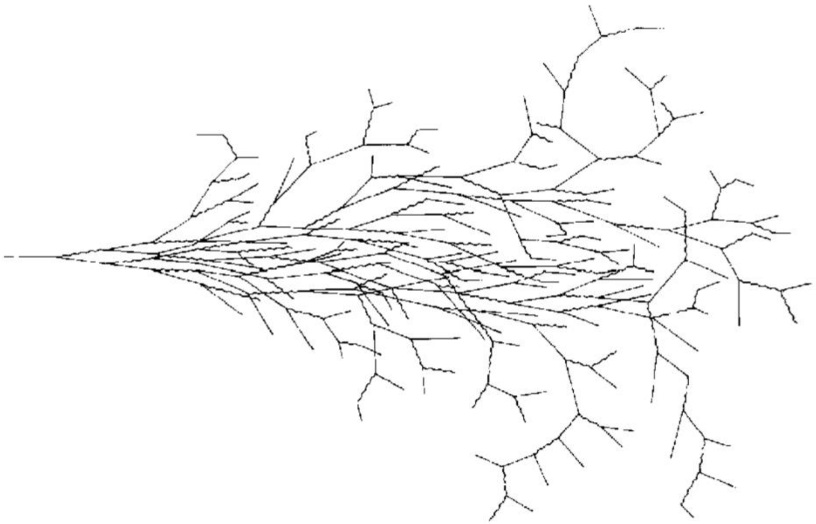

Crystals for Homogeneous EM Calorimetry

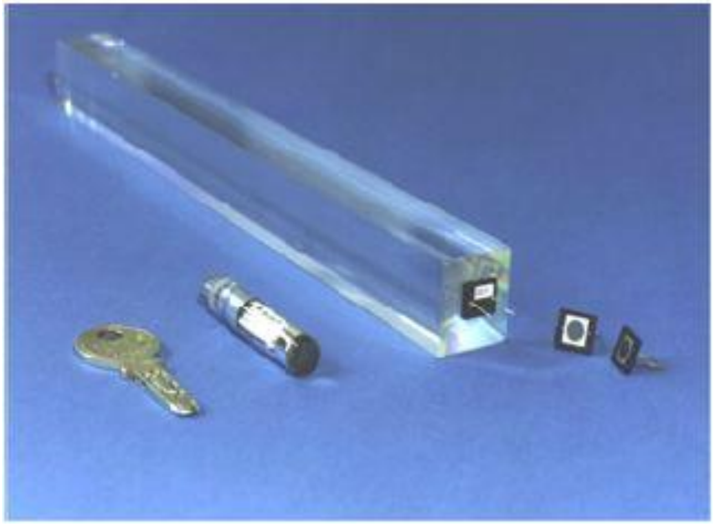

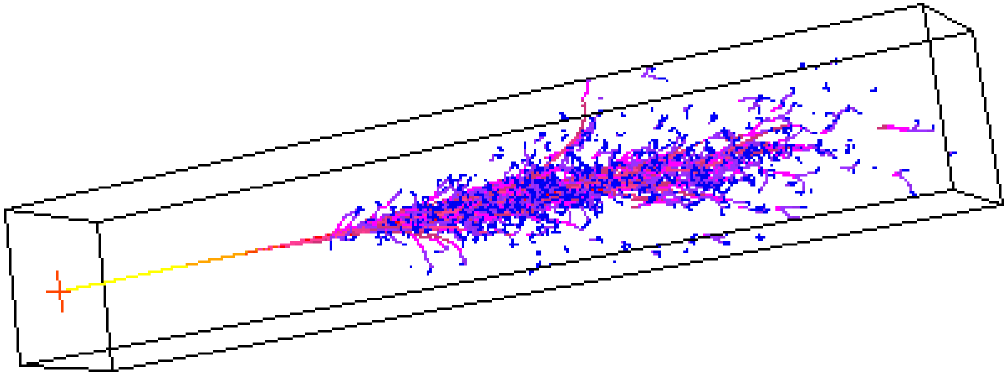

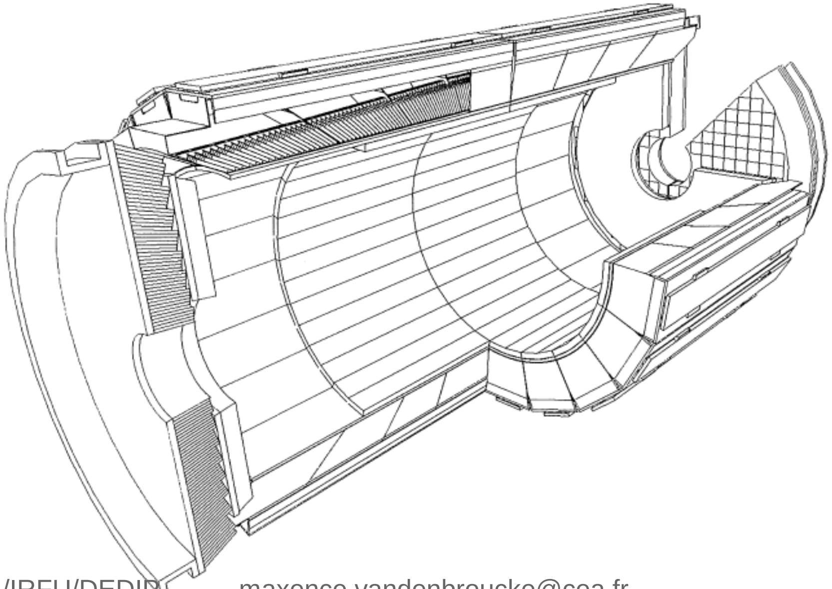

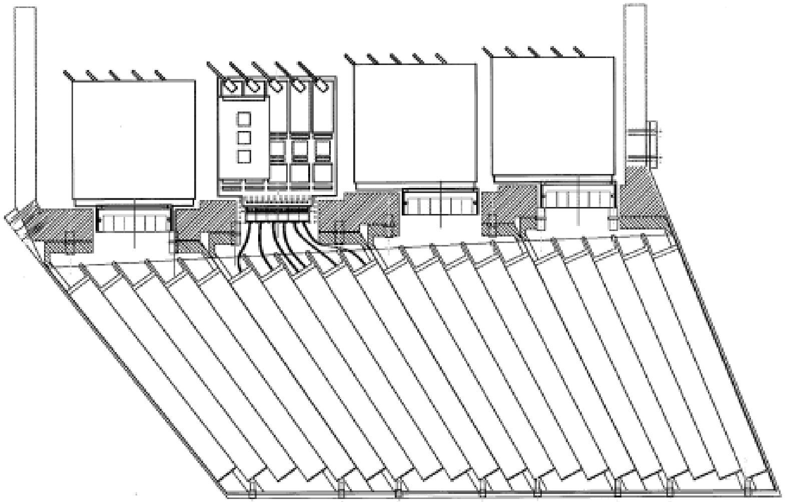

Fig. 2. Longitudinal drawing of module 2, showing the structure and the front-end electronics layout.

Hadron Calorimeters are Large because □ is large

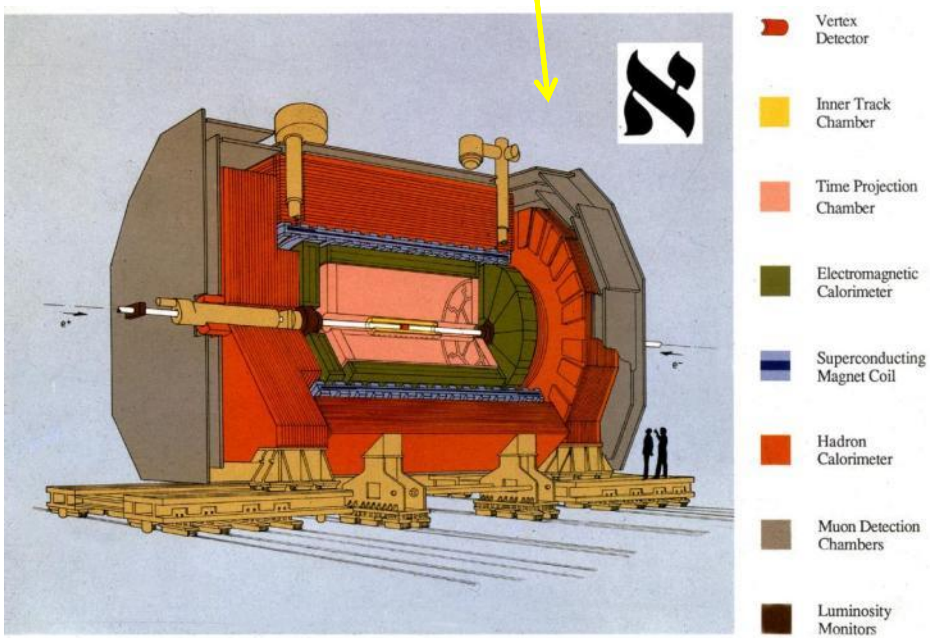

Fig. 1 - The ALEPH Detector

Hadron Calorimeters are large and heavy because the hadronic interaction length □, the 'strong interaction equivalent' to the EM radiation length X_0, is large (5-10 times larger than X_0)

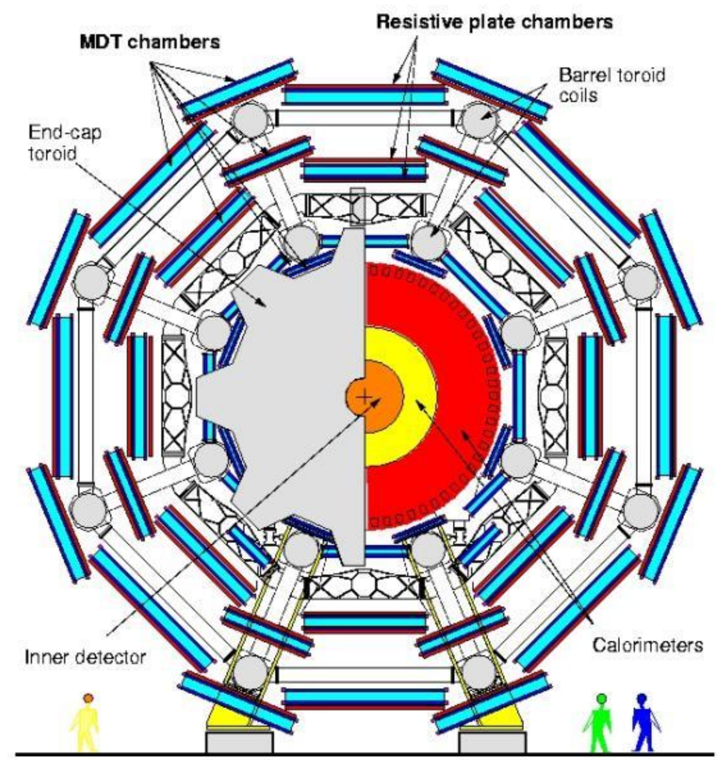

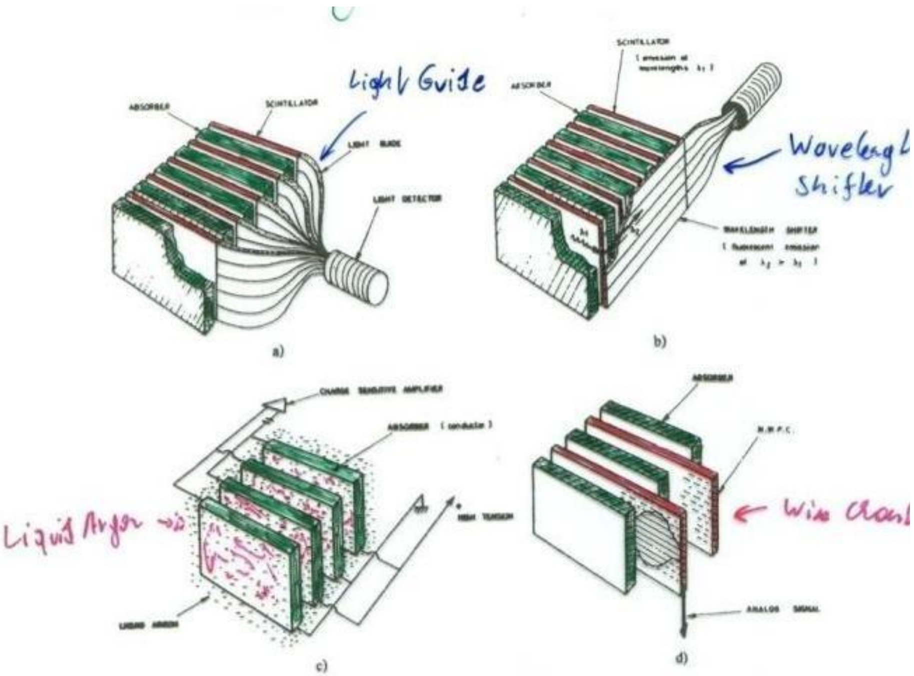
Light Guide
ABSORBER
SCINTILLATOR
LIGHT GUIDE
LIGHT DETECTOR
a)
SCINTILLATOR
ABSORBER
Shifter
WAVELENGTH SHIFTER
b)
CHARGE SENSITIVE AMPLIFIER
ABSORBER (conductor)
HIGH TENSION
Liquid Argon
LIQUID ARGON
c)
ABSORBER
M.W.P.C.
ANALOG SIGNAL
d)

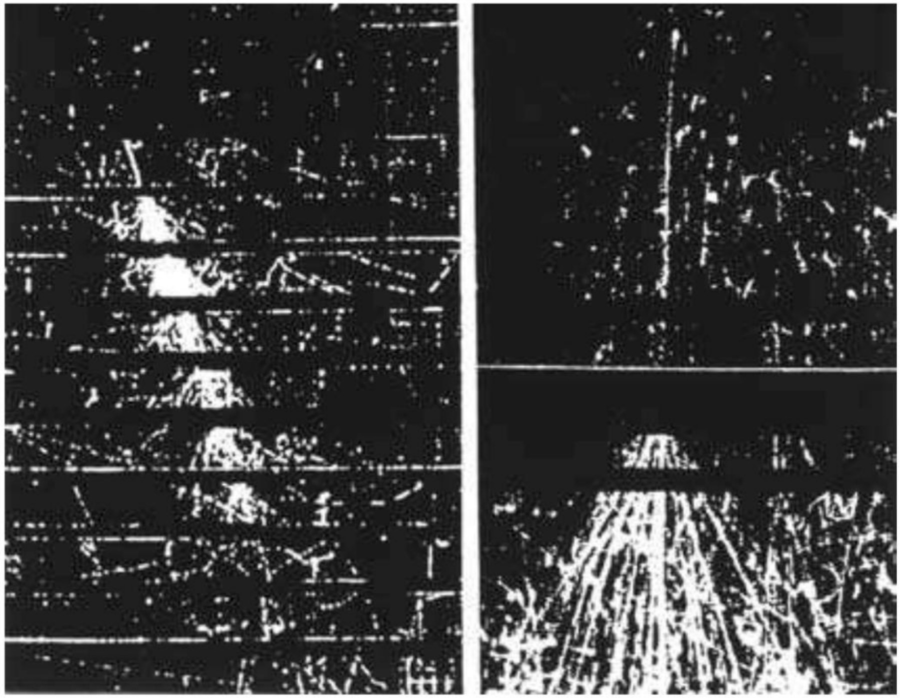

La détection des particules: exemple des détecteurs gazeux

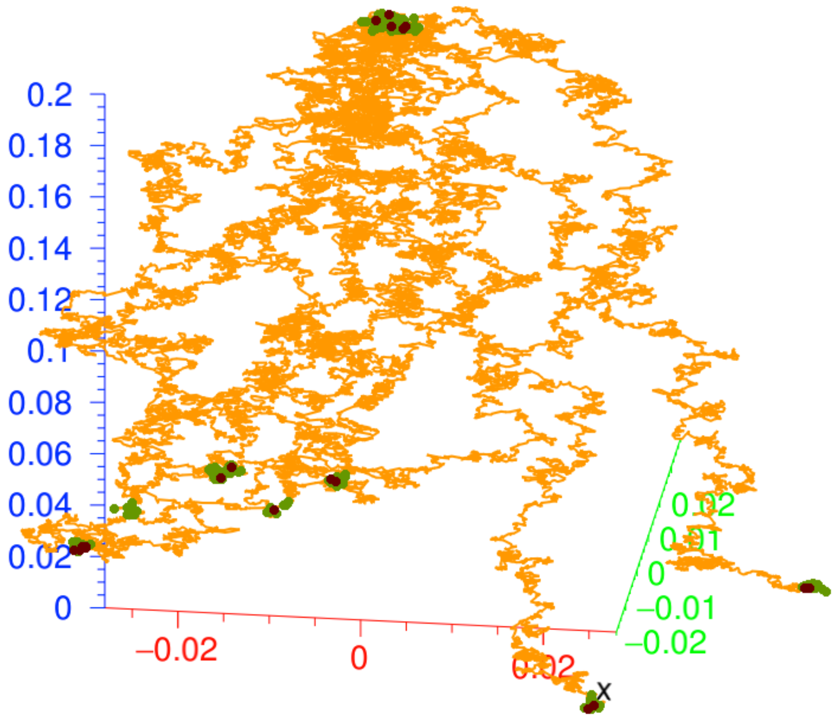

Détecteurs Gazeux

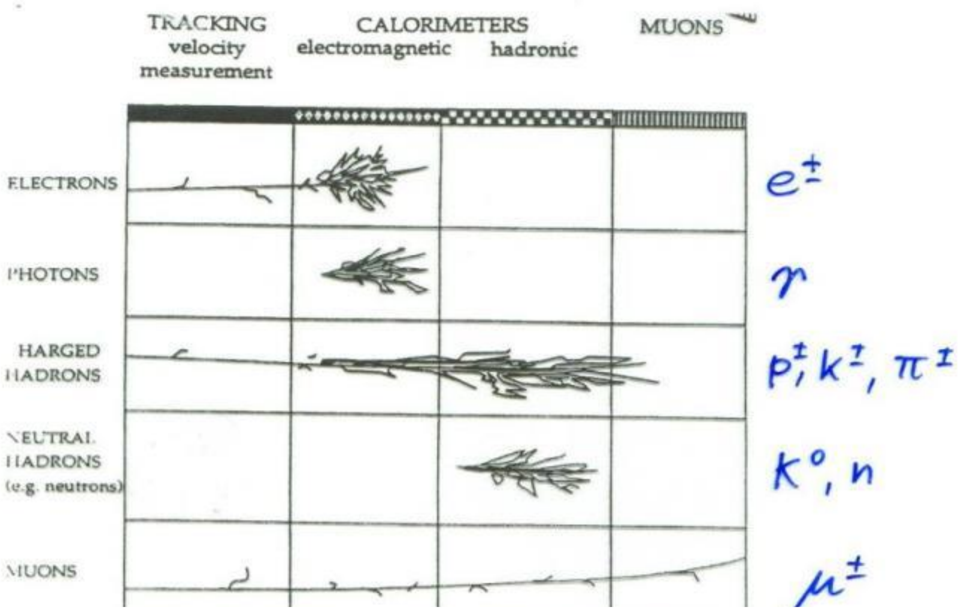

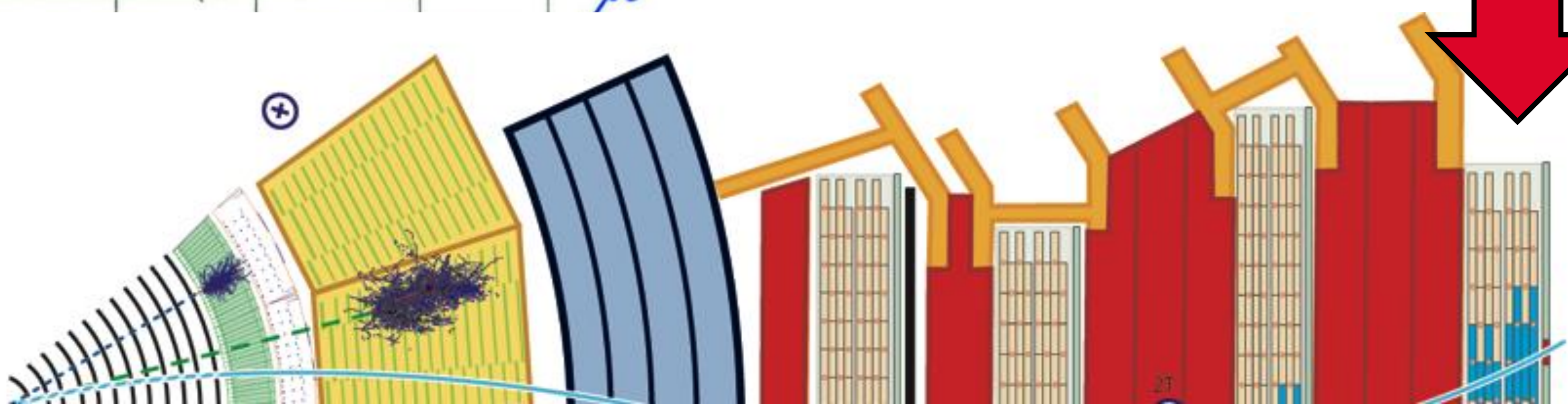

EXEMPLE SIMPLE DE DÉTECTEUR

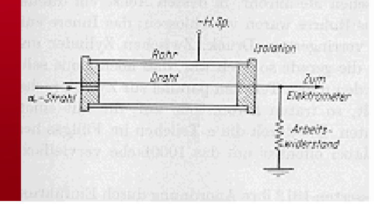

(RADIAL) AVEC: $E = \frac{1}{r}\frac{V_0}{\ln(b/a)}$

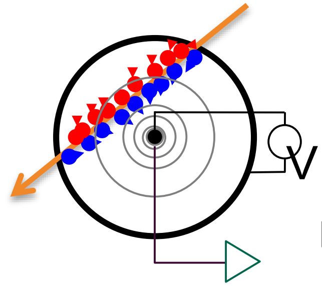

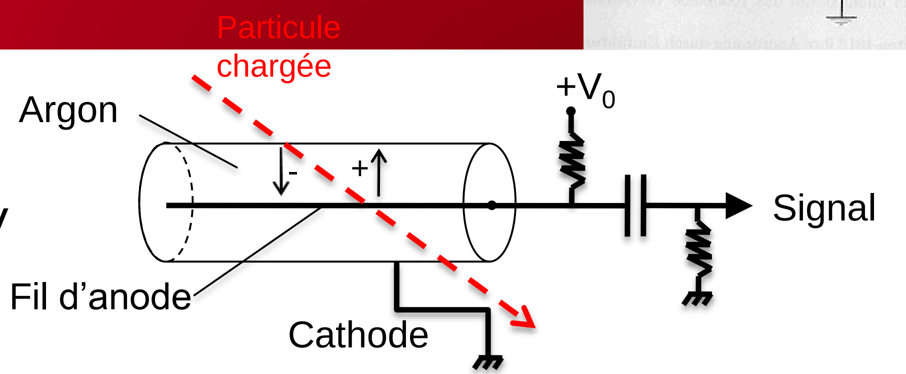

- R : DISTANCE RADIALE À L'AXE
- B : RAYON INTERNE DU CYLINDRE
- A : RAYON DU FIL D'ANODE

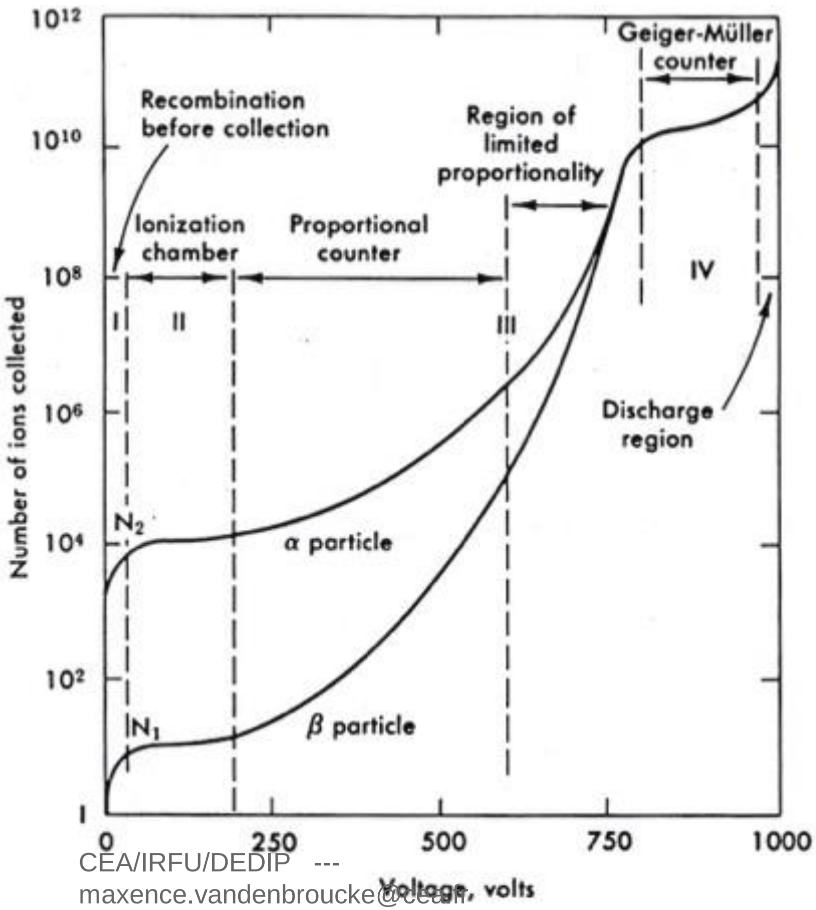

I: tension trop faible→ recombinaison

II: Chambre d'ionisation. Collection des charges sans amplification.

IIIa: Mode **proportionnel**. Le signal est amplifié et proportionnel à l'énergie déposée.

IIIb: Mode **Streamer**. Phénomènes secondaires induits par les photons de la première avalanche → Gaz quencher

IV: Mode **Geiger-Müller**. Avalanche dans tout le détecteur. Le courant de sortie est saturé.

IONISATION PRIMAIRE

Production de paires électron-ion :

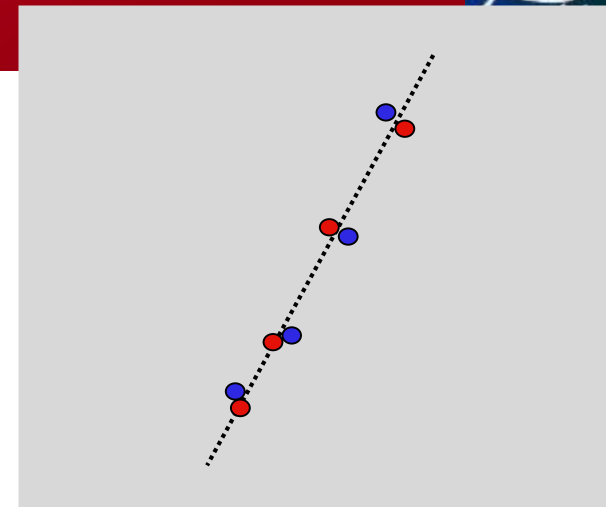

- Les interactions Coulombiennes entre le champ électrique de la particule et les atomes du milieu produisent des paires électron-ion.
- Les ionisations multiples suivent une statistique de Poisson:

$$P_k^n = \frac{n^k}{k!} e^{-n}$$

n : moyen

k : mesuré

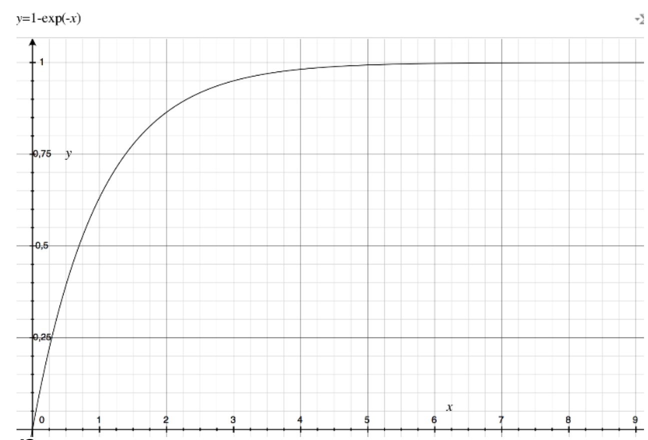

- Efficacité de détection: $e = 1 - P_0^n = 1 - e^{-n}$
- Mécanismes d'ionisation :

• Excitation: $X + p \rightarrow X^* + p$ puis $X^* \rightarrow X^+ + e^-$
• Ionisation: $X + p \rightarrow X^+ + p + e^-$
• *Effet Penning*: $Ne^* + Ar \rightarrow Ne + Ar^+ + e^-$

IONISATION TOTALE

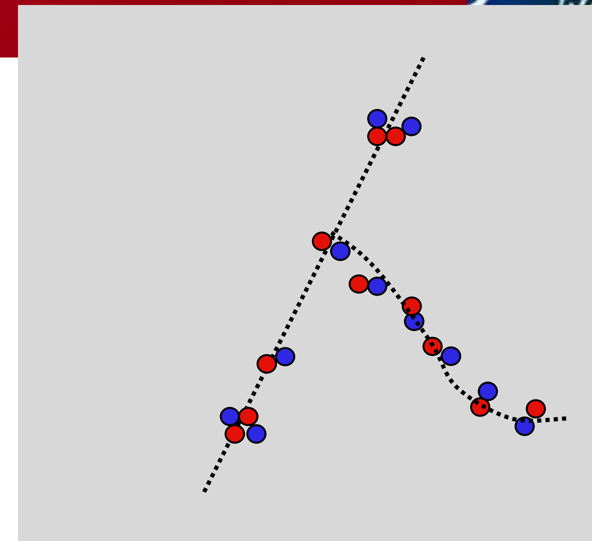

- Les électrons primaires ionisent à nouveau le milieu et produisent localement de nouveaux groupes de paires électron-ion. Si l'électron secondaire a suffisament d'énergie il peut produire une longue trace (électronδ).

- Nombre total de paires:

$$n_T = \frac{\Delta E}{w_i}$$

ΔE : perte d'énergie de la particule
w_i : énergie moyenne par paire

M.I.P. dans l'argon:

– ΔE= 2,65 keV/cm $\quad w_i$ = 25 eV

– $n_T \approx$ 106 paires électron-ion/cm

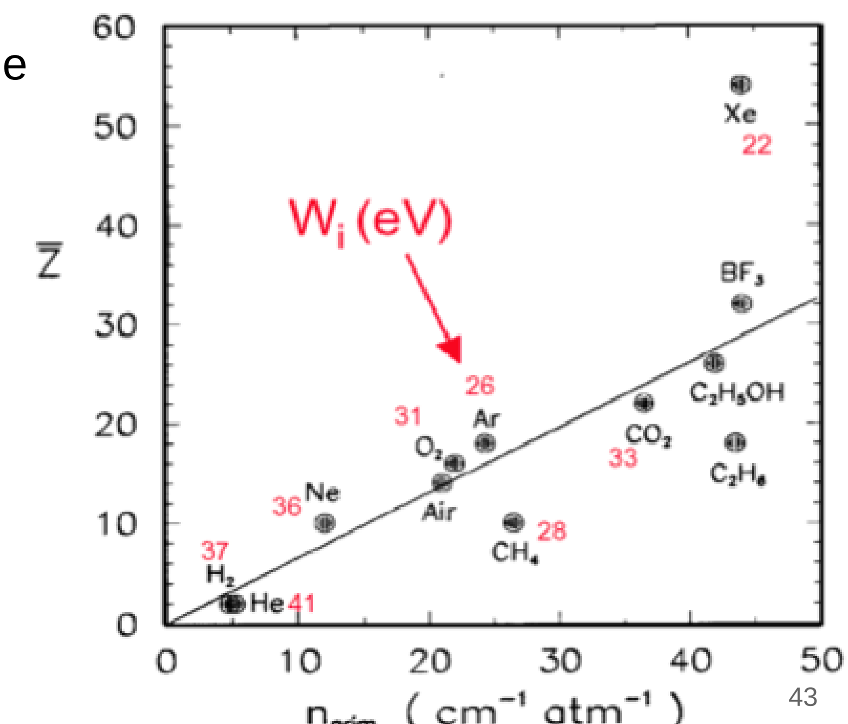

PHÉNOMÈNE D'AVALANCHE AUTOUR D'UN FILS

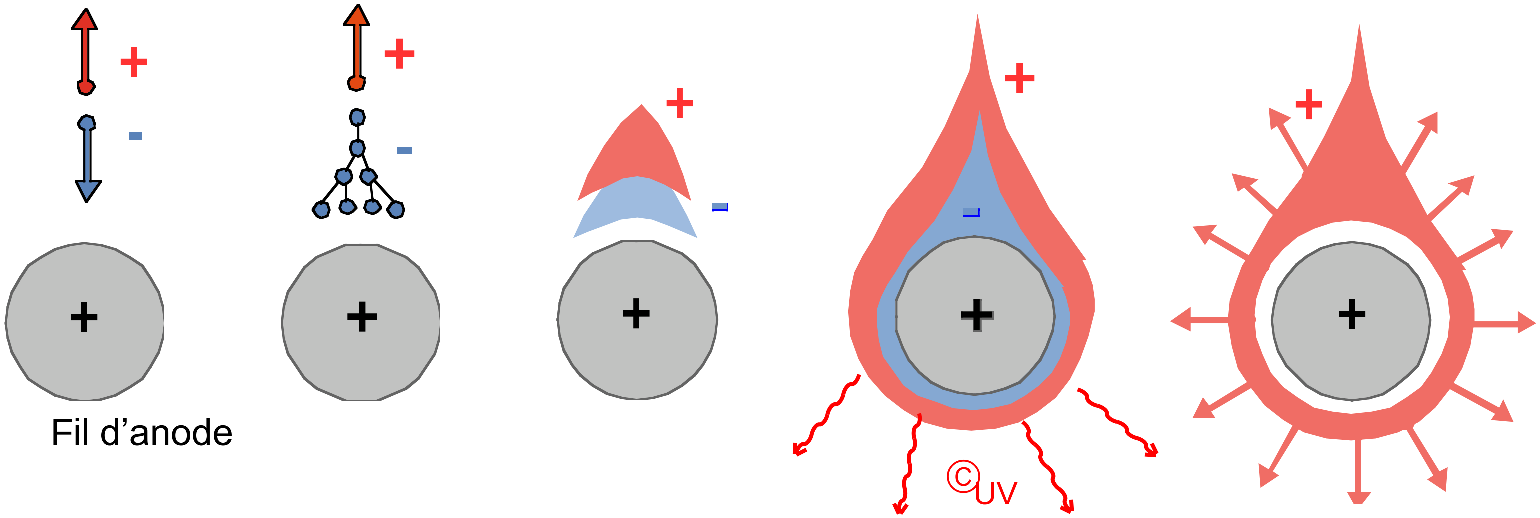

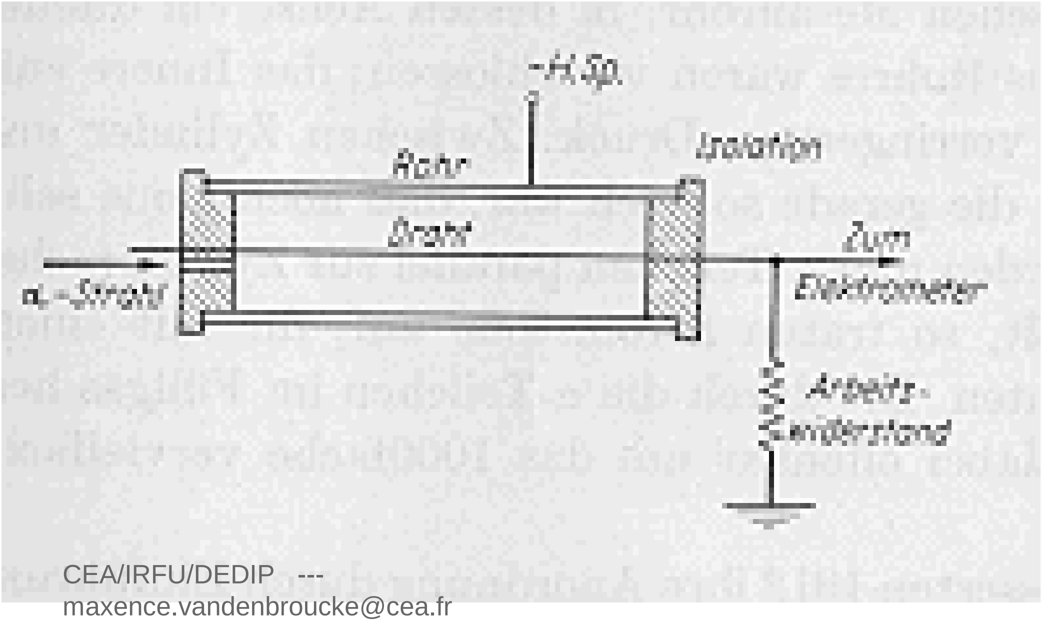

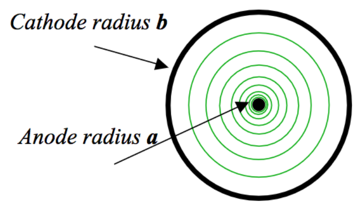

ELECTRIC FIELD AND POTENTIAL:

$$E(r) = \frac{CV_0}{2\pi\varepsilon_0}\frac{1}{r}$$

$$V(r) = \frac{CV_0}{2\pi\varepsilon_0}\ln\frac{r}{a}$$

$$C = \frac{2\pi\varepsilon_0}{\ln(b/a)}$$ capacitance per unit length

MWPCS

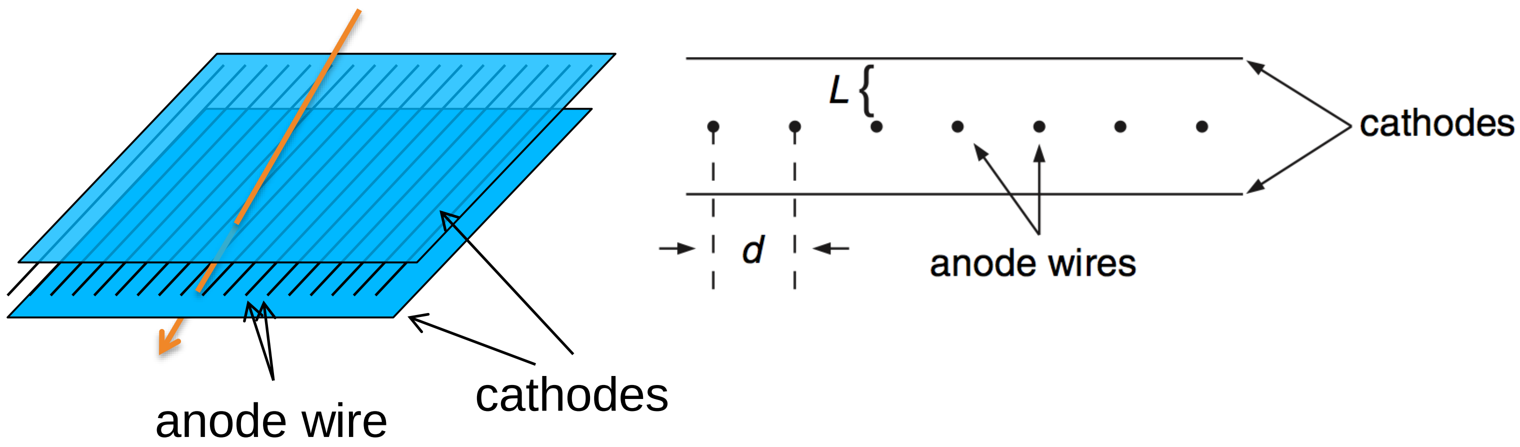

GRANDE CHAMBRE À FILS (1972)

EN COMPARAISON DES CHAMBRES À ÉTINCELLES ET DES CHAMBRES À BULLES, LES CHAMBRES À FILS SONT PLUS RAPIDES, PRÉSENTENT DE MEILLEURES RÉSOLUTIONS SPATIALE ET TEMPORELLE, SANS TEMPS MORT SIGNIFICATIF ET RÉSISTANTES AUX RADIATIONS.

PRIX NOBEL DE PHYSIQUE 1992

The Royal Swedish Academy of Sciences awards the 1992 Nobel Prize in Physics to **Georges Charpak** for his invention and development of particle detectors, in particular the multiwire proportional chamber.

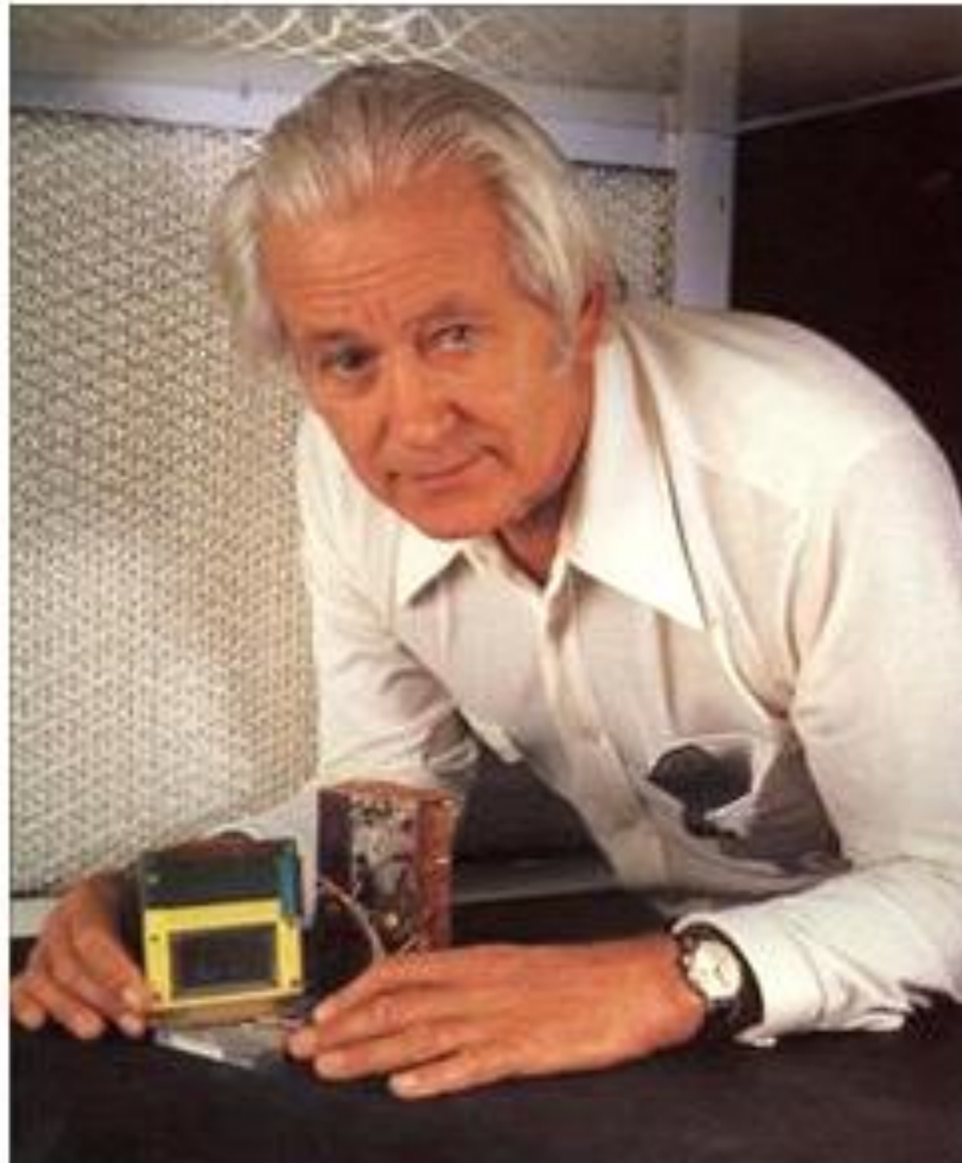

Photo: D. Parker, Science Photo Lab. UK

Georges Charpak
CERN, Geneva, Switzerland

NOBEL PRICES FOR INSTRUMENTATION

1927: C.T.R. Wilson, Cloud Chamber
1939: E. O. Lawrence, Cyclotron & Discoveries
1948: P.M.S. Blacket, Cloud Chamber & Discoveries
1950: C. Powell, Photographic Method & Discoveries
1954: Walter Bothe, Coincidence method & Discoveries
1960: Donald Glaser, Bubble Chamber
1968: L. Alvarez, Hydrogen Bubble Chamber & Discoveries
1992: Georges Charpak, Multi Wire Proportional Chamber

Time Projection Chamber (TPC):

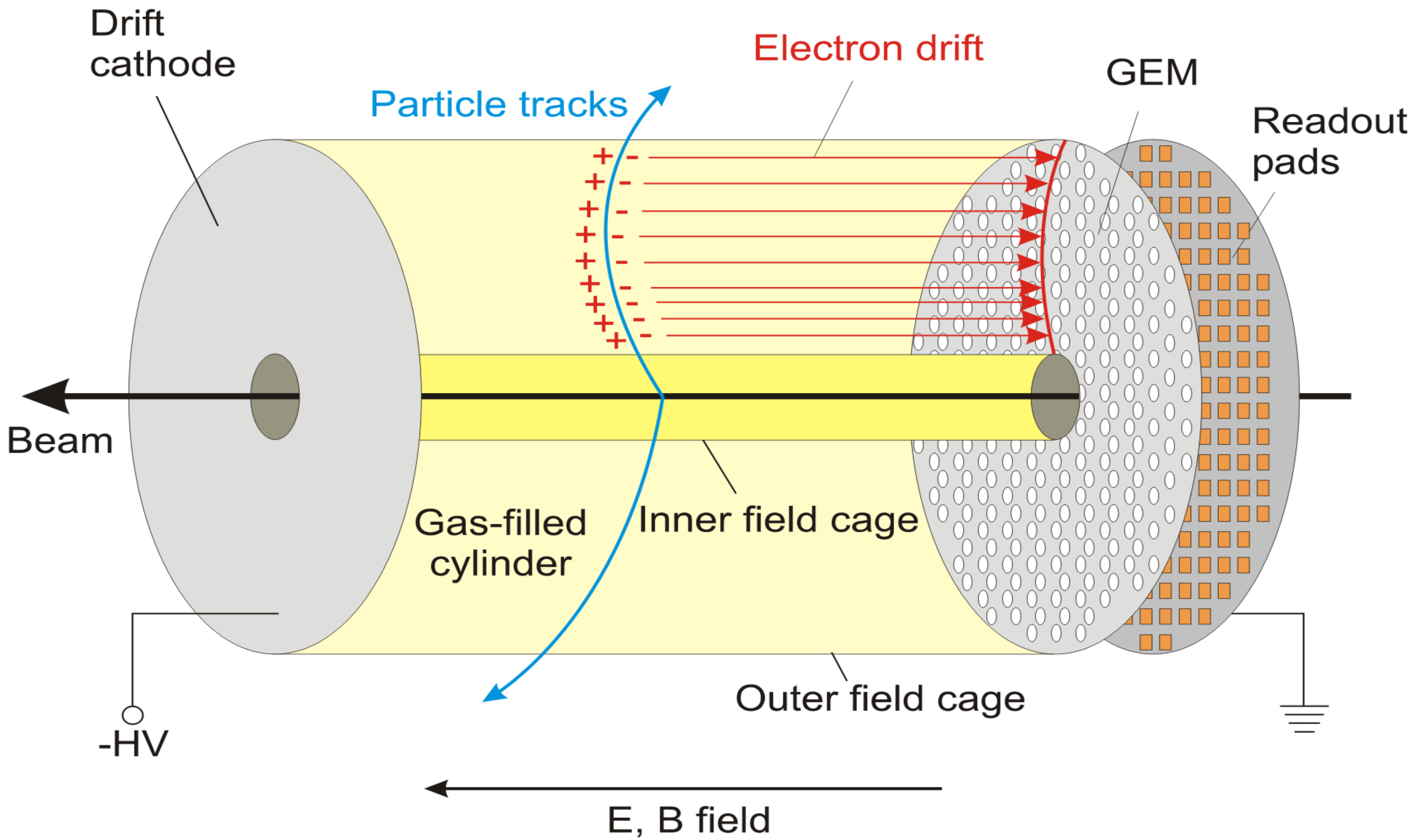

Time Projection Chamber (TPC):

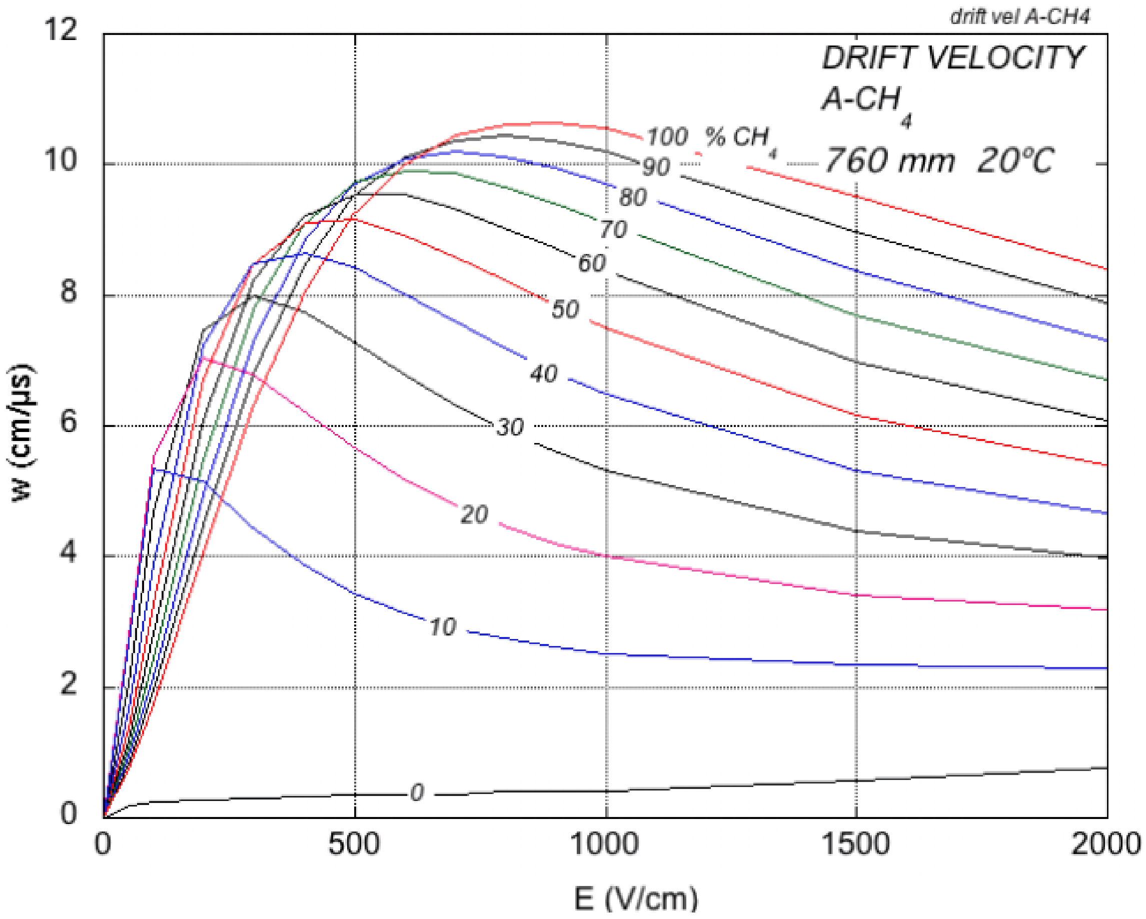

EXAMPLE: Ar-CH_4 90-10 , E=1kVcm^{-1} w^- = 2.5 cm μs^{-1}

STAR TPC (BNL)

Event display of a Au Au collision at CM energy of 130 GeV/n.

Typically around 200 tracks per event.

Great advantage of a TPC: The only material that is in the way of the particles is gas → very low multiple scattering → very good momentum resolution down to low momenta !

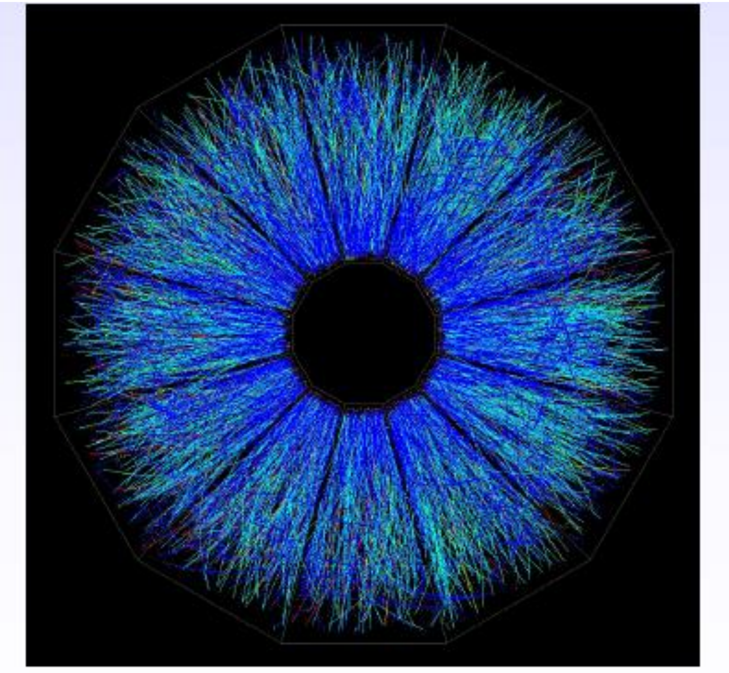

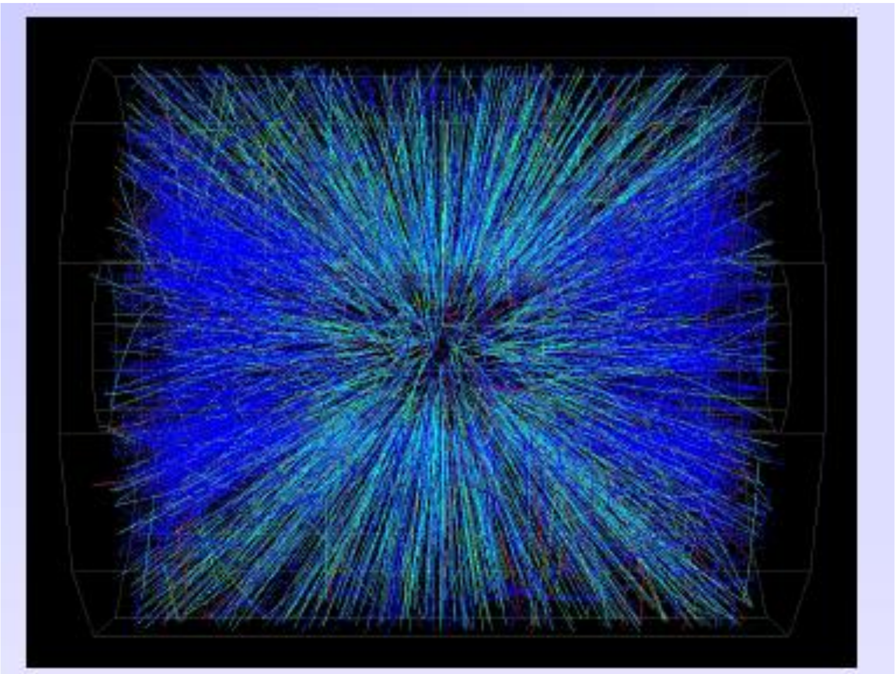

ALICE TPC: Detector Parameters

- **Gas Ne/ CO_2 90/10%**
- **Field 400V/cm**
- **Gas gain >10^4**
- **Position resolution σ= 0.25mm**
- **Diffusion: σ_t= 250μm**
- **Pads inside: 4x7.5mm**
- **Pads outside: 6x15mm** $\sqrt{cm}$
- **B-field: 0.5T**
- **Largest TPC:**
  - **Length 5m**
  - **Diameter 5m**
  - **Volume 88m^3**
  - **Detector area 32m^2**
  - **Channels ~570 000**
- **High Voltage:**
  - **Cathode -100kV**

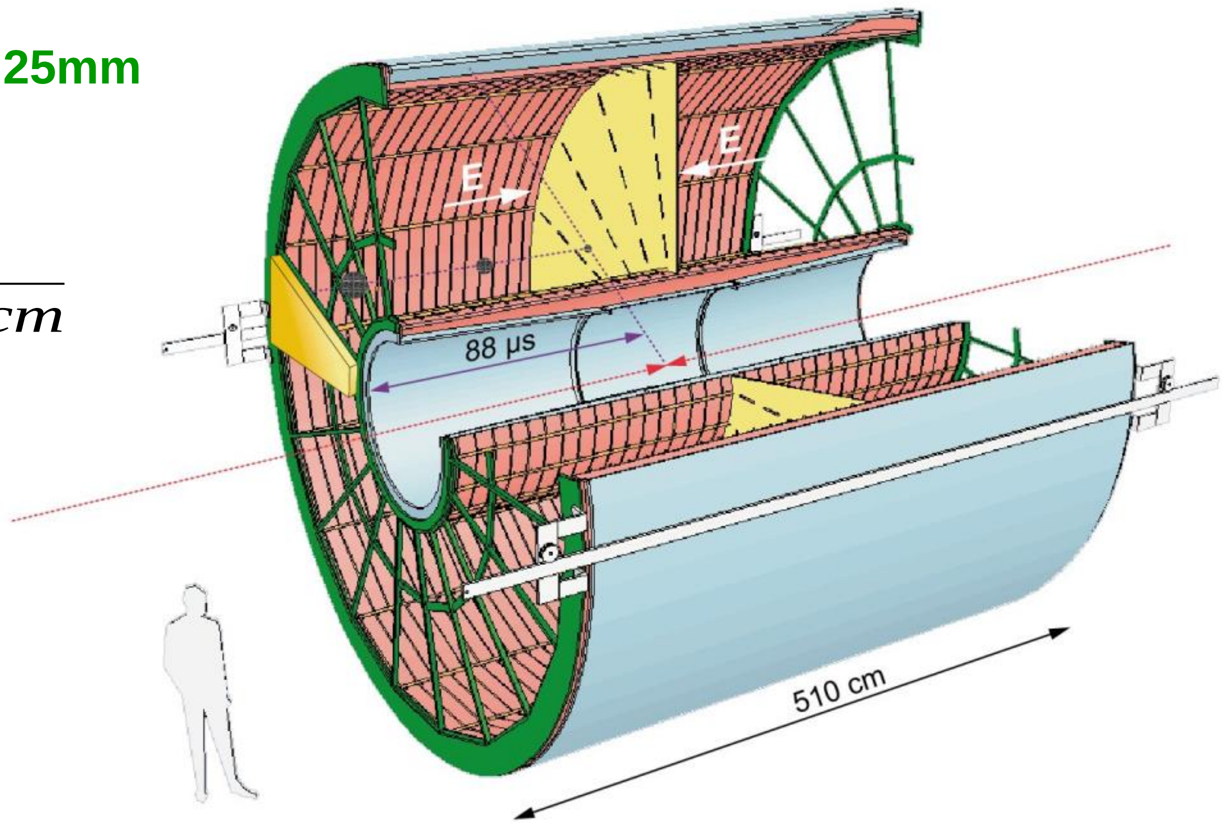

TPC installed in the ALICE Experiment

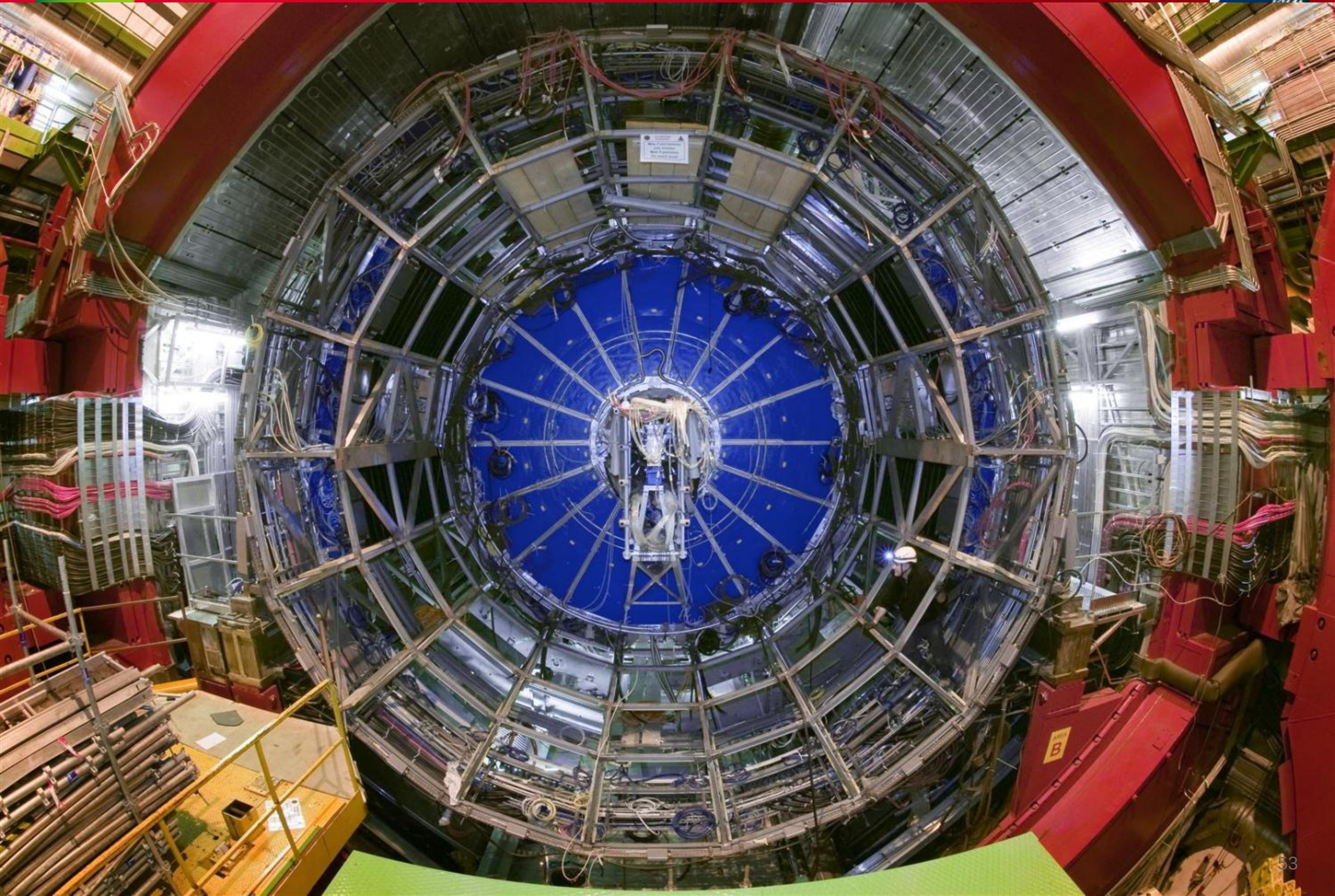

ALICE : Simulation of Particle Tracks

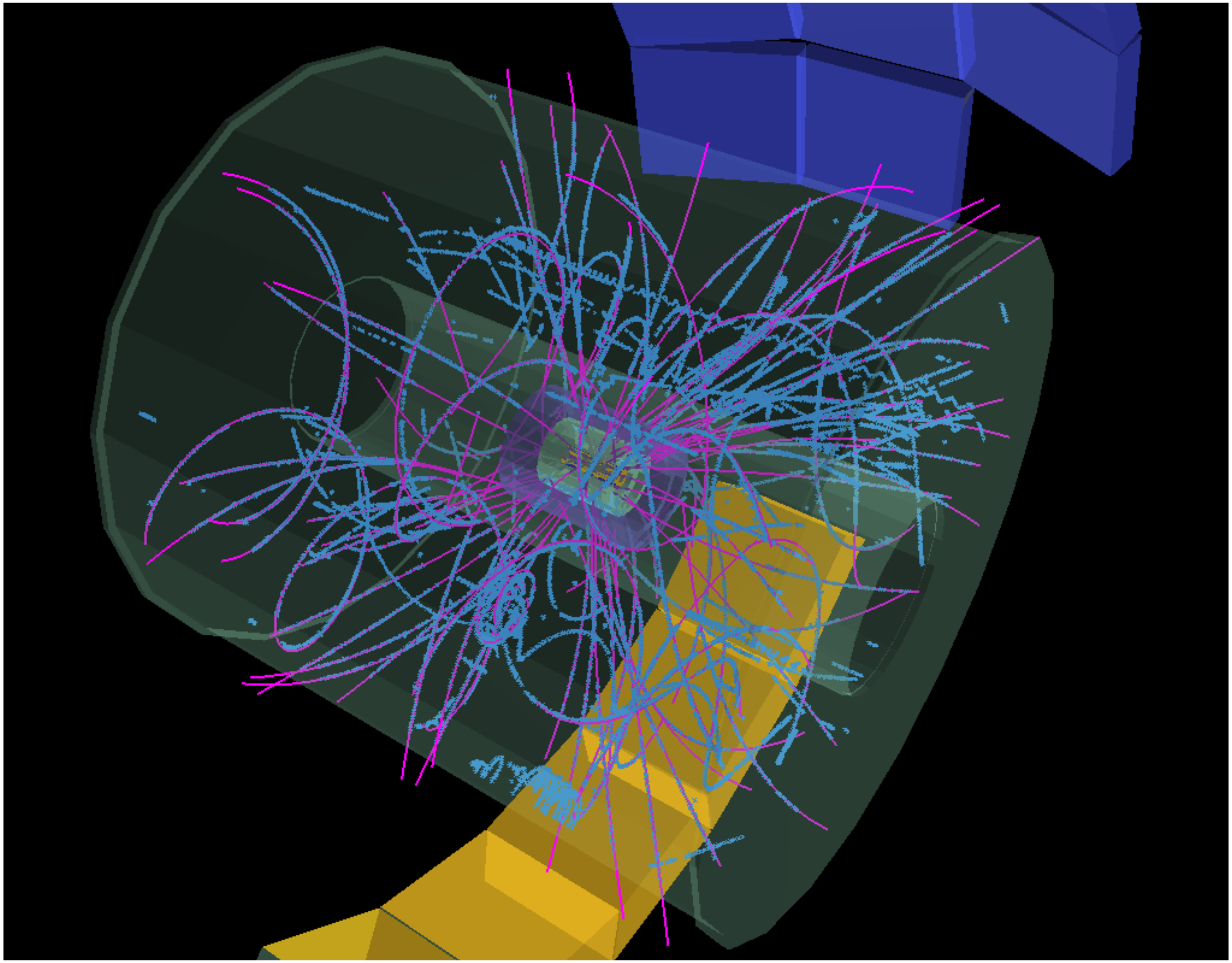

TENUE À HAUT FLUX

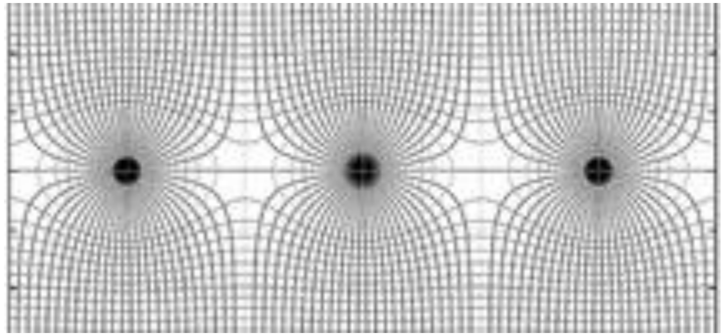

?

DRIFT CHAMBERS (1980):

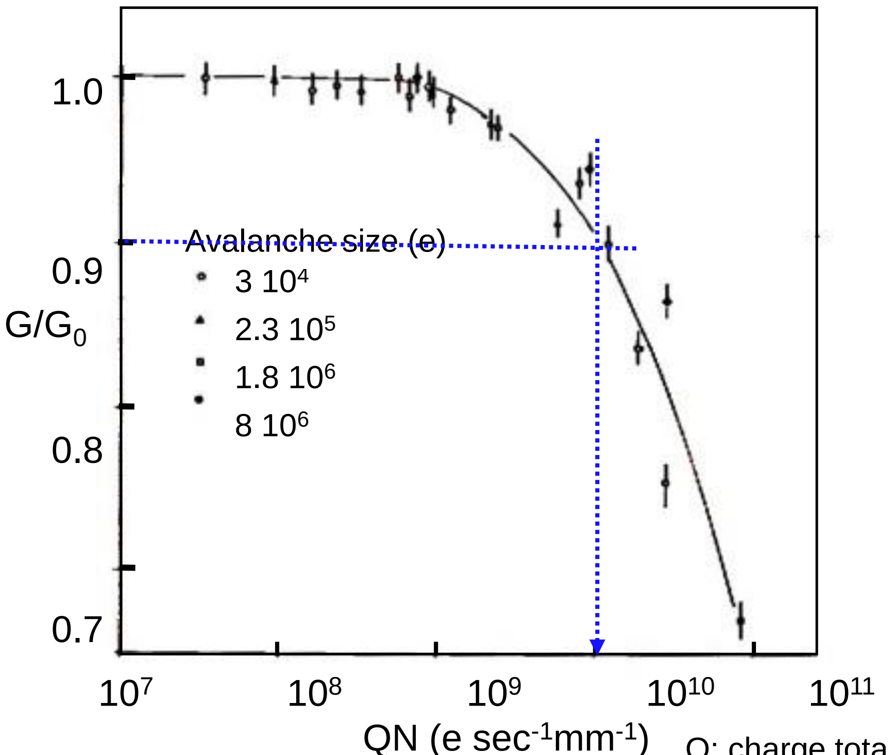

ATLAS MONITORED DRIFT TUBES (2000):

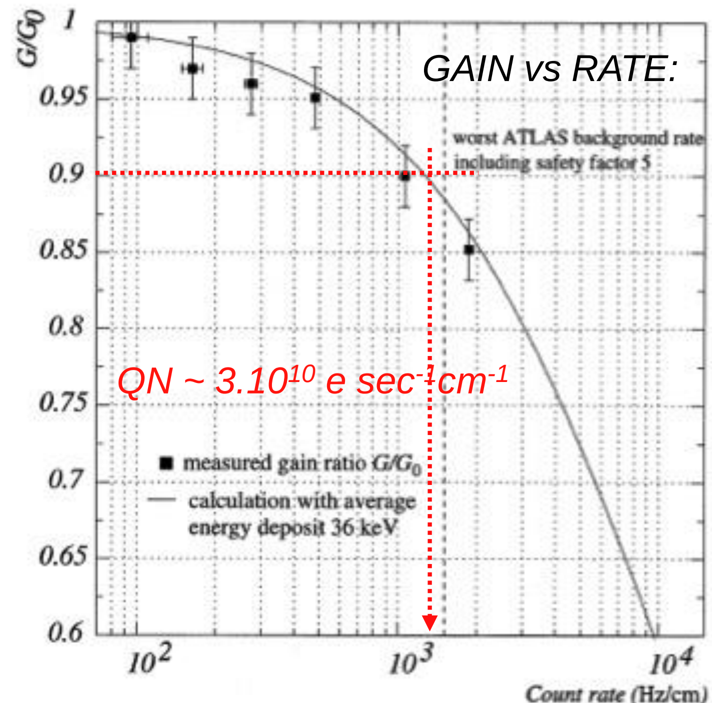

Q: charge totale de l'avalanche
N: flux de particules / longueur de fil

LES MPGDS OU COMMENT CONCENTRER LES LIGNES DE CHAMPS

Électrode de dérive

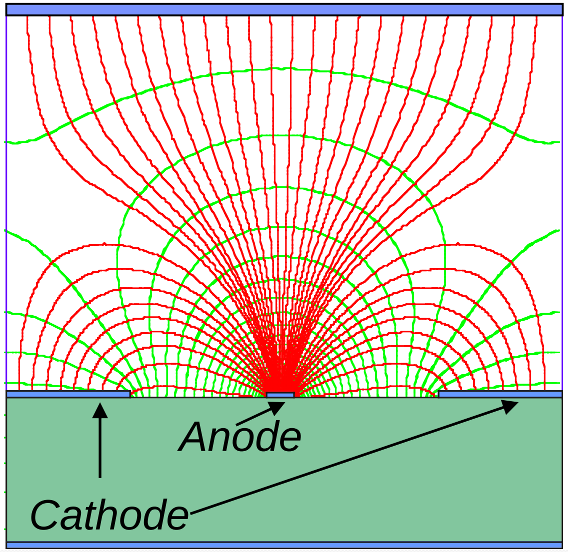

MICRO-PIN ARRAY (MIPA)

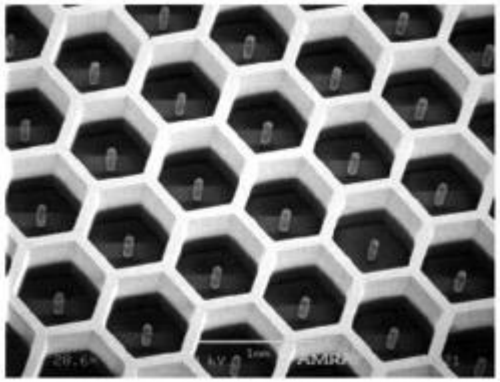

MICRO-GROOVE CHAMBER

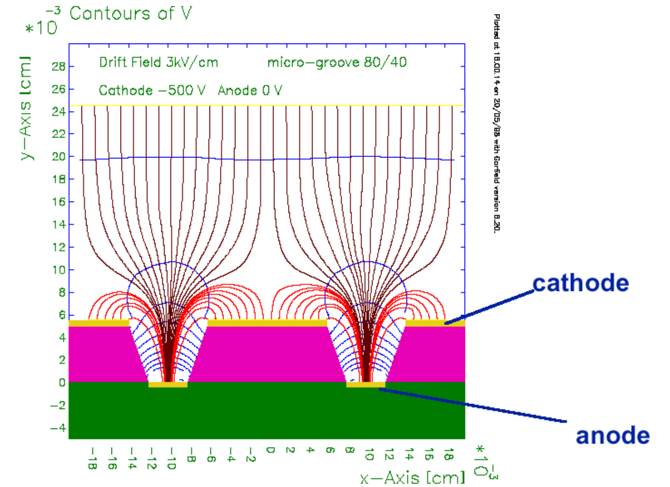

Equipotential and drift lines (with zero diffusion)

MICRO-PIXEL CHAMBER

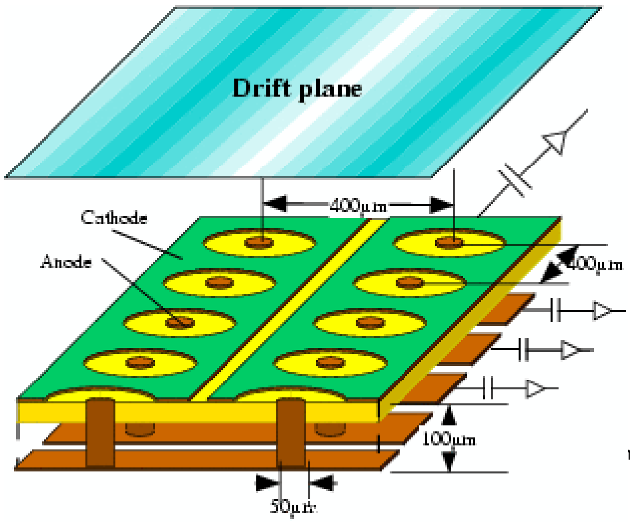

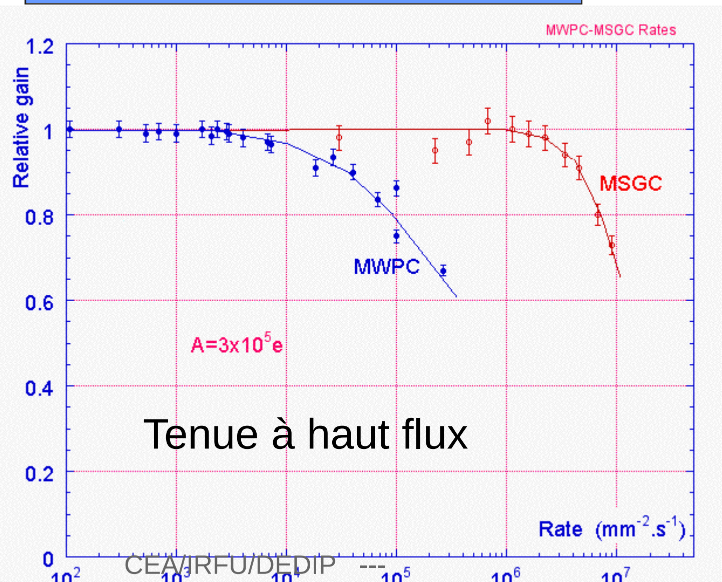

Tenue à haut flux

MICRO-GAP CHAMBER

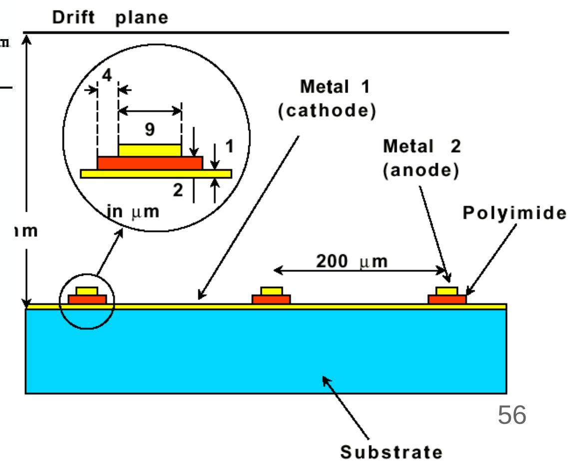

GEM : GASEOUS ELECTRON MULTIPLIER

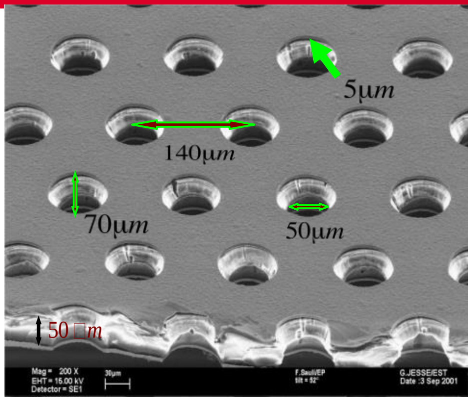

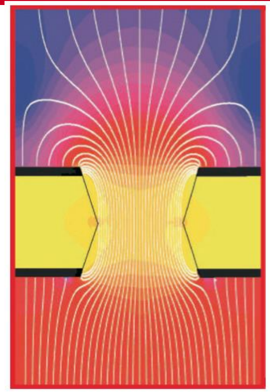

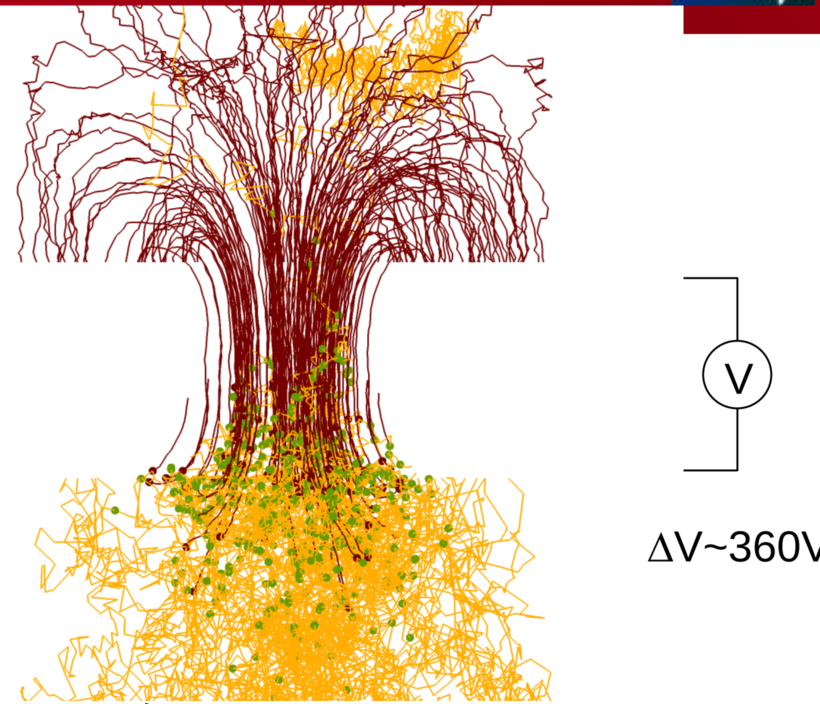

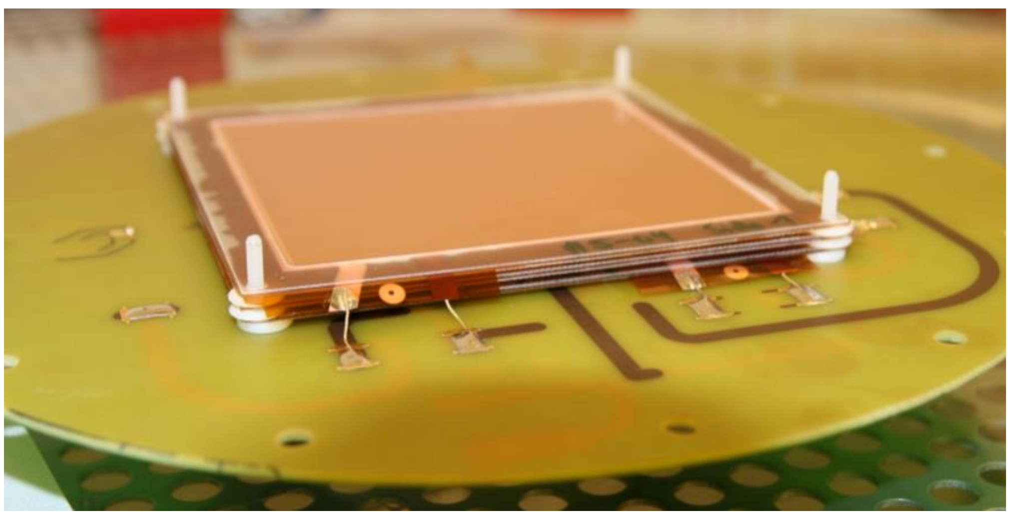

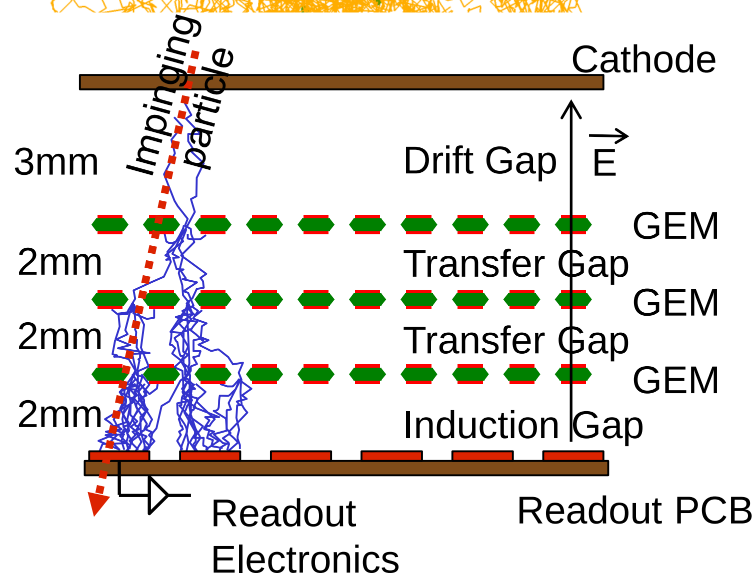

CEA/IRFU/DEDIP --- maxence.vandenbroucke@cea.fr

MICROMEGAS

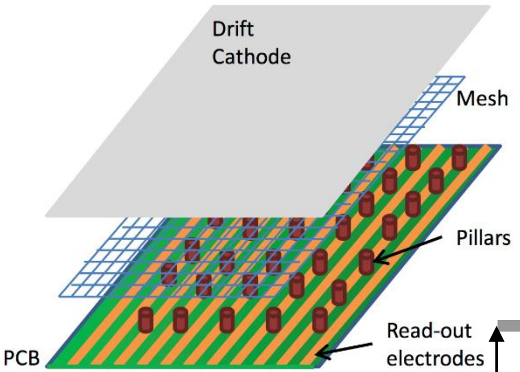
Drift
Cathode
Mesh
Pillars
PCB
Read-out
electrodes

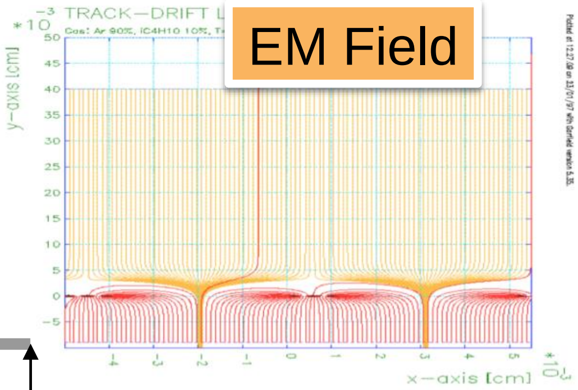
TRACK—DRIFT
y—axis [cm]
x—axis [cm]
EM Field

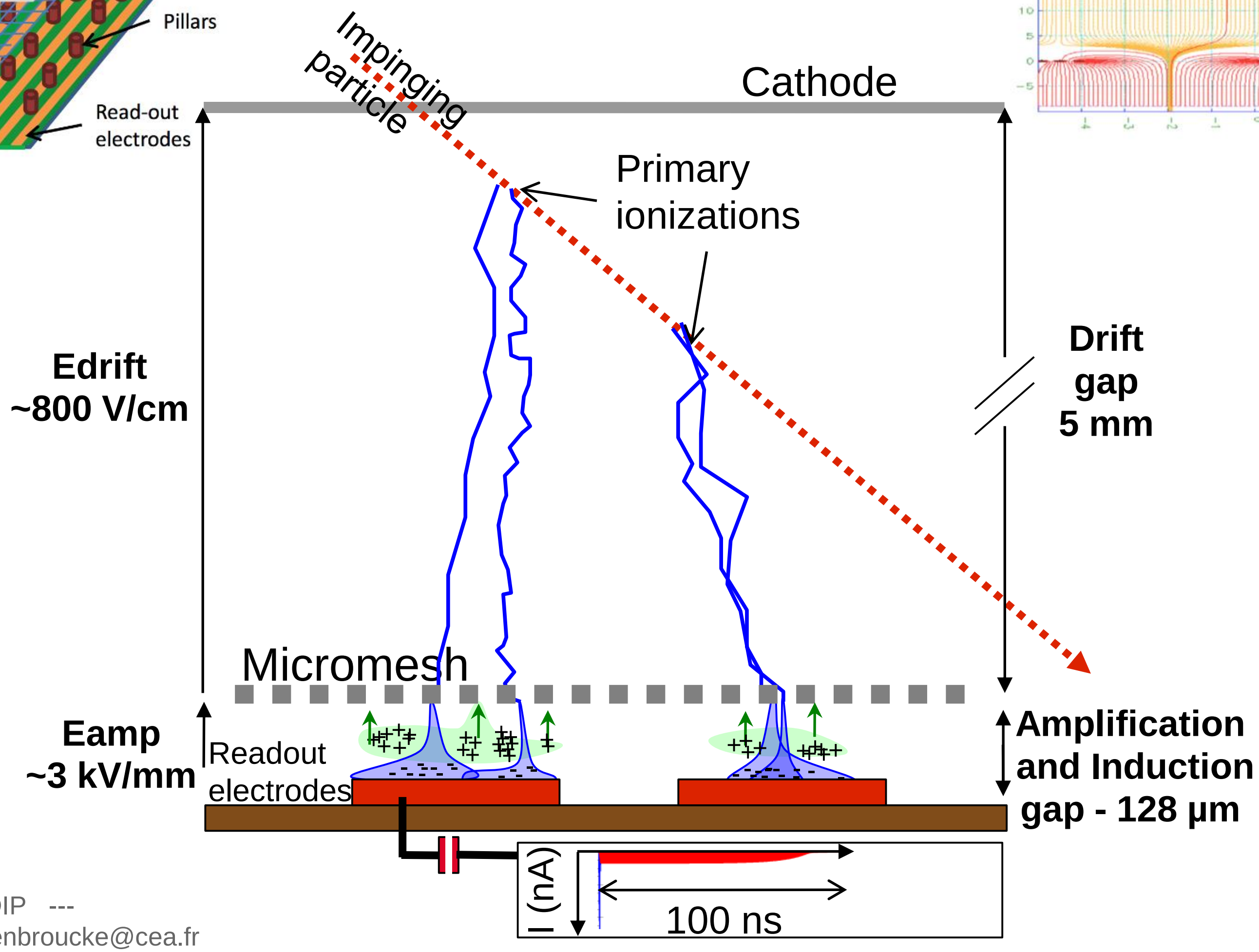
Impinging
particle
Cathode
Primary
ionizations
Edrift
~800 V/cm
Drift
gap
5 mm
Micromesh
Eamp
~3 kV/mm
Readout
electrodes
Amplification
and Induction
gap - 128 µm
I (nA)
100 ns

APPLICATIONS EN PHYSIQUE…

Grands détecteurs pour le système à muons d'ATLAS/HL-LHC

TPC pour l'ILC

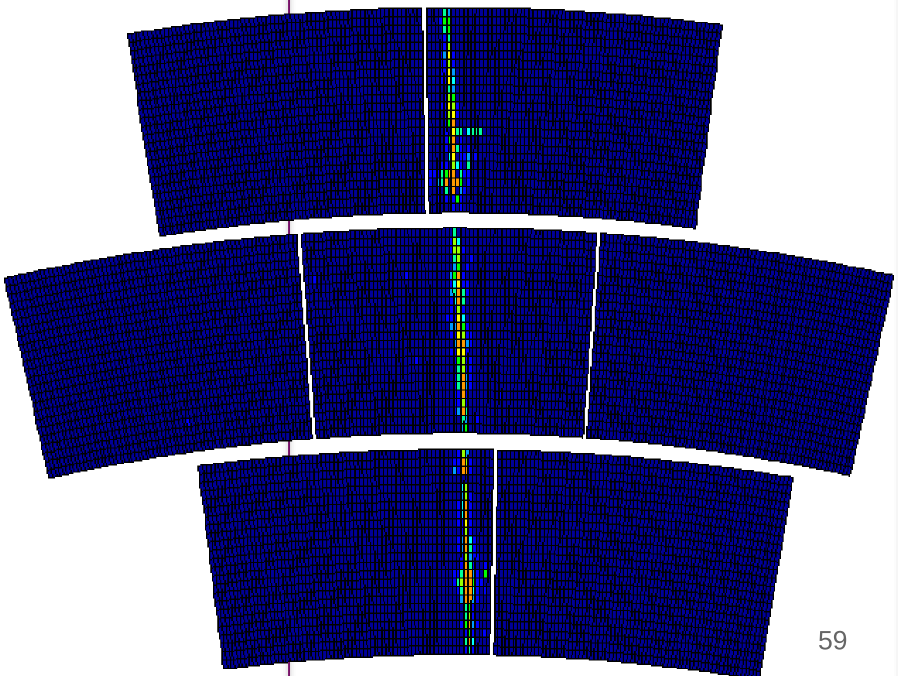

CLAS 12

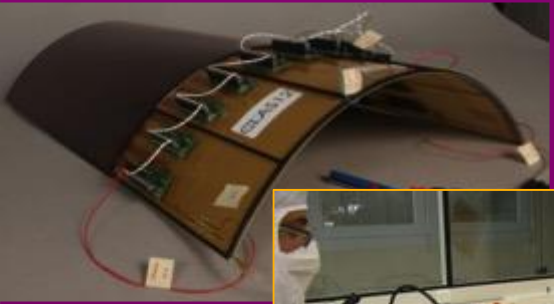

Tuile pour le trajectographe cylindrique

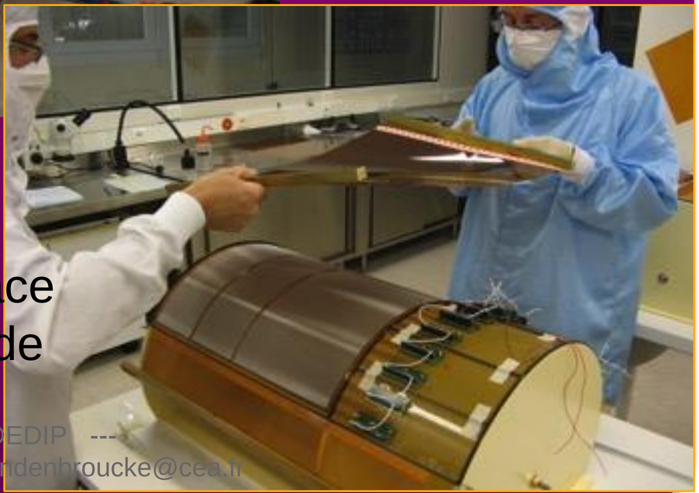

Mise en place de l'électrode de dérive

MUONGRAPHY 2015-2017

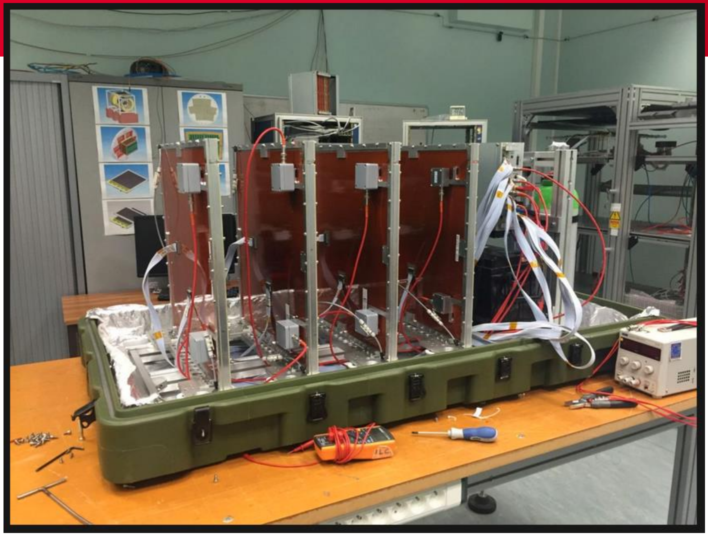

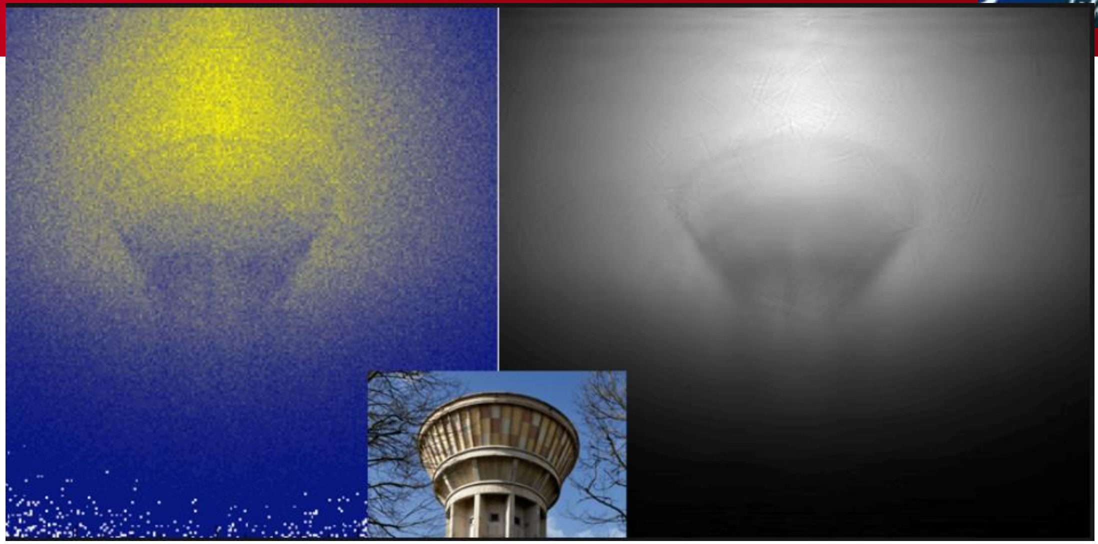

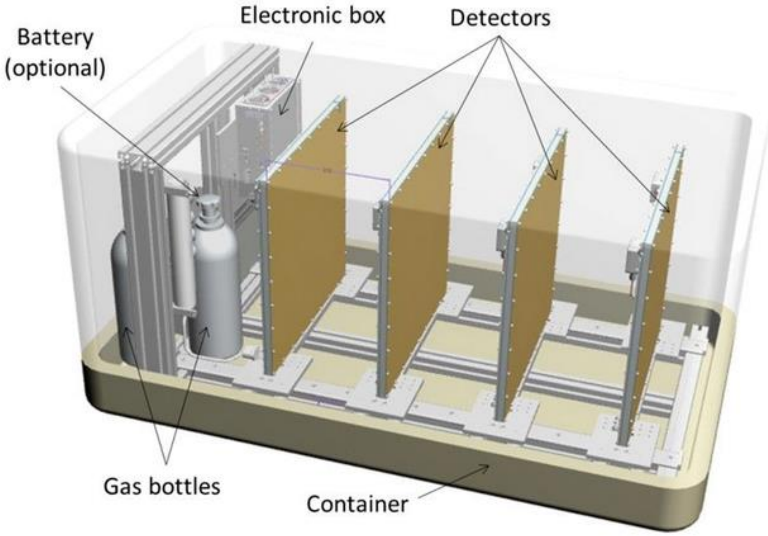

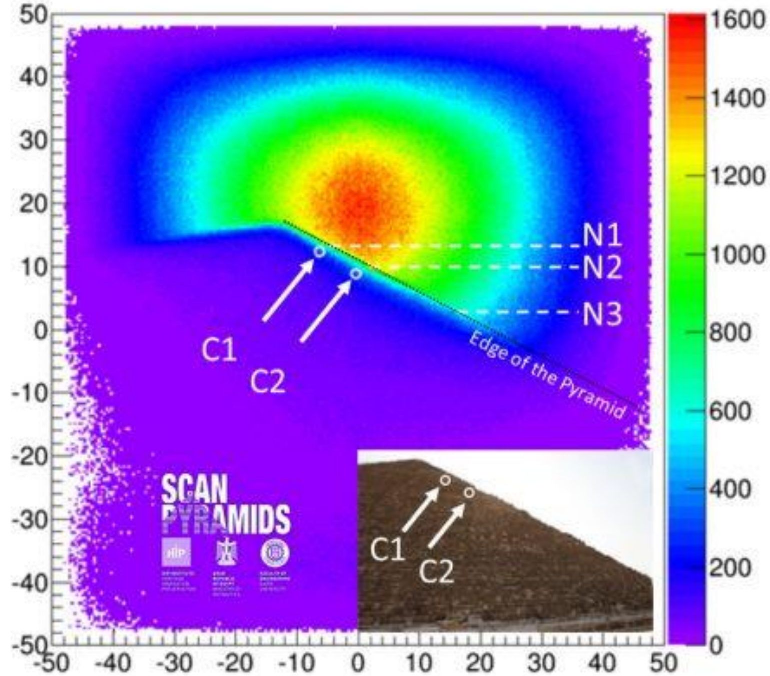

PLAN DES COURS

Cours 1 : Généralités

-Introduction générale sur l'importance de la mesure
-Qu'est-ce qu'une expérience de physique subatomique ?
-Que veut-on observer à propos d'une particule?
-Architecture générale d'une expérience en physique subatomique

Cours 2 : Les détecteurs de particules

- Trajectographie :
  - -Détecteurs Gazeux
  - -Détecteurs au Silicium
- Calorimétrie
- Scintillation

Cours 3 : Exemple d'expériences

- Autour du Neutrino
- Nucléaire et Hadronique
- Rayons Cosmiques
- Antimatière

Cours 3 : Exemple d’expériences

- **Autour du Neutrino**
- **Nucléaire et Hadronique**
- **Rayons Cosmiques**
- **Antimatière**

Oberserver les neutrinos

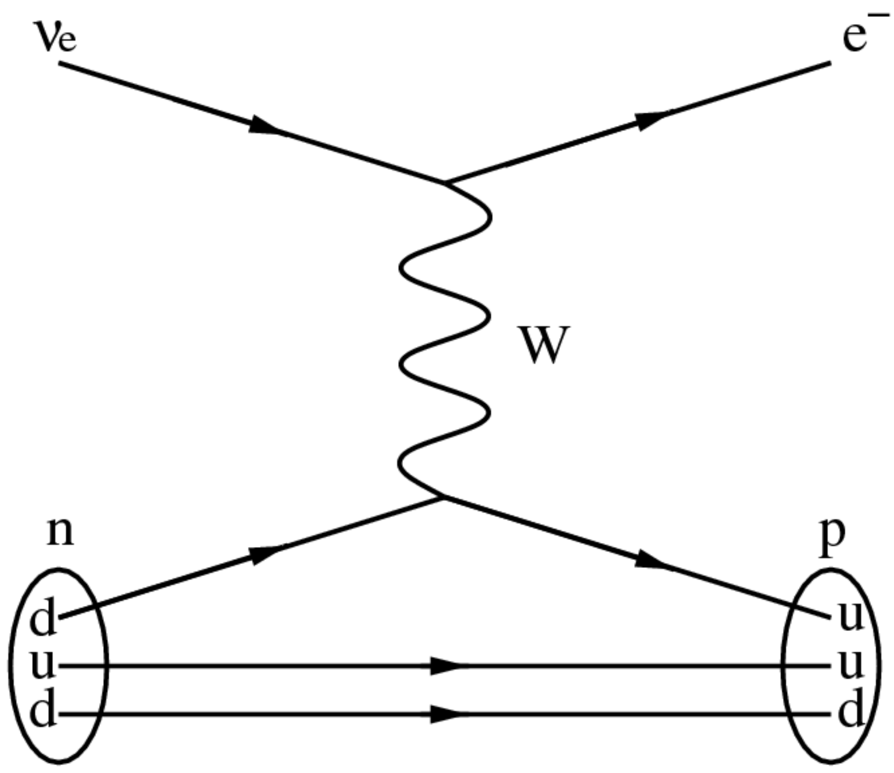

Super Kamiokande

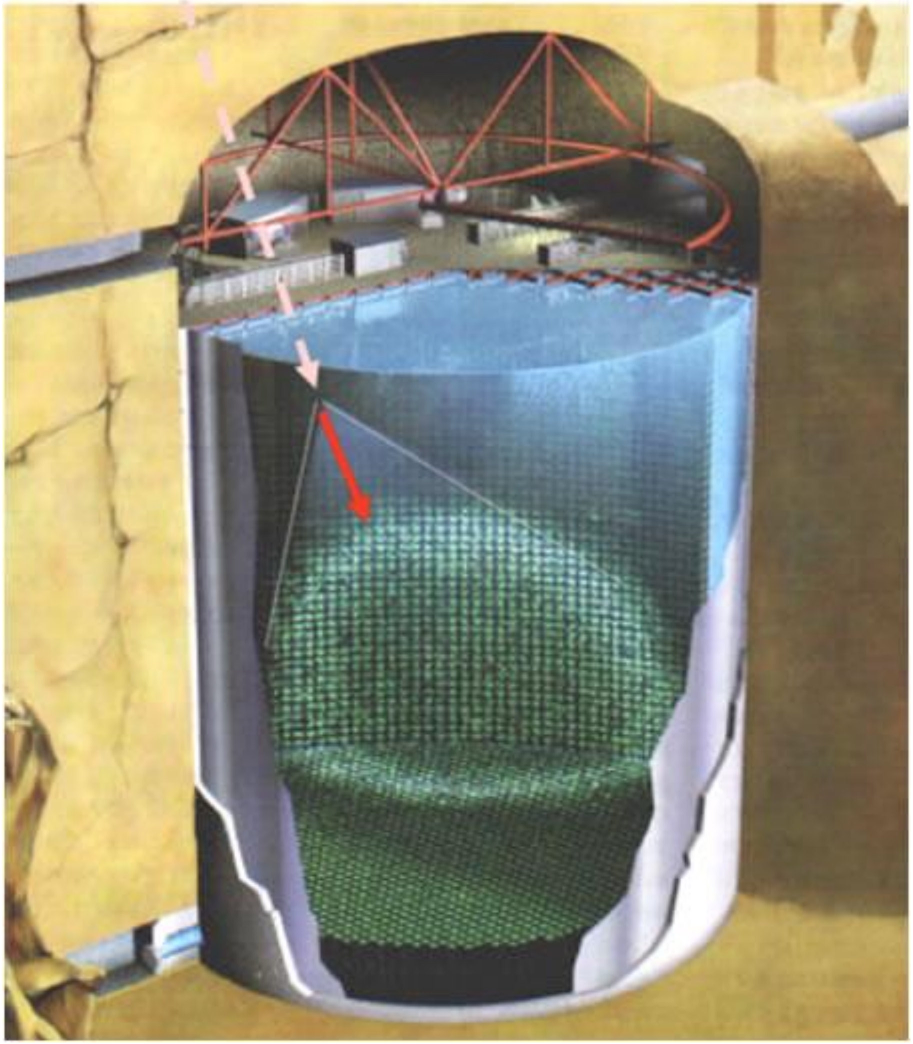

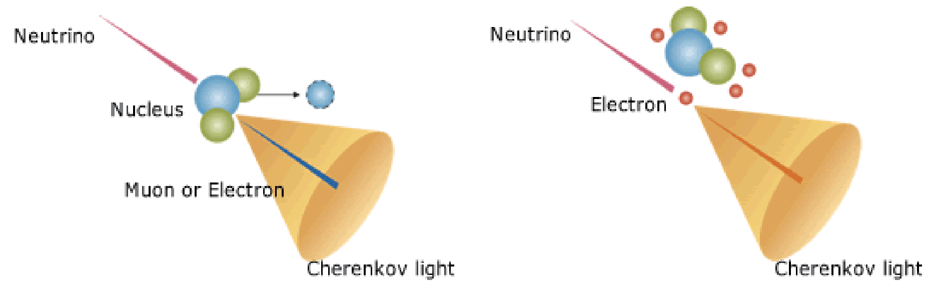

The generated charged particle emits the Cherenkov light.

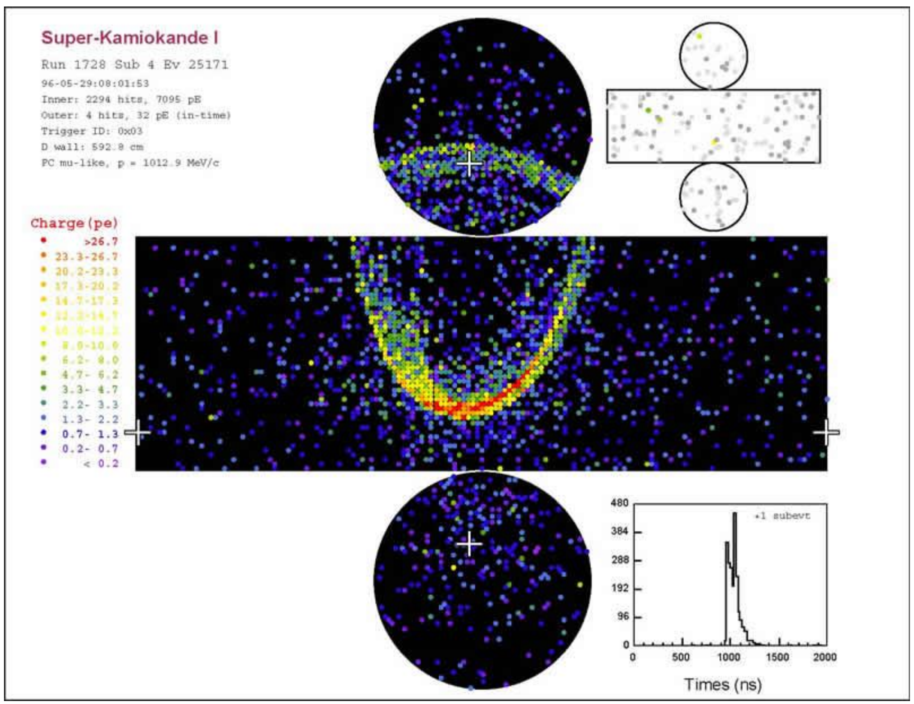

Super Kamiokande

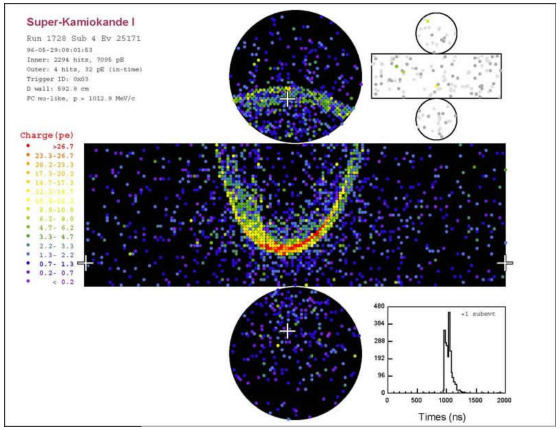

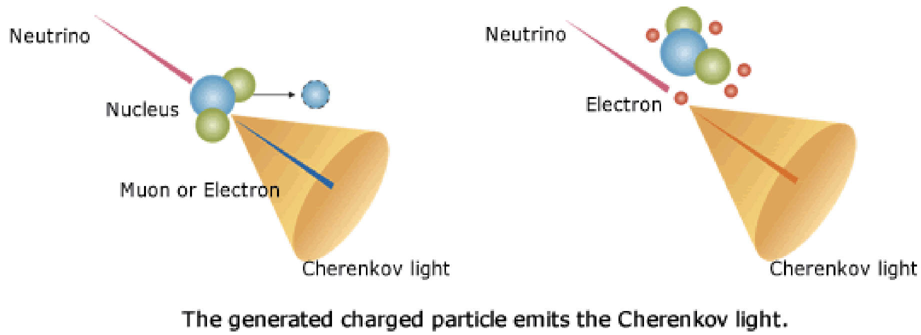

Image du soleil en Neutrino Electronique

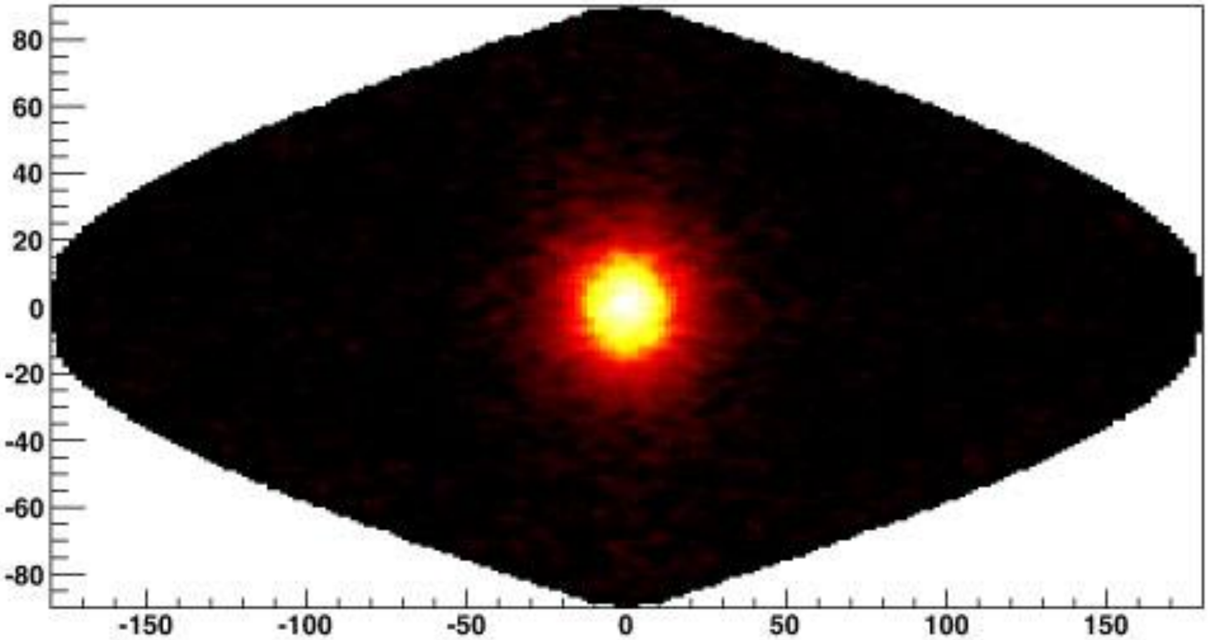

Antares

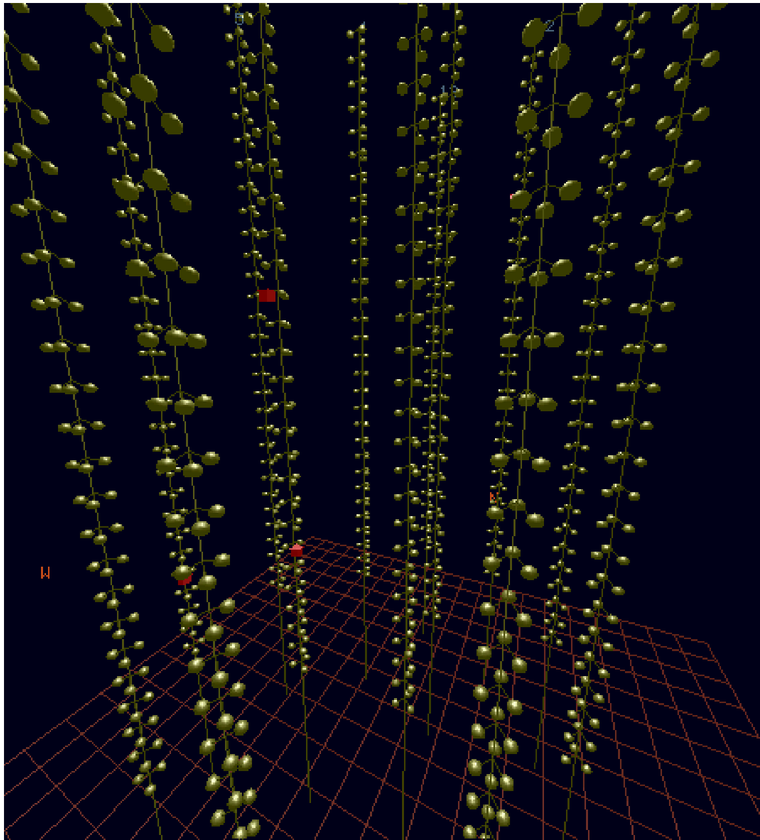

AMANDA

Antarctic **M**uon **A**nd **N**eutrino **D**etector **A**rray

AMANDA

South Pole

AMANDA

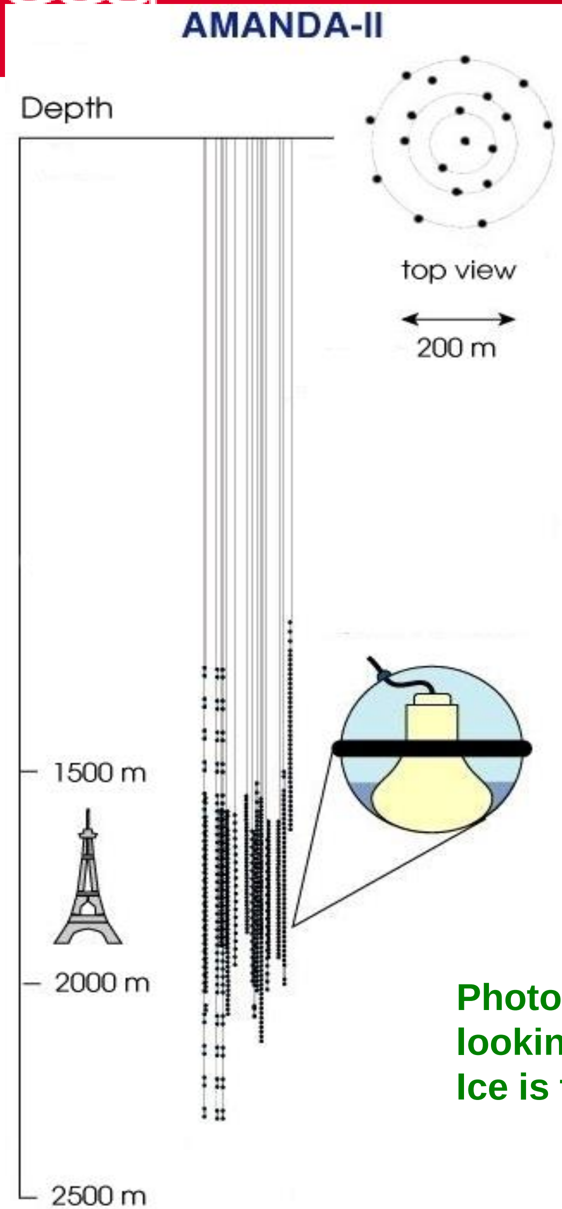

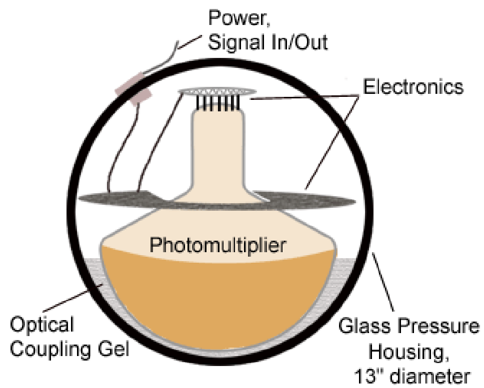

Photomultipliers in the Ice, looking downwards.
Ice is the detecting medium.

AMANDA

Look for upwards going Muons from Neutrino Interactions.
Cherekov light propagating through the ice.

→ **Find neutrino point sources in the universe !**

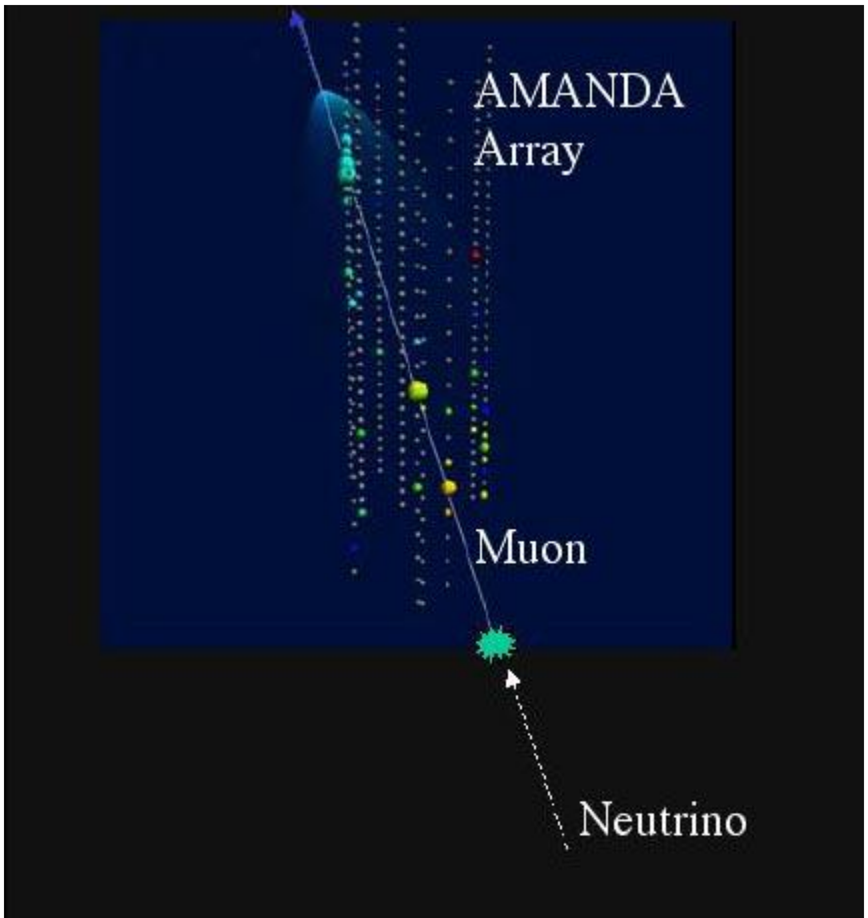

AMANDA – ICE CUBE

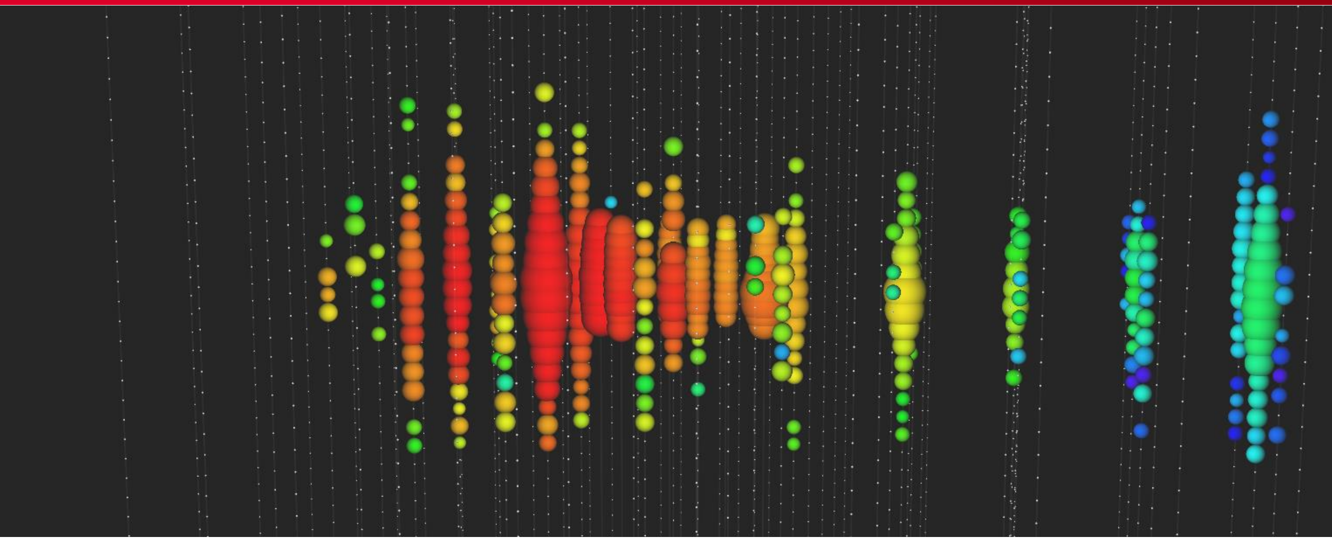

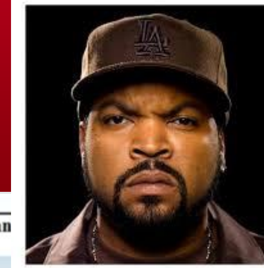

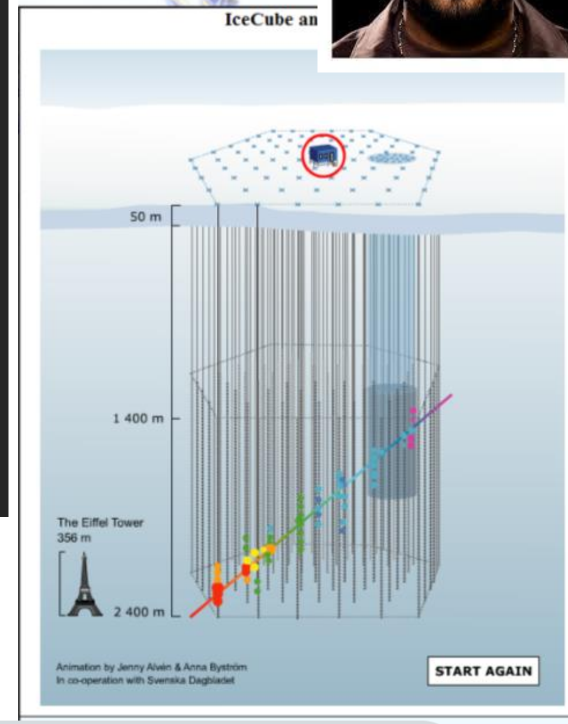

A very high energy neutrino detected in IceCube on November 12, 2010, with an energy of 71 TeV.
Image: IceCube Collaboration

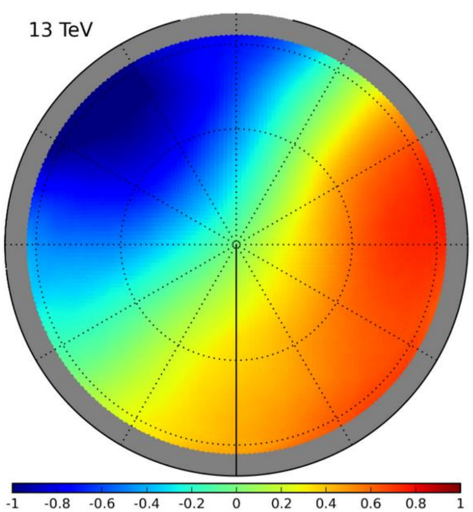

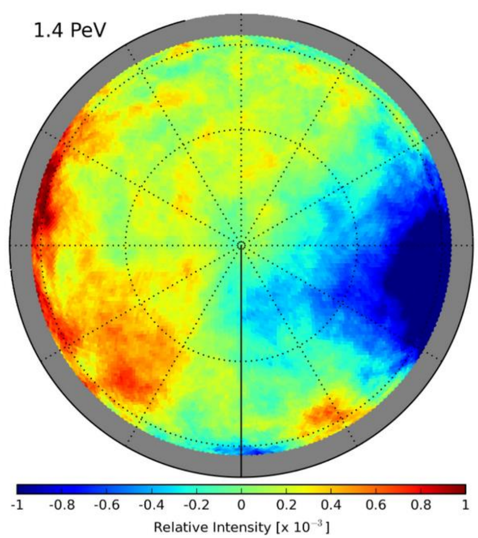

Detector Design

- 1 gigaton of instrumented ice
- 5,160 light sensors, or digital optical modules (DOMs), digitize and time-stamp signals
- 1 square kilometer surface array, IceTop, with 324 DOMs
- 2 nanosecond time resolution
- IceCube Lab (ICL) houses data processing and storage and sends 100 GB of data north by satellite daily

CERN Neutrino Gran Sasso

(CNGS)

CNGS

If neutrinos have mass:

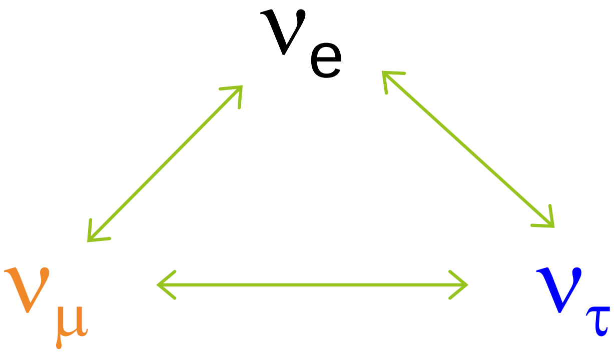

Muon neutrinos produced at CERN.
See if tau neutrinos arrive in Italy.

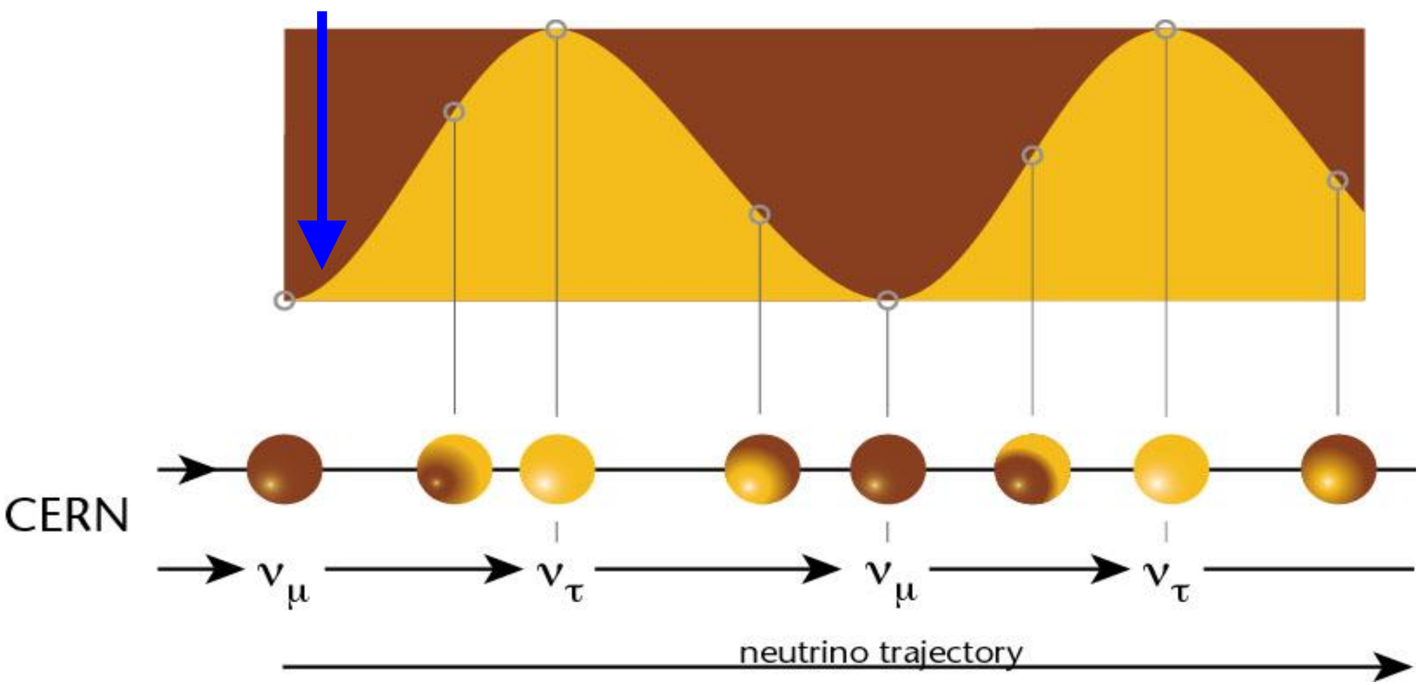

CNGS PROJECT

CNGS (CERN Neutrino Gran Sasso)

- A long base-line neutrino beam facility (732km)
- Send N_M beam produced at CERN
- Detect N_T appearance in OPERA experiment at Gran Sasso

➔ direct proof of ν_μ - ν_τ oscillation (appearance experiment)

CNGS

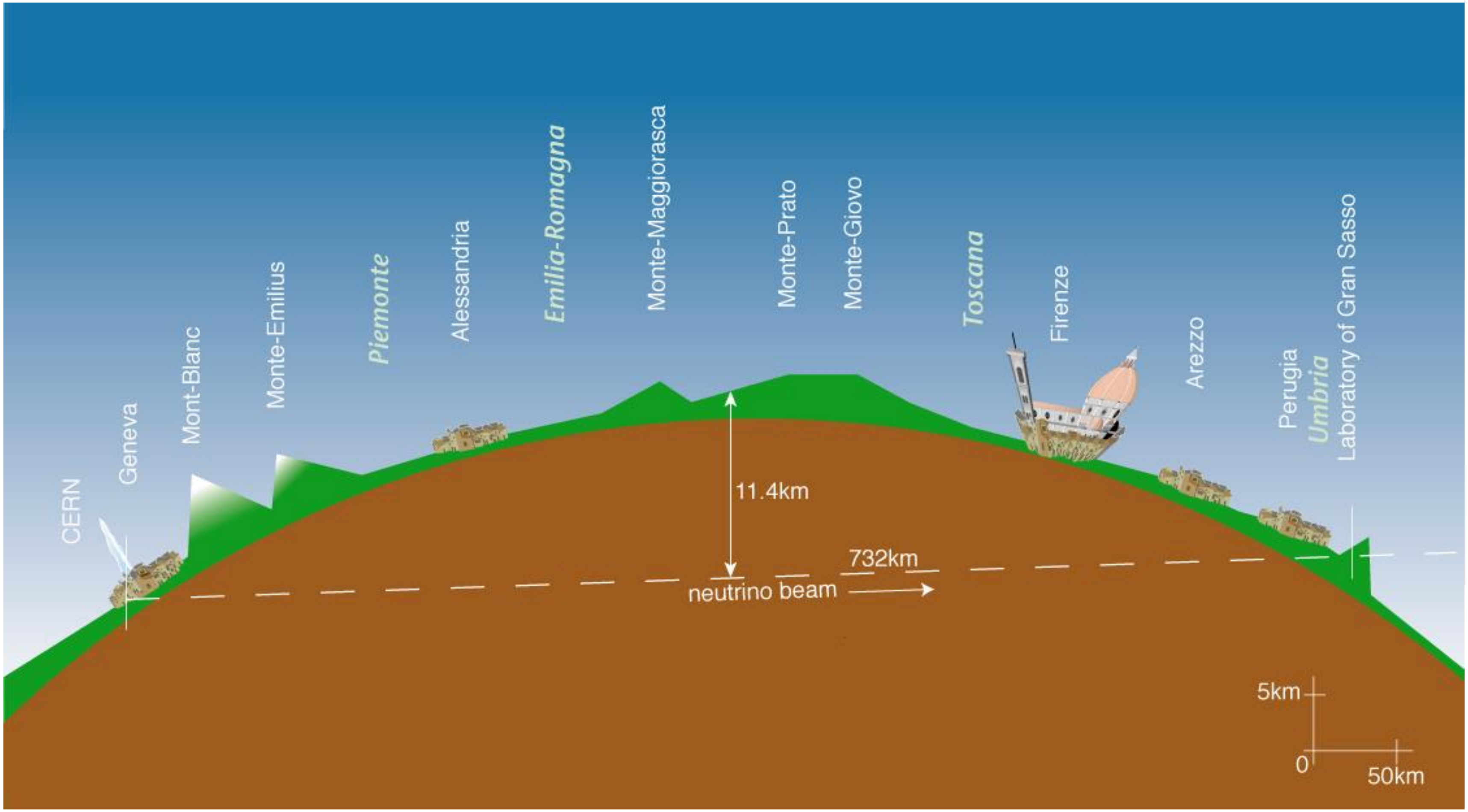

CERN
Geneva
Mont-Blanc
Monte-Emilius
Piemonte
Alessandria
Emilia-Romagna
Monte-Maggiorasca
Monte-Prato
Monte-Giovo
Toscana
Firenze
Arezzo
Perugia
Umbria
Laboratory of Gran Sasso
11.4km
732km
neutrino beam
5km
0
50km

NEUTRINOS AT CNGS: SOME NUMBERS

For 1 day of CNGS operation, we expect:

protons on target	2×10^{17}
pions / kaons at entrance to decay tunnel	3×10^{17}
ν_μ in direction of Gran Sasso	10^{17}
ν_μ in 100 m^2 at Gran Sasso	3×10^{12}

ν_μ events per day in OPERA	$\approx$ 25 per day
ν_τ events (from oscillation)	$\approx$ 2 per year

CNGS LAYOUT

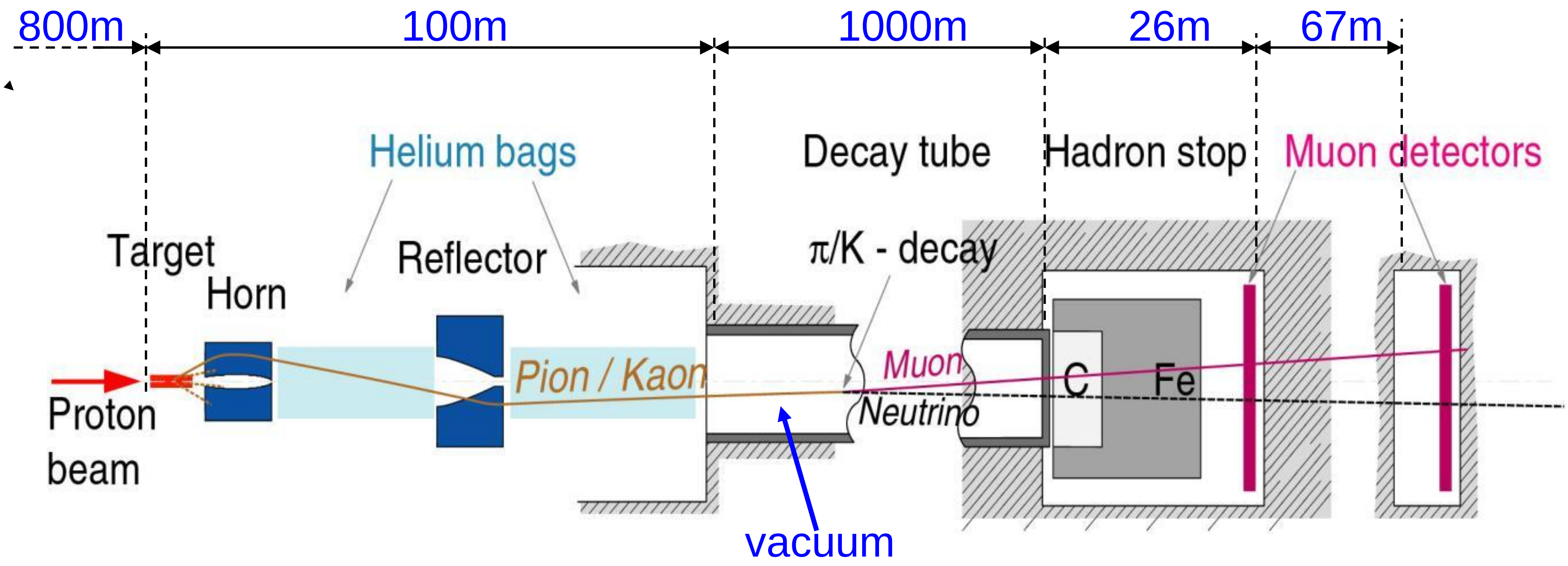

$p + C \rightarrow$ (interactions) $\rightarrow \pi^+, K^+ \rightarrow$ (decay in flight) $\rightarrow \mu^+ + \nu_\mu$

CNGS

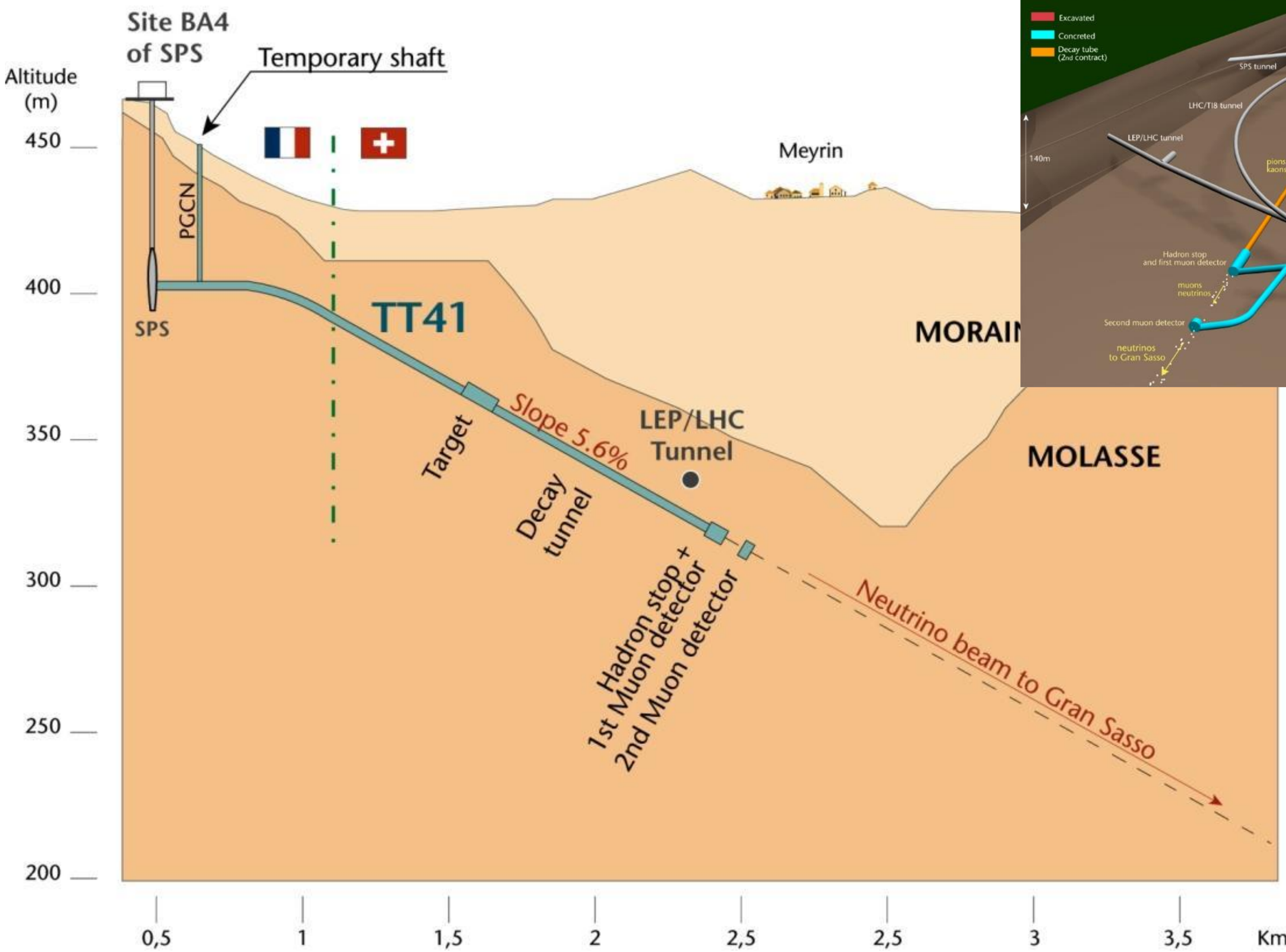

Site BA4
of SPS
Temporary shaft
Altitude
(m)
450
400
350
300
250
200
PGCN
SPS
TT41
Meyrin
MORAI
MOLASSE
Target
Slope 5.6%
LEP/LHC
Tunnel
Decay
tunnel
Hadron stop +
1st Muon detector
2nd Muon detector
Neutrino beam to Gran Sasso
0,5
1
1,5
2
2,5
2,5
3
3,5
Km

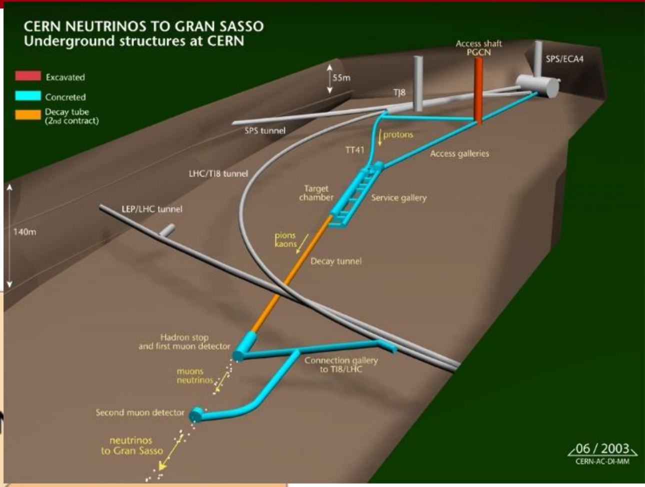

CERN NEUTRINOS TO GRAN SASSO
Underground structures at CERN
Excavated
Concreted
Decay tube
(2nd contract)
55m
140m
Access shaft
PGCN
SPS/ECA4
TJ8
SPS tunnel
protons
TT41
Access galleries
LHC/TI8 tunnel
LEP/LHC tunnel
Target
chamber
Service gallery
pions
kaons
Decay tunnel
Hadron stop
and first muon detector
Connection gallery
to TI8/LHC
muons
neutrinos
Second muon detector
neutrinos
to Gran Sasso
06 / 2003
CERN-AC-DI-MM

Opera Experiment at Gran Sasso

$$\nu_\tau N \rightarrow \tau^- X$$

$$\tau^- \rightarrow \mu^- \nu_\mu \bar{\nu}_\tau \quad with \quad BR = 17.36 \pm 0.05\% \tag{1}$$

$$\tau^- \rightarrow e^- \nu_e \bar{\nu}_\tau \quad with \quad BR = 17.85 \pm 0.05\% \tag{2}$$

$$\tau^- \rightarrow h^- (n\pi^0) \bar{\nu}_\tau \quad with \quad BR = 49.52 \pm 0.07\% \tag{3}$$

$$\tau^- \rightarrow 2h^- h^+ (n\pi^0) \bar{\nu}_\tau \quad with \quad BR = 15.19 \pm 0.08\%. \tag{4}$$

https://arxiv.org/pdf/1305.2513.pdf

Basic unit: brick

56 Pb sheets + 56 photographic films (emulsion sheets)

Lead plates: massive target
Emulsions: micrometric precision

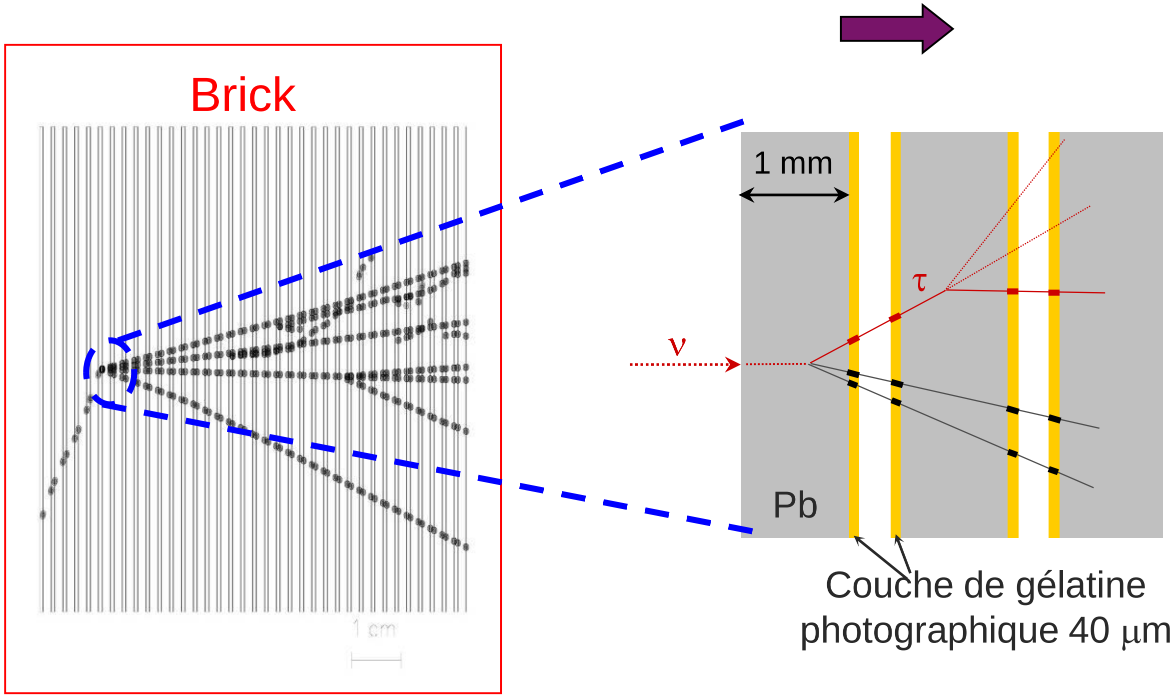

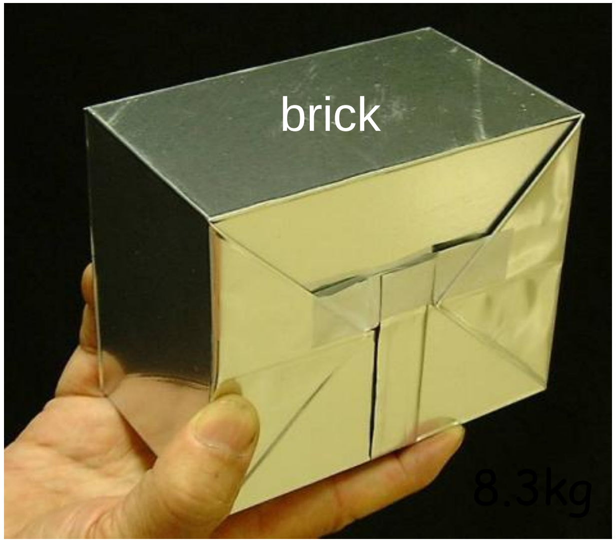

10.2 x 12.7 x 7.5 cm^3

Opera Experiment at Gran Sasso

31 target planes / supermodule

In total: 206336 bricks, 1766 tons

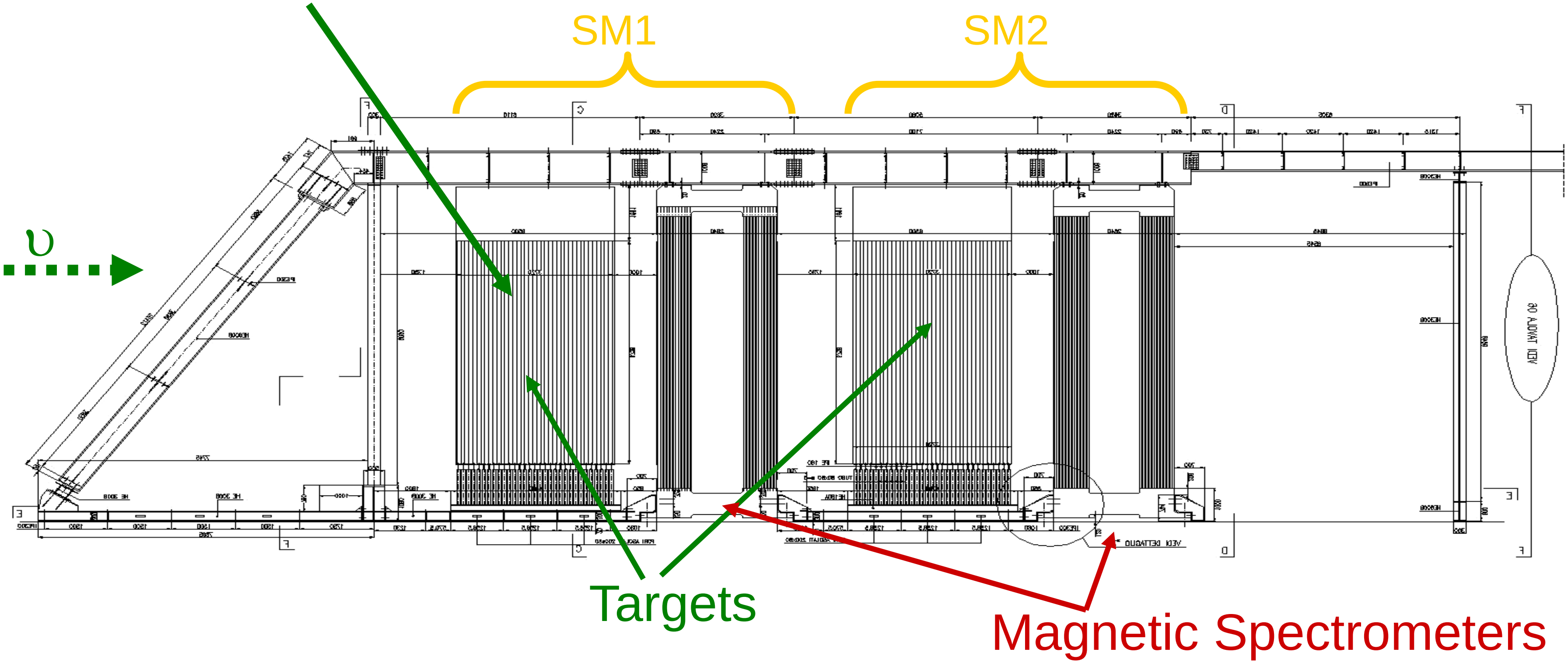

First observation of CNGS beam neutrinos : August 18th, 2006

Opera Experiment at Gran Sasso

Second Super-module

Scintillator planes 5900 m^2

8064 7m long drift tubes

Details of the first spectrometer

3050 m^2 Resistive Plate Counters

2000 tons of iron for the two magnets

Opera Experiment at Gran Sasso

The Brick Manipulator System (BMS) prototype:
a lot of fun for children and adults !

Tests with the prototype wall

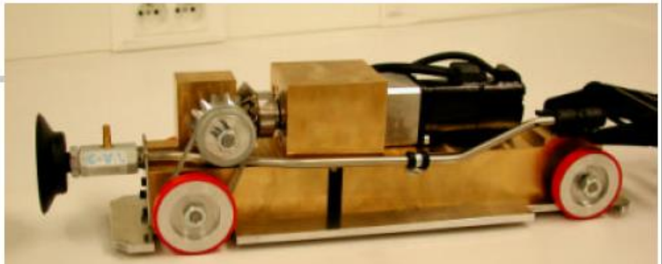

The robotised "Ferrari" for insertion/extraction of bricks with vacuum grip by Venturi valve

"Carousel" brick dispensing and storage system

Physique Hadronique

COMPASS et CLAS12

COMPASS at CERN

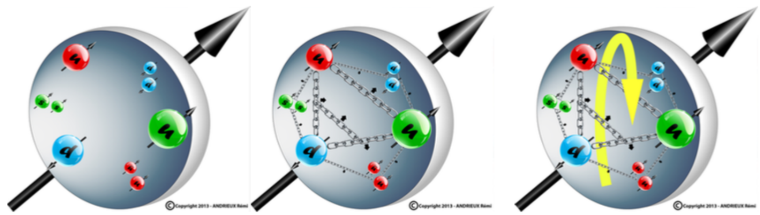

Différentes contributions

$$\frac{1}{2} = \underbrace{\frac{1}{2}(\Delta u + \Delta d + \Delta s)} + \underbrace{\Delta G} + \underbrace{L_g + L_q}$$

Spin des quarks
$\Delta\Sigma \sim 0.3$

Spin des gluons
$|\Delta G| < 0.5$

Moments orbitaux
$L_{q+g} = ??$

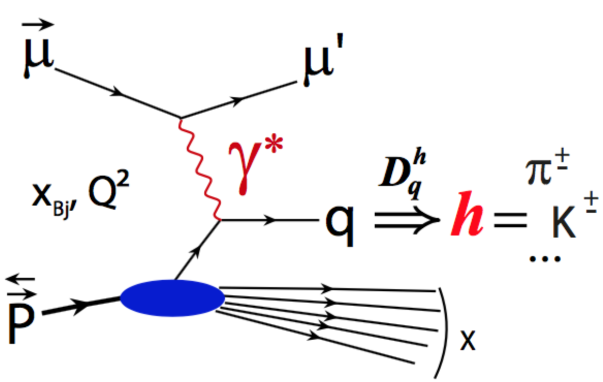

Section efficace DIS

$$\frac{d^2\sigma}{dxdQ^2} = \underbrace{c_1\, F_1(x,Q^2) + c_2\, F_2(x,Q^2)}_{\textit{fonctions de structure non-polarisées}} + \underbrace{c_3^{s,S}\, g_1(x,Q^2) + c_4^{s,S}\, g_2(x,Q^2)}_{\textit{fonctions de structure polarisées}}$$

COMPASS at CERN

- Faisceau polarisé de μ^+ du SPS
  - $1 \cdot 10^8 / 2 \cdot 10^8$ μ par déversement de ~ 10 s
  - 200 GeV/160 GeV
  - $P_\mu = 80\%$

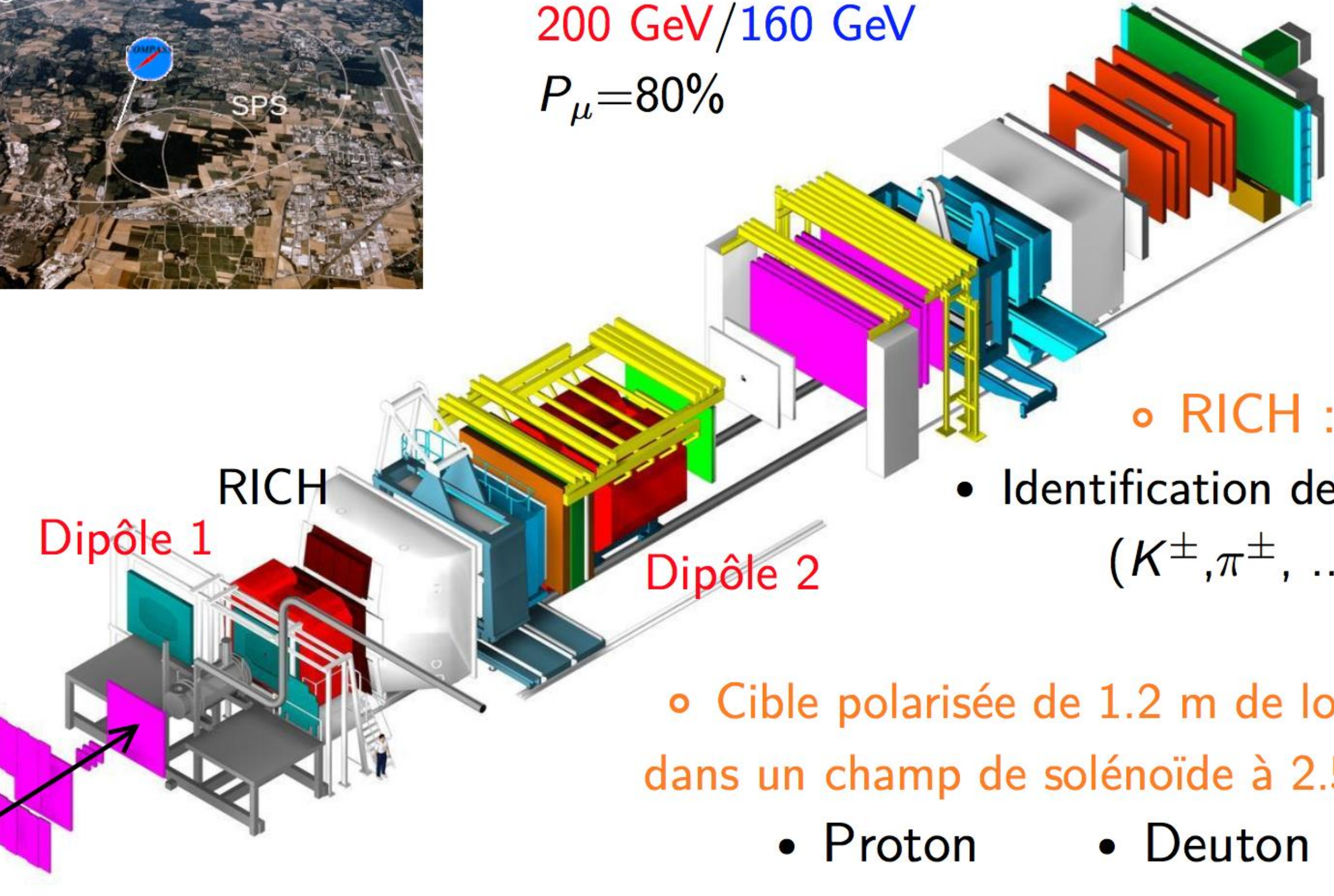

- RICH :
  - Identification des hadrons ($K^\pm$, $\pi^\pm$, ...)

- Cible polarisée de 1.2 m de long dans un champ de solénoïde à 2.5 T
  - Proton
  - Deuton

Diffusion Compton profondément virtuelle (DVCS)

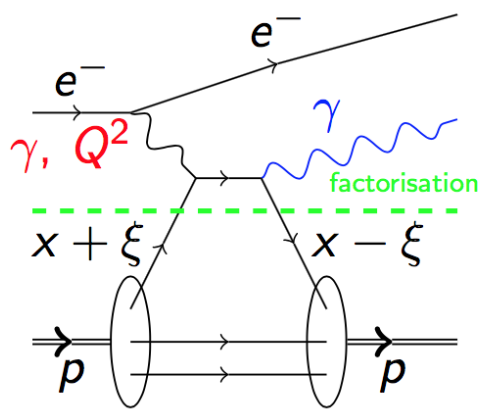

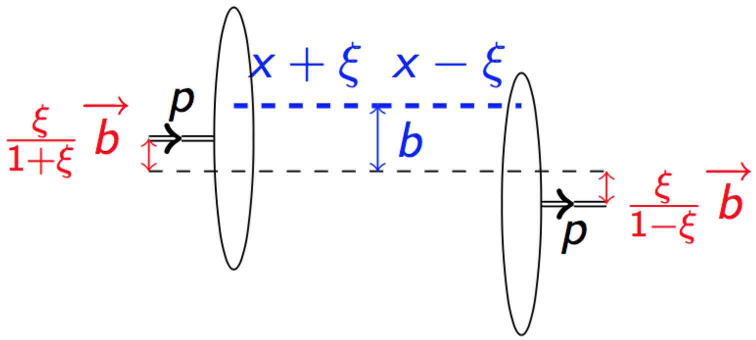

Vers une visualisation en 3d du nucléon !

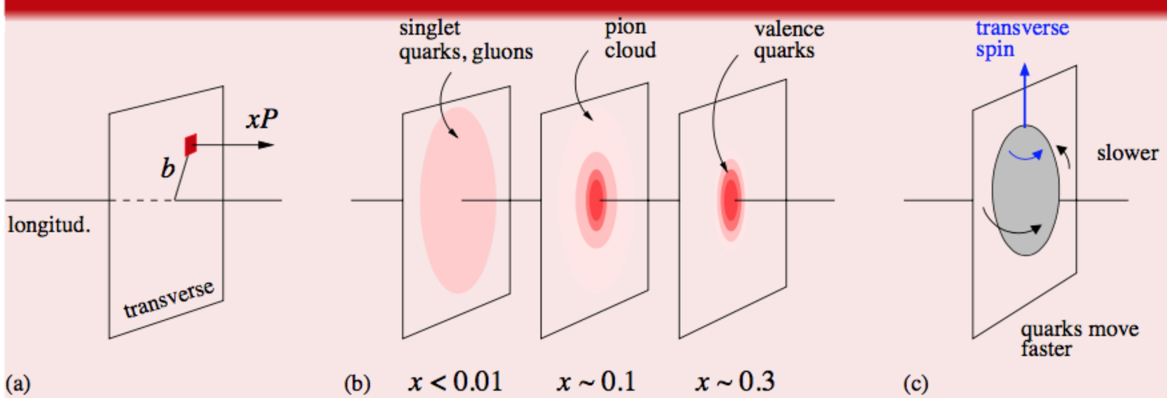

C. Weiss, AIP Conf. Proc. 1149, 150 (2009)

CLAS12 at Jefferson Lab

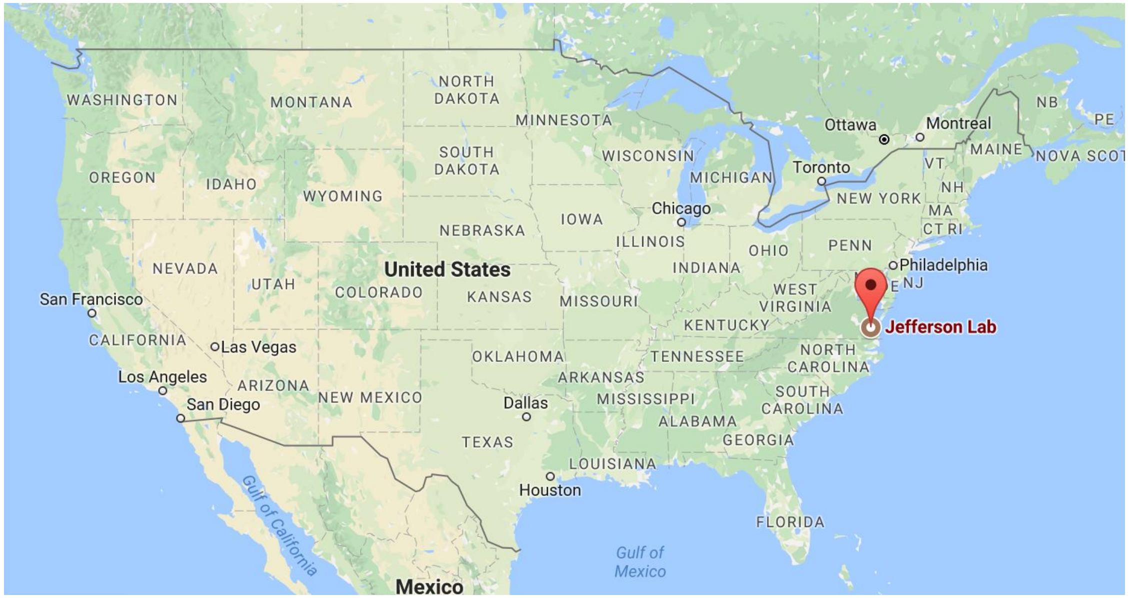

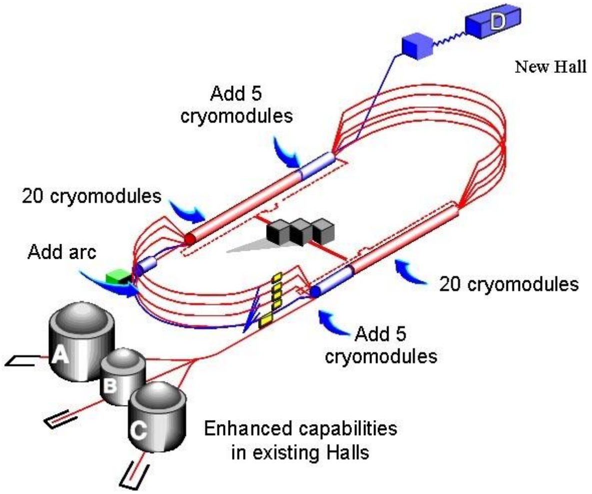

CLAS12 at Jefferson Lab

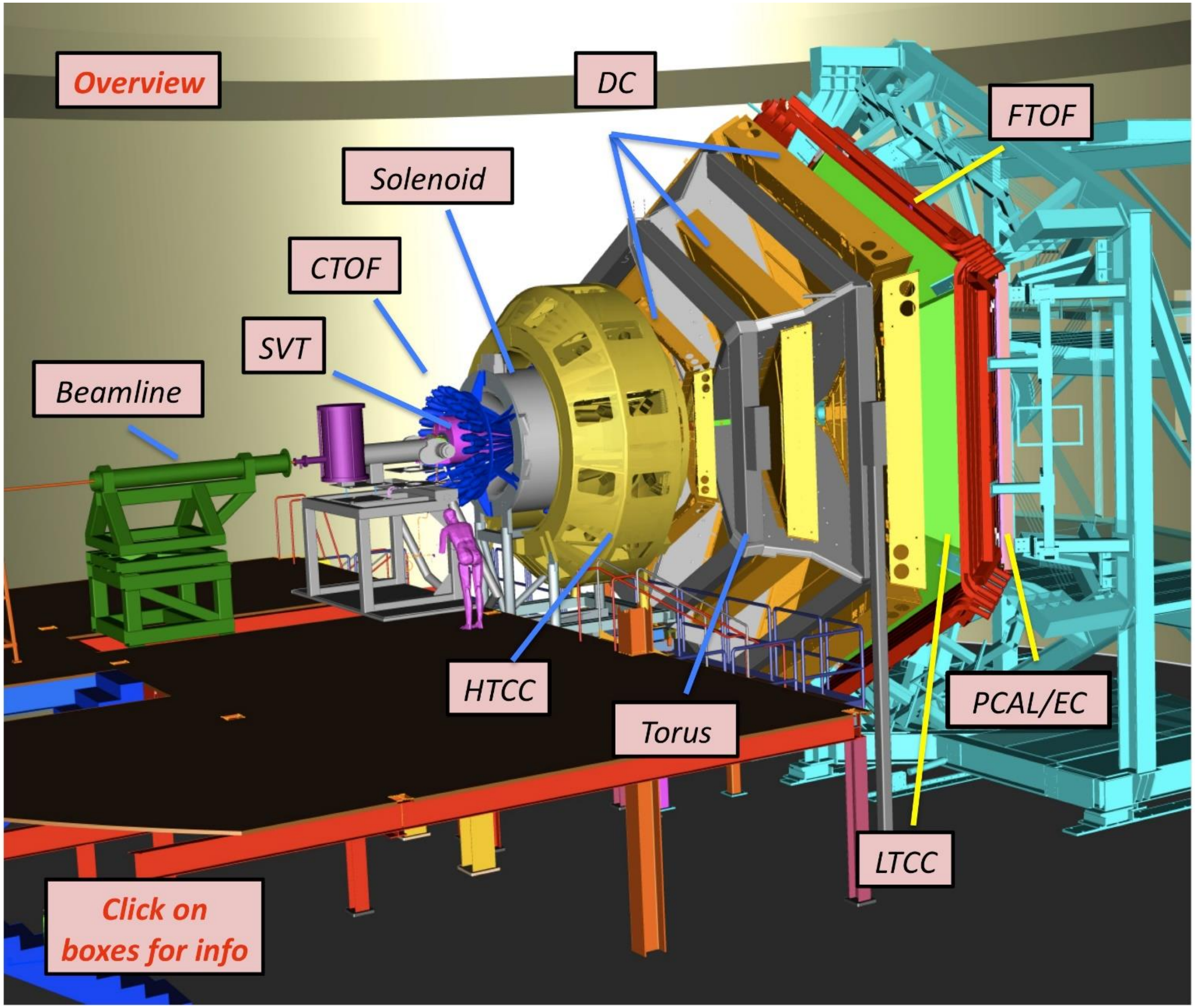

CLAS12 at Jefferson Lab

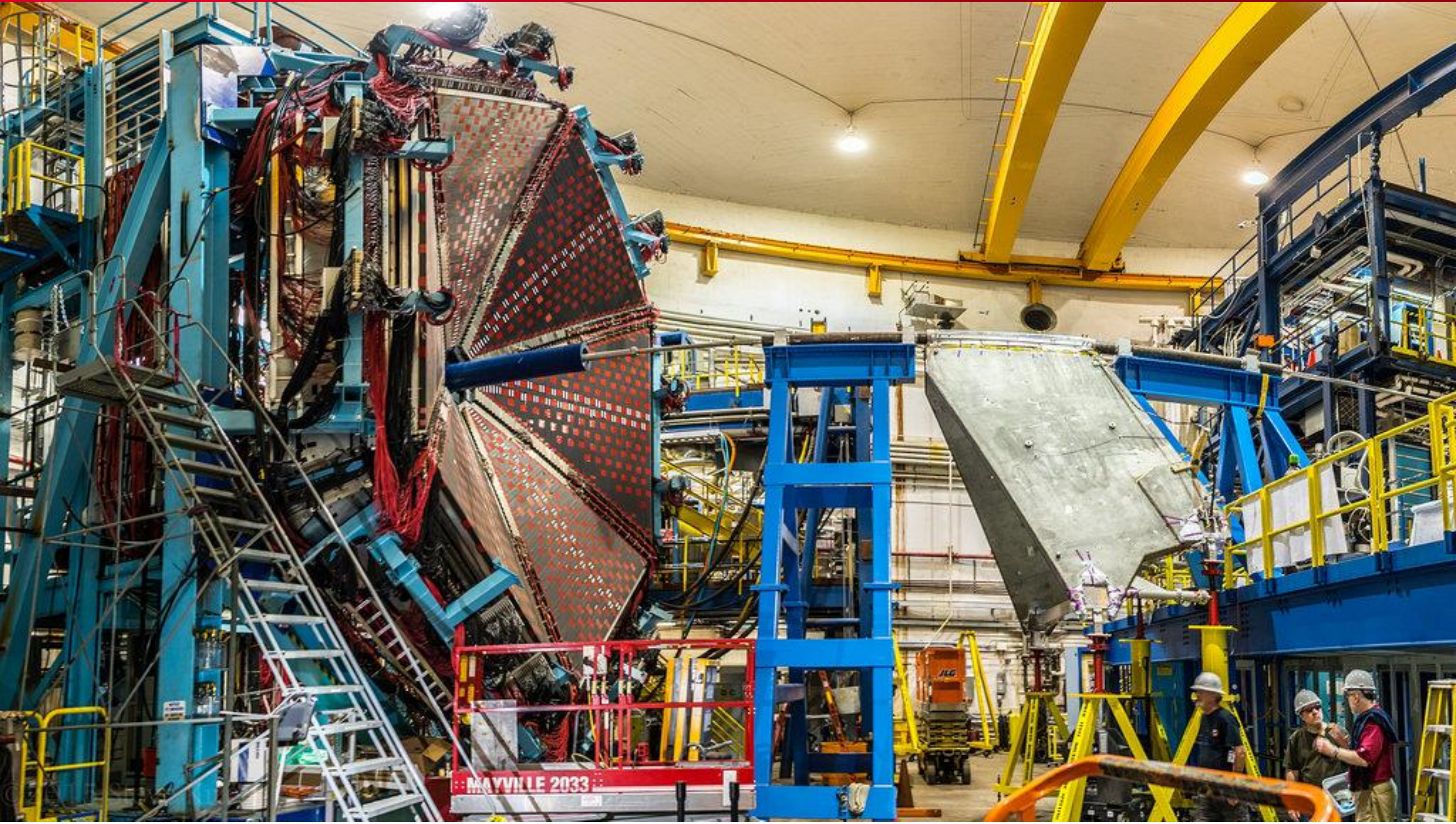

CLAS12 – Central Tracker

CLAS12 - THE MICROMEGAS VERTEX TRACKER

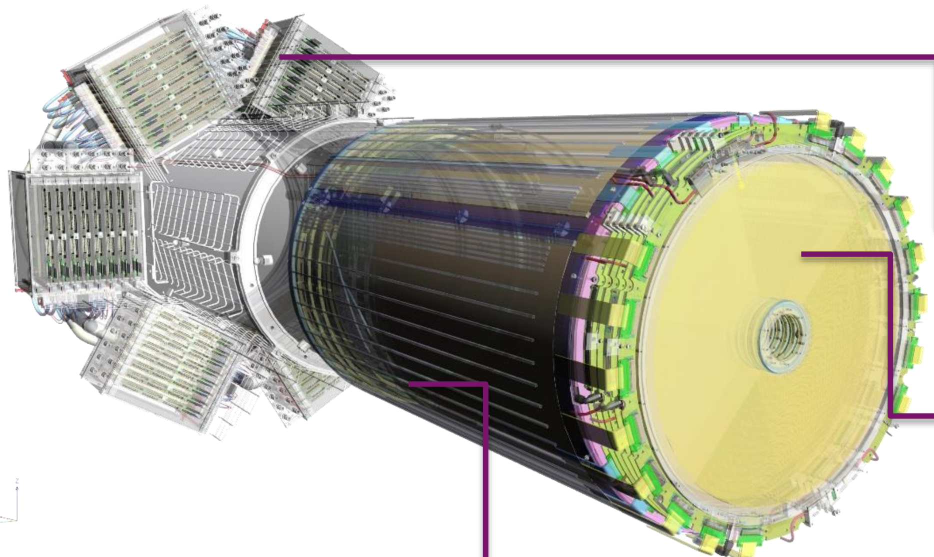

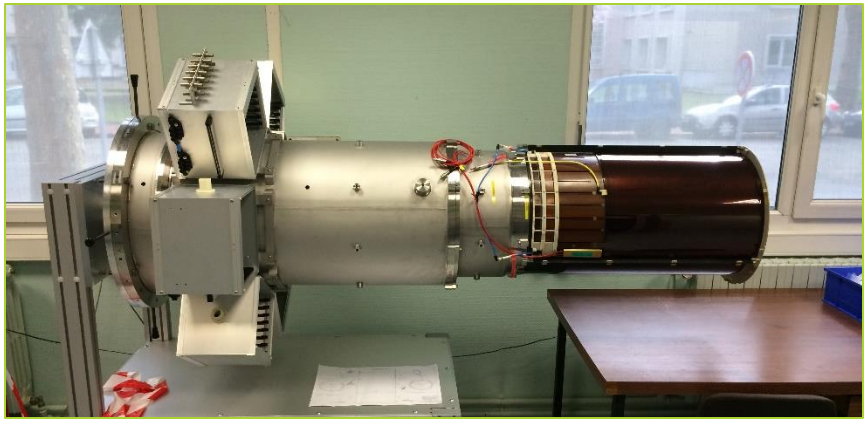

- 4 m² of Micromegas detectors to be installed in 2017
- DREAM based Front-End Electronics
- Remote off-detector frontend electronics connected with 2m micro-coaxial cables
- Forward Detectors
  - High particle rate (30MHz) => Fast detectors
  - Resistive strips divided in 2 zones inner/outer
  - Dimensions: 6x 430 mm diameter disk with a 50 mm diameter hole at the center
- Cylindrical Barrel
  - Low momentum particles => Light Detectors
  - Limited space of ~10 cm for 6 layers
  - High magnetic field (5T)
  - Phase 1 (2016) : 2 Layers (6 Det. of 120°)
  - Phase 2 (2017) : 6 Layers (18 Det.)

CLAS12 - THE MICROMEGAS VERTEX TRACKER

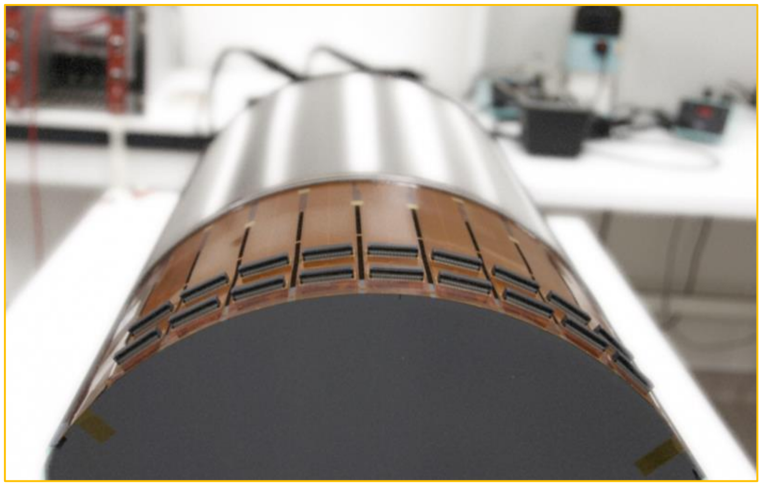

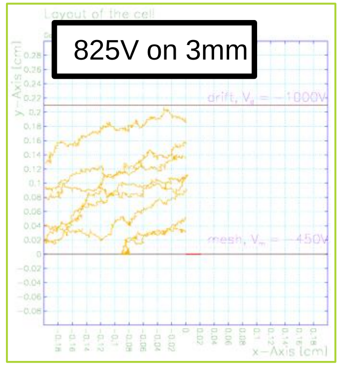

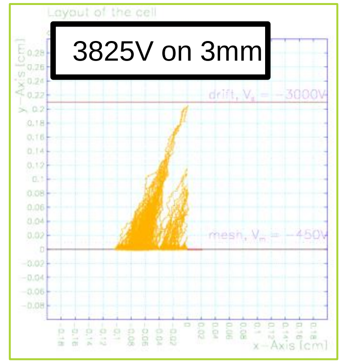

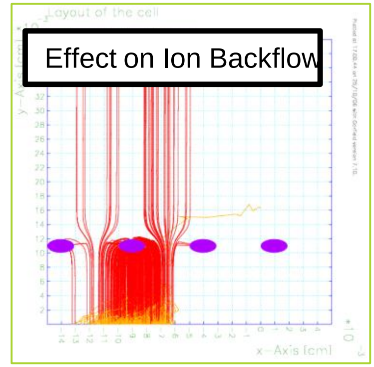

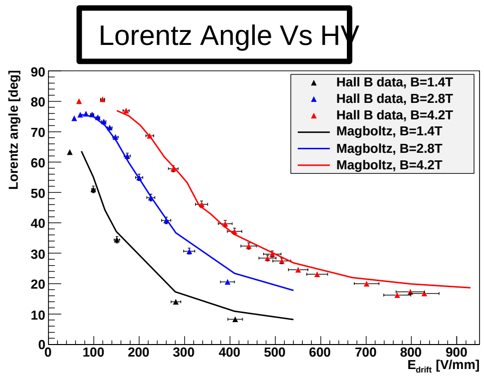

=> Clas-note 2007-004: Simulations of Micromegas detectors for the CLAS12 experiment (S. Procureur)

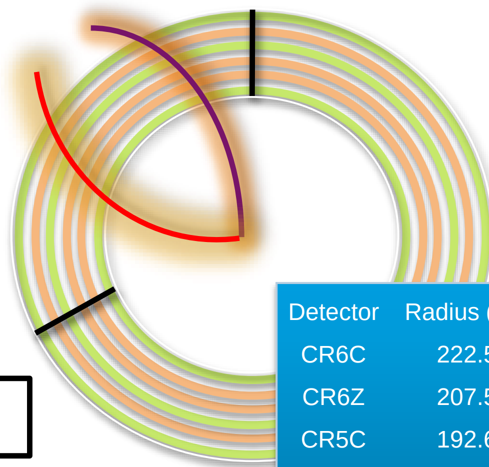

Detector	Radius (mm)
CR6C	222.53
CR6Z	207.54
CR5C	192.65
CR5Z	177.57
CR4Z	162.56
CR4C	147.57

CLAS12 – MVT ASSEMBLY

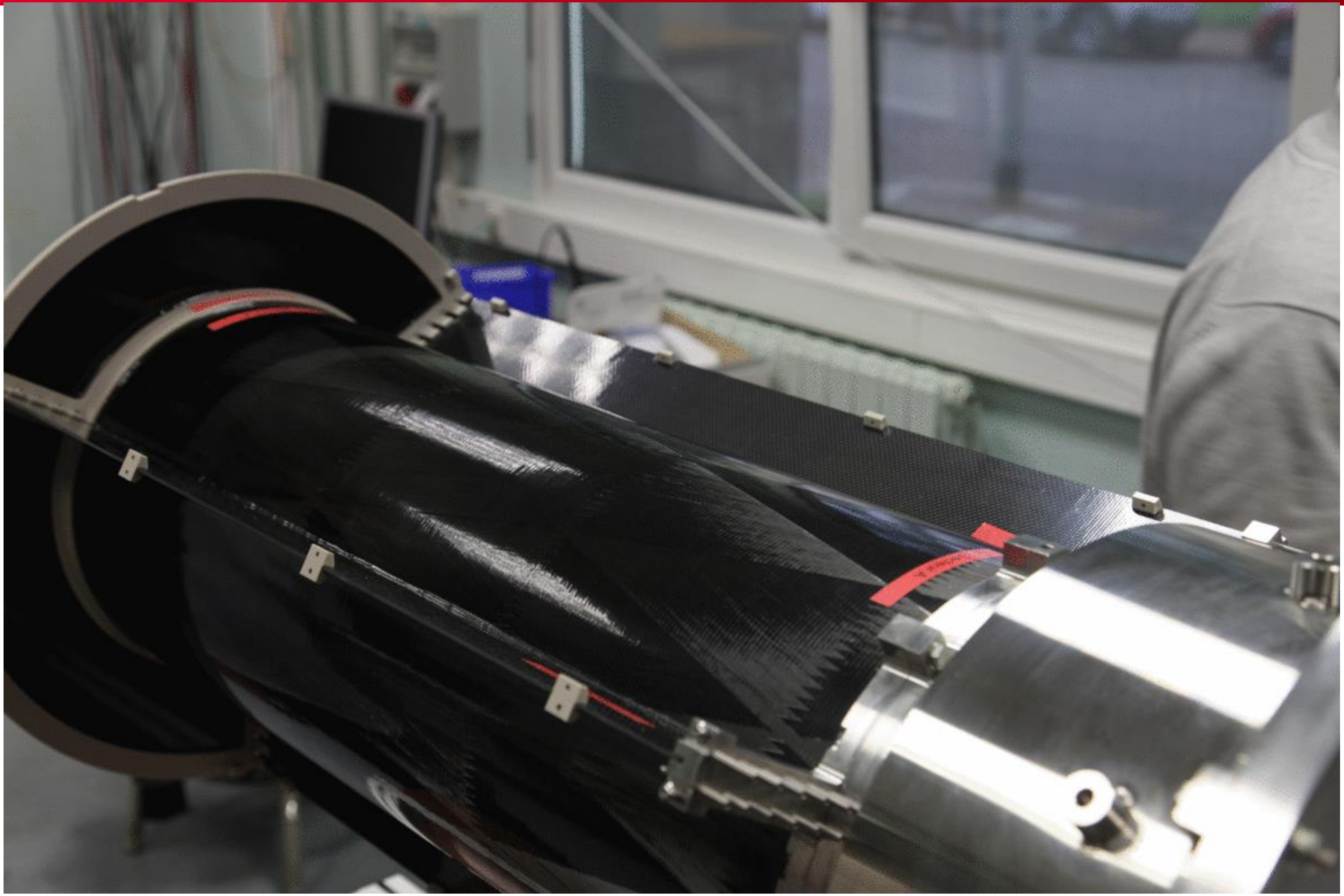

ALICE A heavy Ion Experiment at the LHC

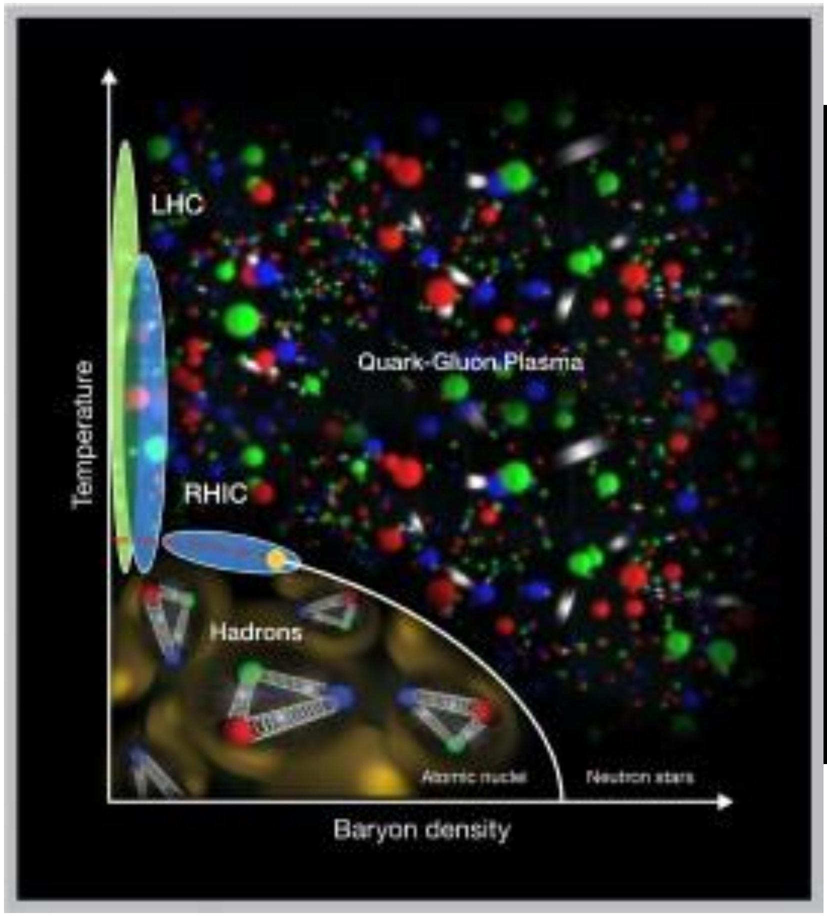

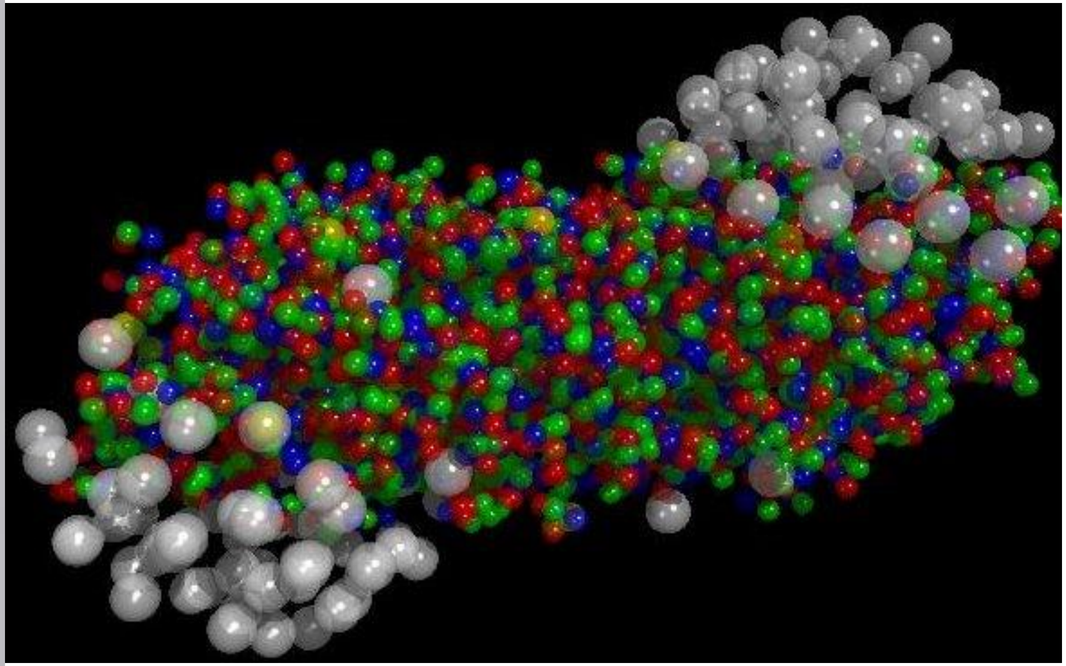

ALICE

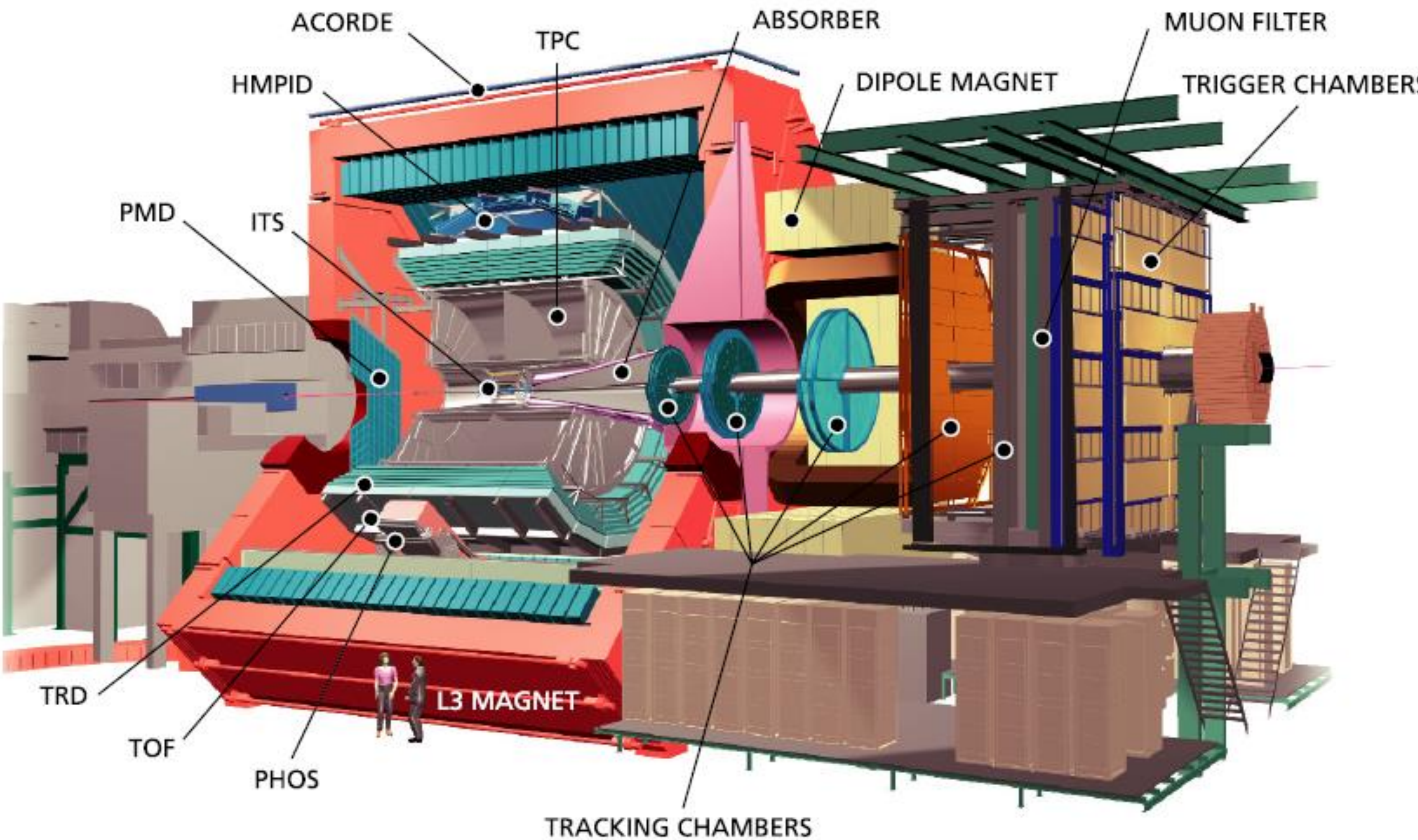
ACORDE
TPC
ABSORBER
MUON FILTER
HMPID
DIPOLE MAGNET
TRIGGER CHAMBERS
PMD
ITS
TRD
TOF
PHOS
L3 MAGNET
TRACKING CHAMBERS

ALICE Particle ID

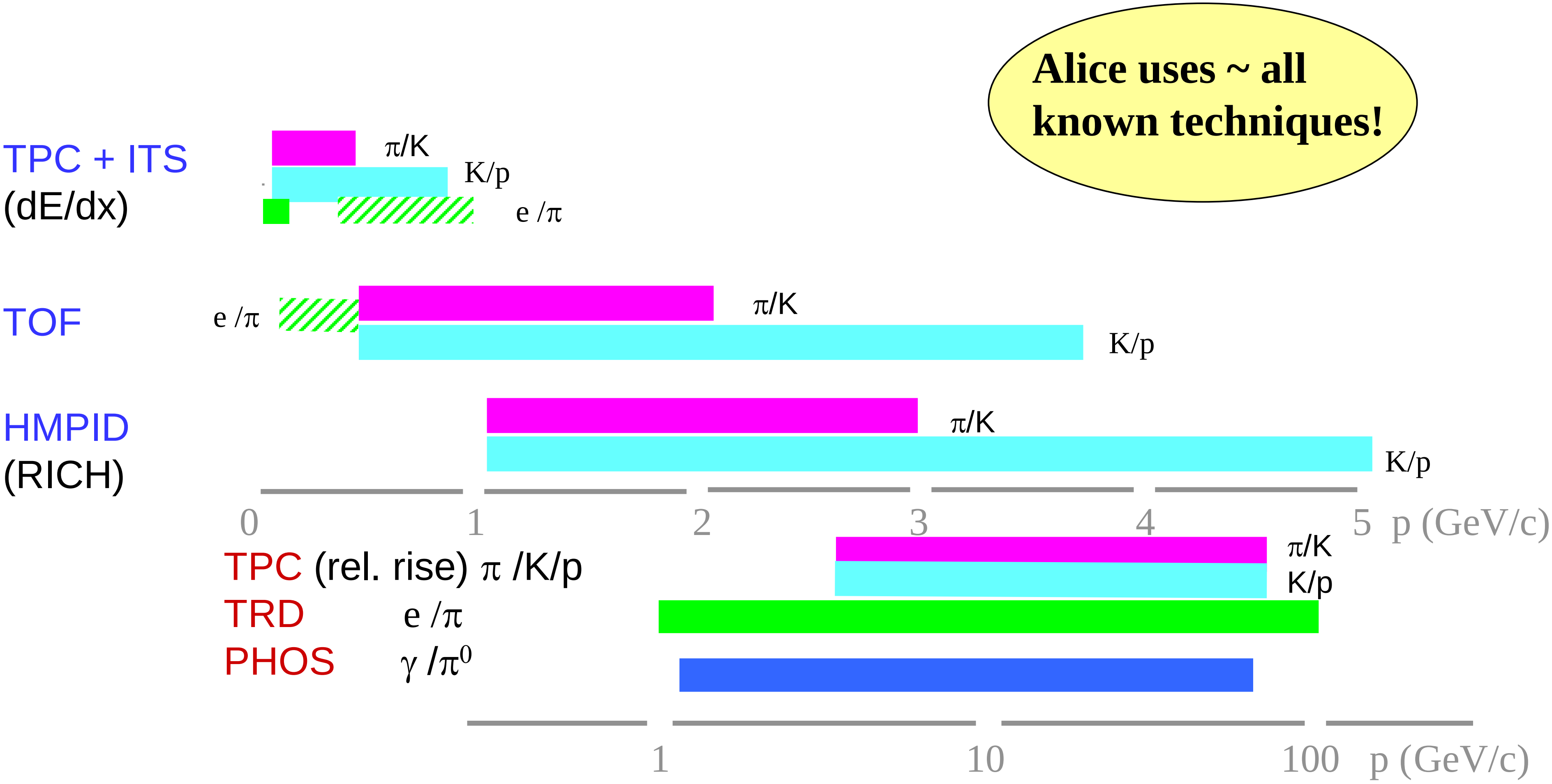

ALICE

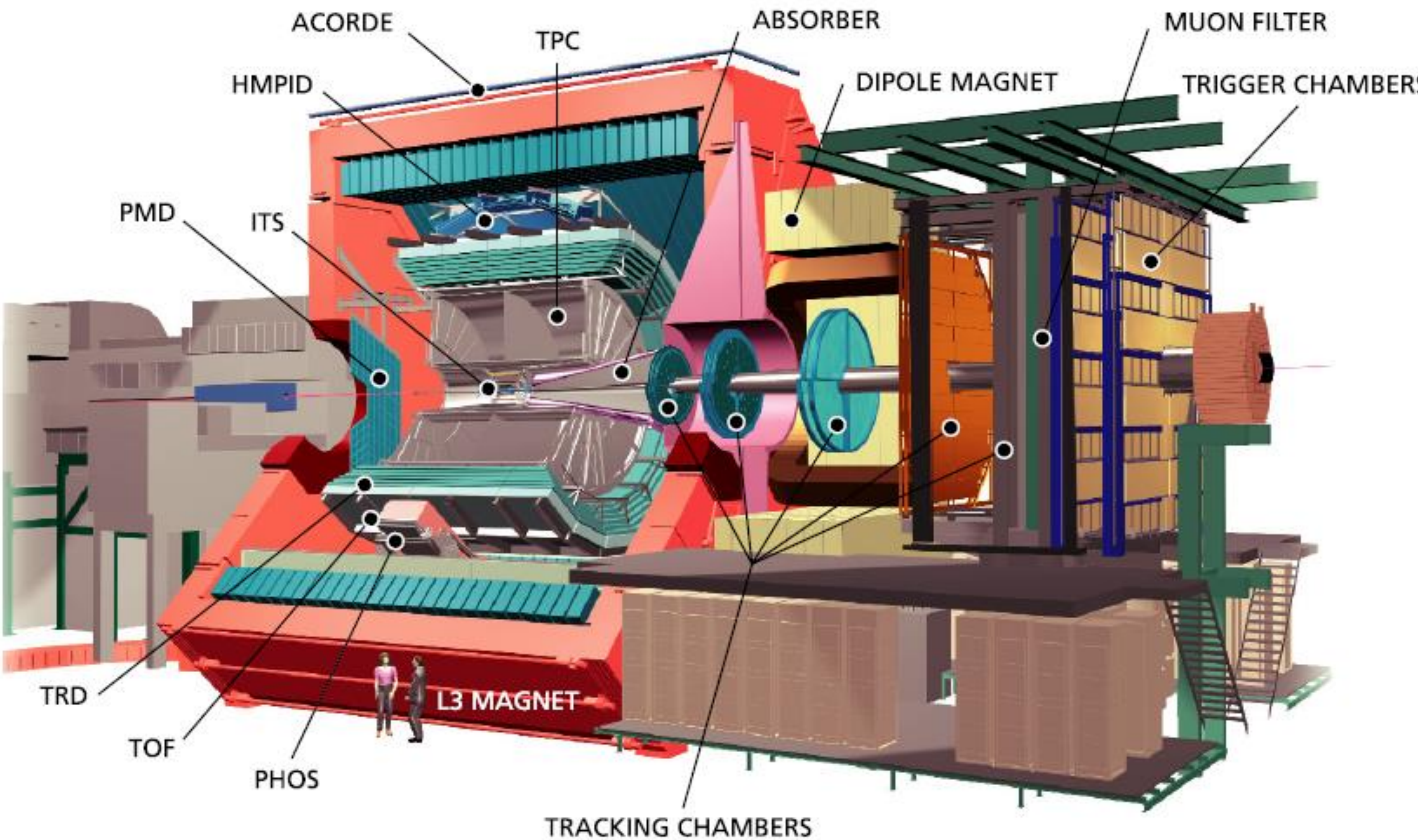
ACORDE
TPC
ABSORBER
MUON FILTER
HMPID
DIPOLE MAGNET
TRIGGER CHAMBERS
PMD
ITS
TRD
TOF
PHOS
L3 MAGNET
TRACKING CHAMBERS

Pierre Auger Cosmic Ray Observatory

Pierre Auger Cosmic Ray Observatory

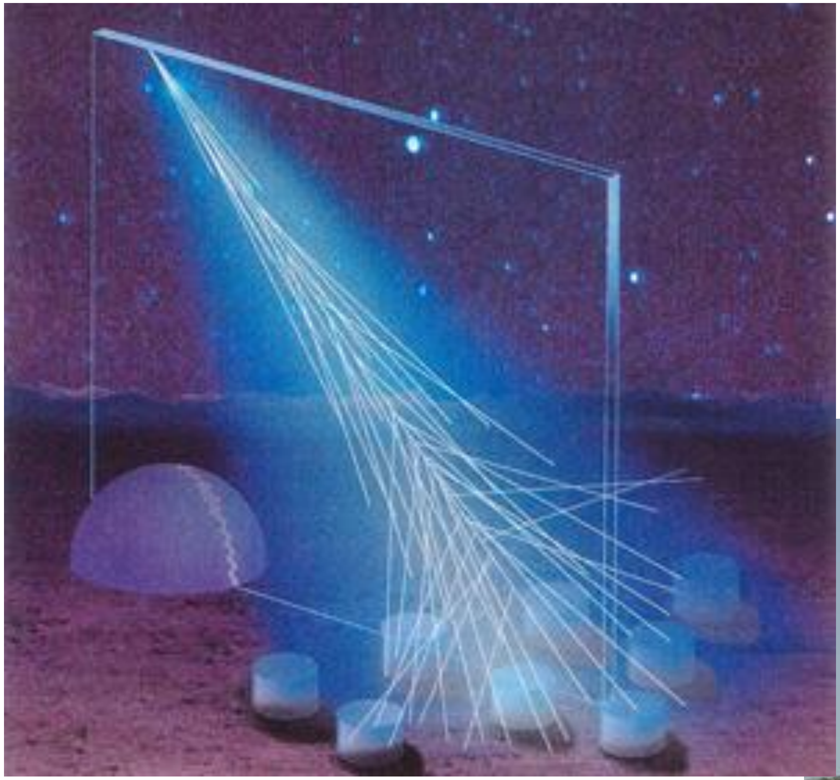

Use earth's atmosphere as a calorimeter. 1600 water Cherenkov detectors with 1.5km distance.

Placed in the Pampa Amarilla in western Argentina.

Pierre Auger Cosmic Ray Observatory

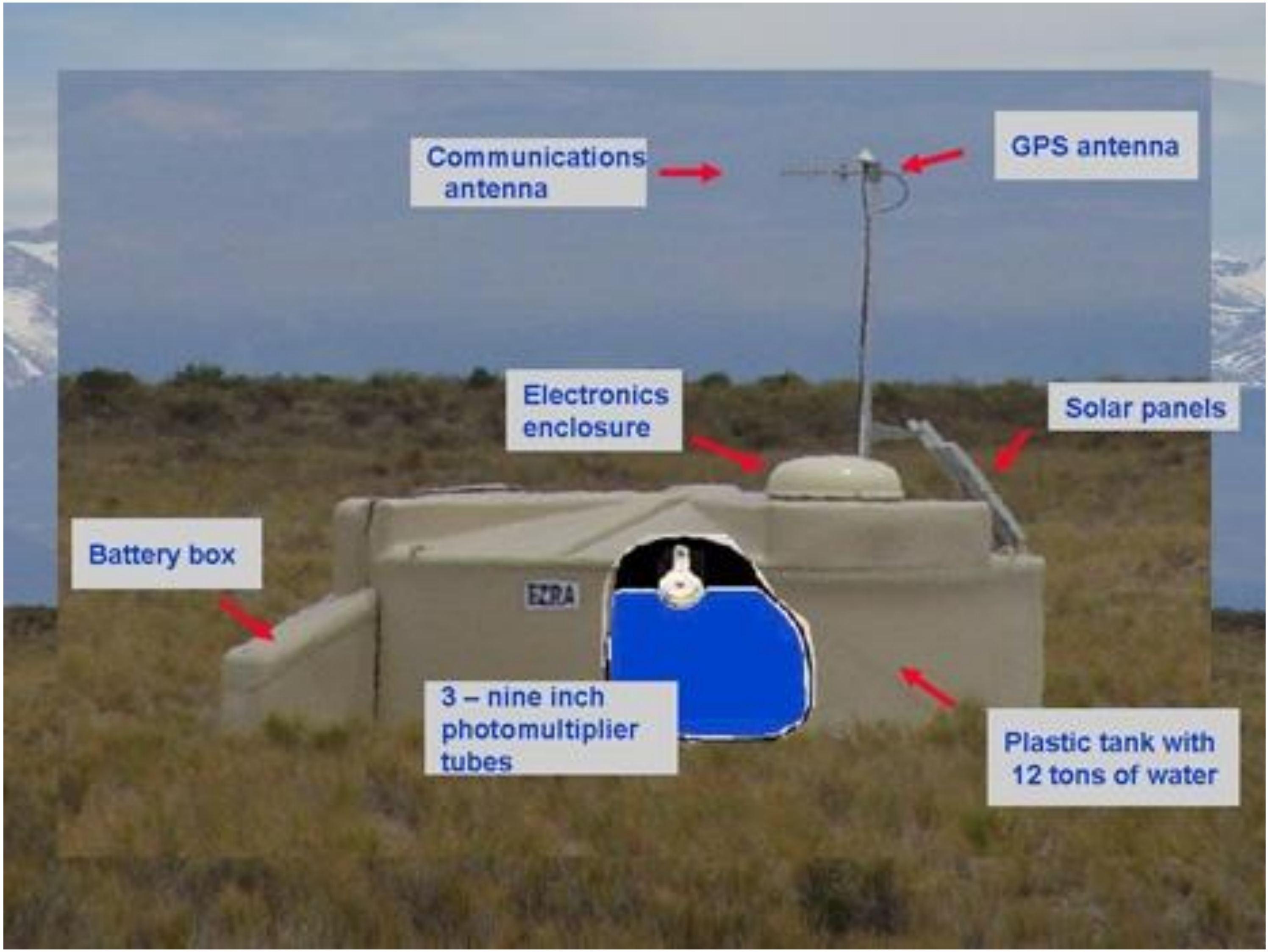

Pierre Auger Cosmic Ray Observatory

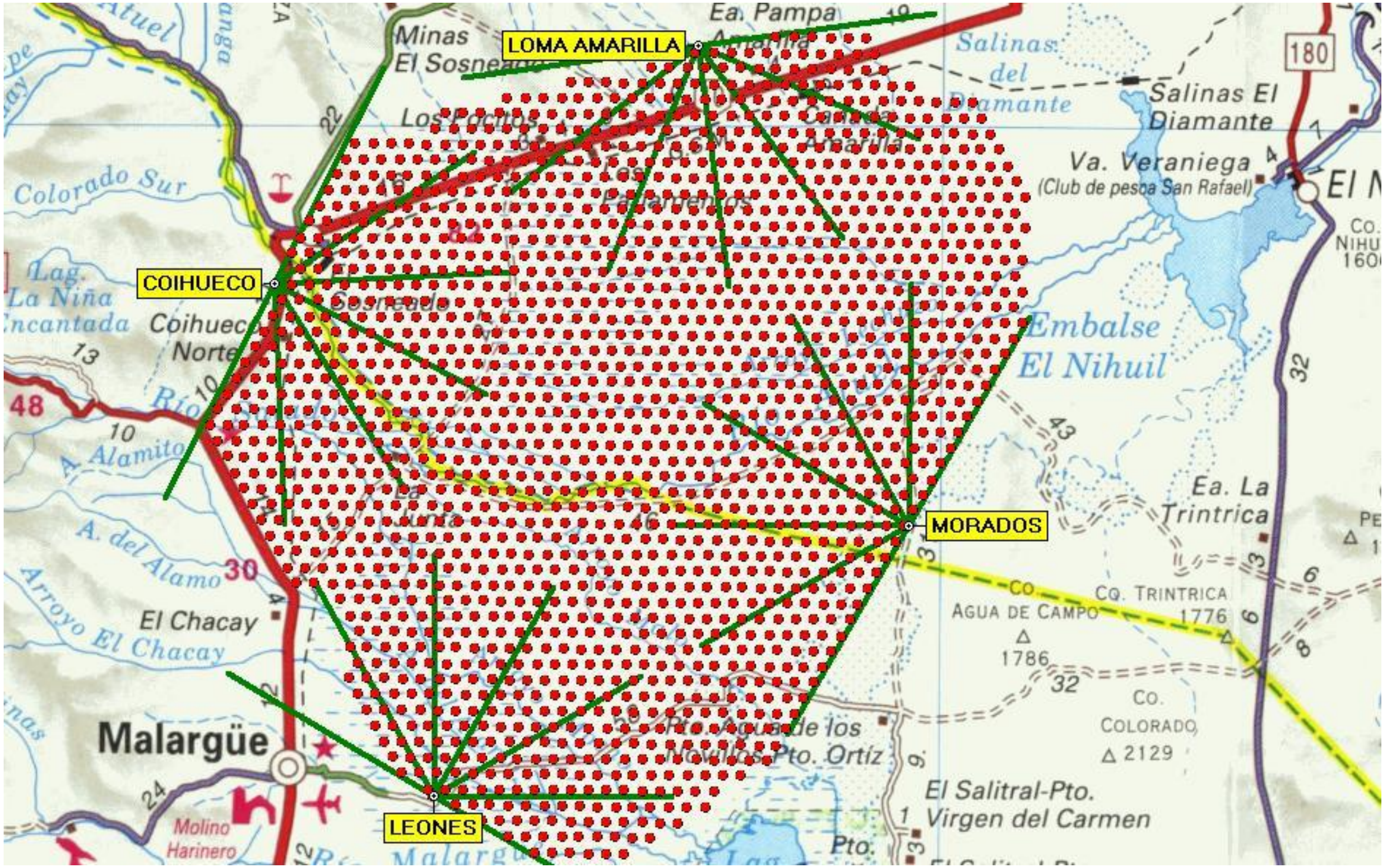

Pierre Auger Cosmic Ray Observatory

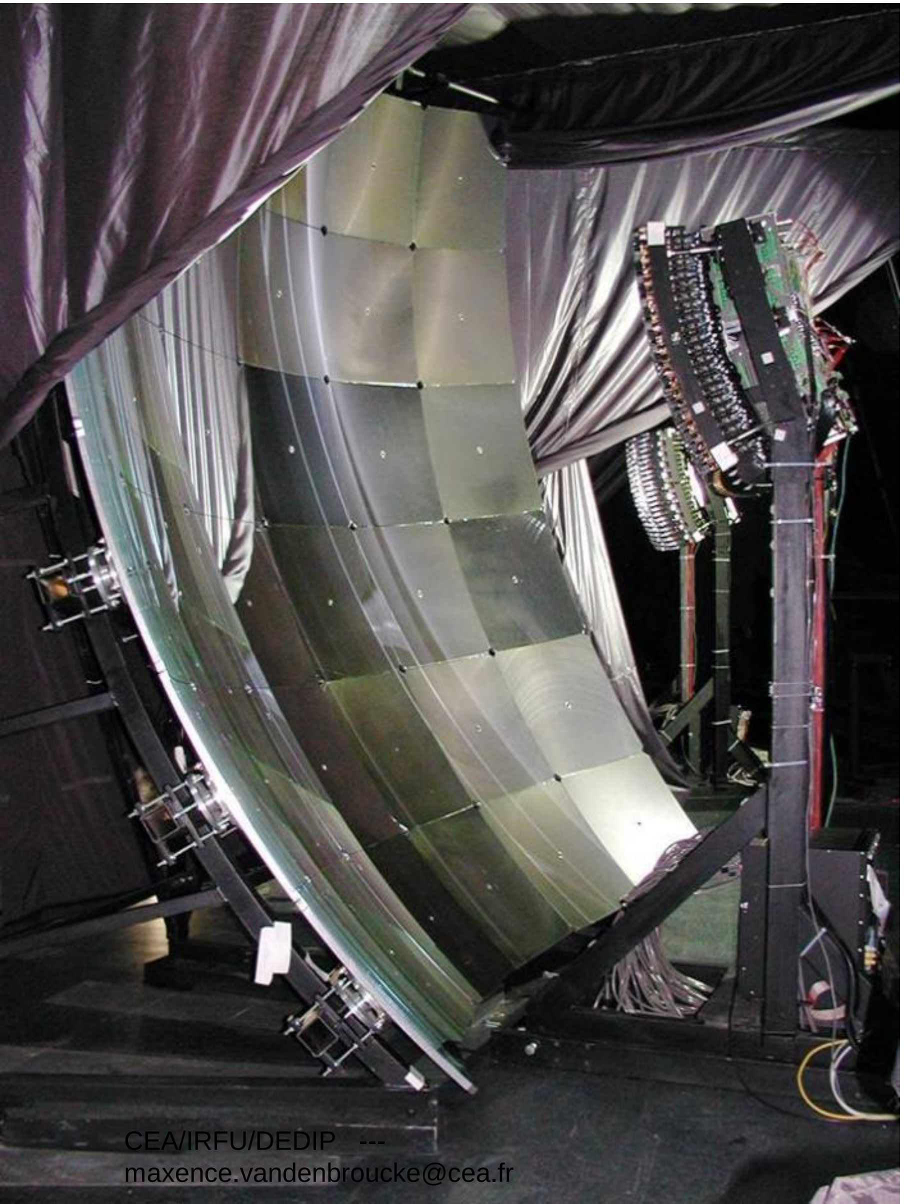

In addition: Fluorescence detectors around the array of water tanks.

Event 1234800

See CR incoming direction | See individual station data

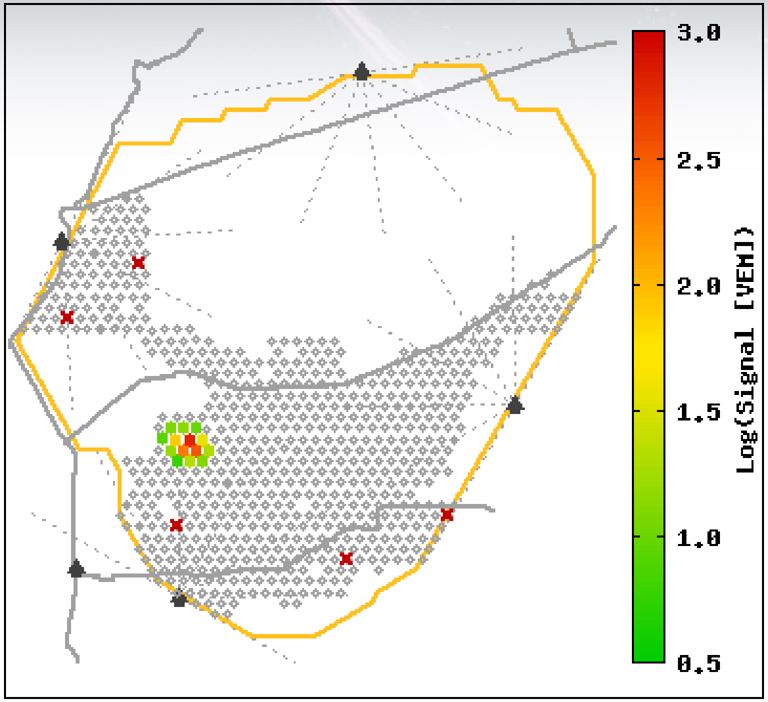

37 EeV = Exa Electron Volt = 37 x 10^{18} eV

Generic Information	
Id	1234800
Date	Sat Mar 5 15:54:48 2005
Nb Station	14
Energy	37.4 ± 1.2 EeV
Theta	43.4 ± 0.1 deg
Phi	-27.3 ± 0.2 deg
Curvature	15.8 ± 0.8 km
Core Easting	460206 ± 20 m
Core Northing	6089924 ± 11 m
Reduced Chi^2	2.30

Event 1234800

See event reconstruction data | See CR incoming direction

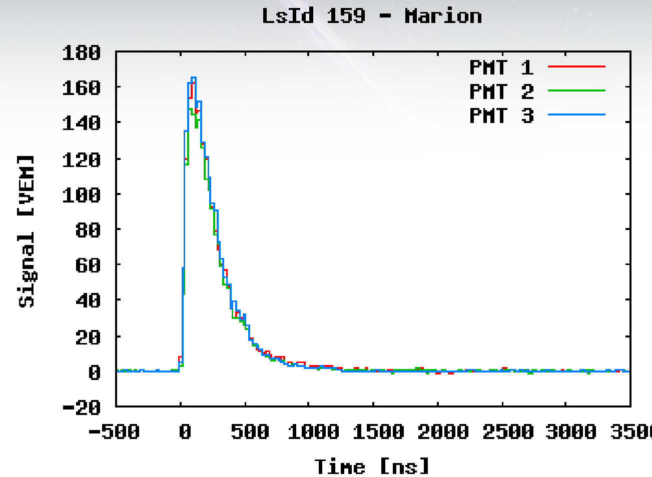

Signal in VEM for the 3 PMTs of station 159 (Marion) as a function of time

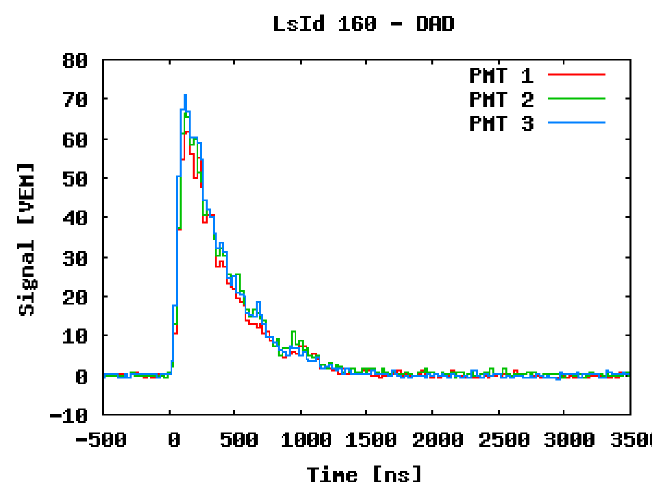

Signal in VEM for the 3 PMTs of station 160 (DAD) as a function of time

AMS

ALPHA MAGNETIC SPECTROMETER

Try to find Antimatter in the primary cosmic rays.
Study cosmic ray composition etc. etc.

Will be installed on the space station.

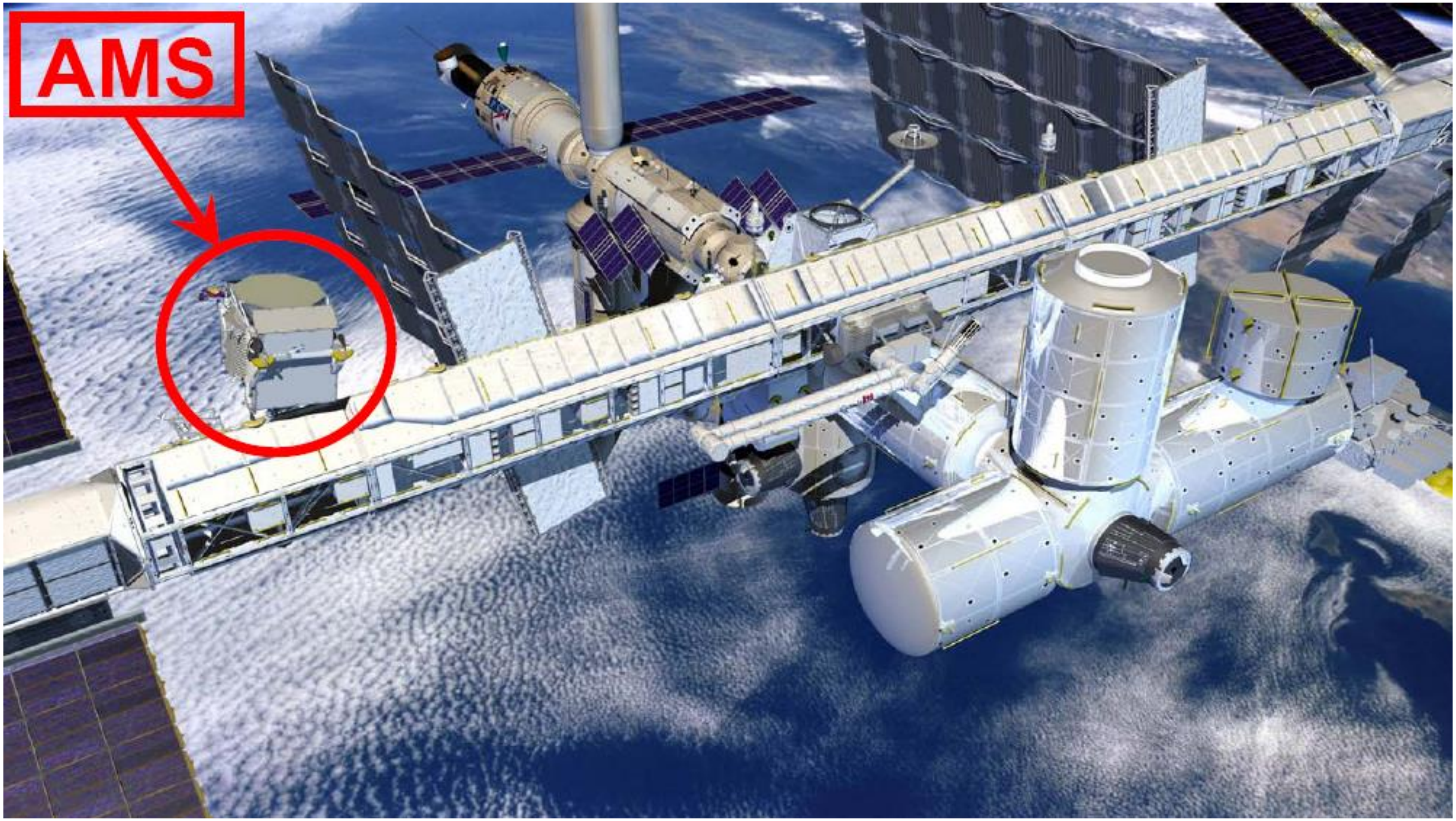

AMS

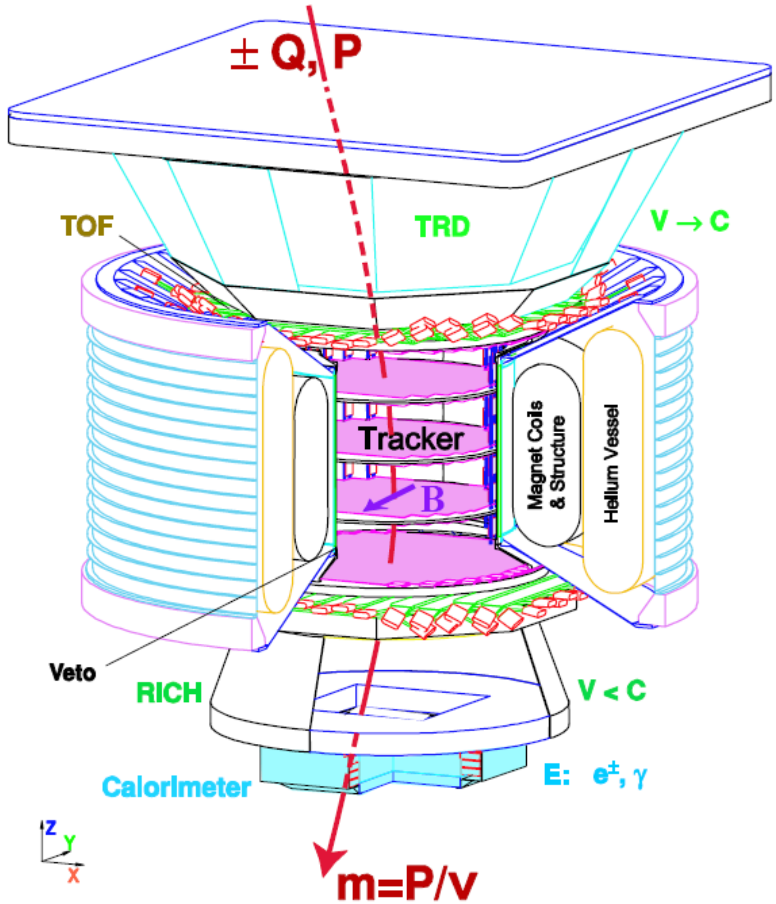

± Q, P
TOF
TRD
V → C
Tracker
B
Magnet Coils & Structure
Helium Vessel
Veto
RICH
V < C
Calorimeter
E: e±, γ
Z
Y
X
m=P/v

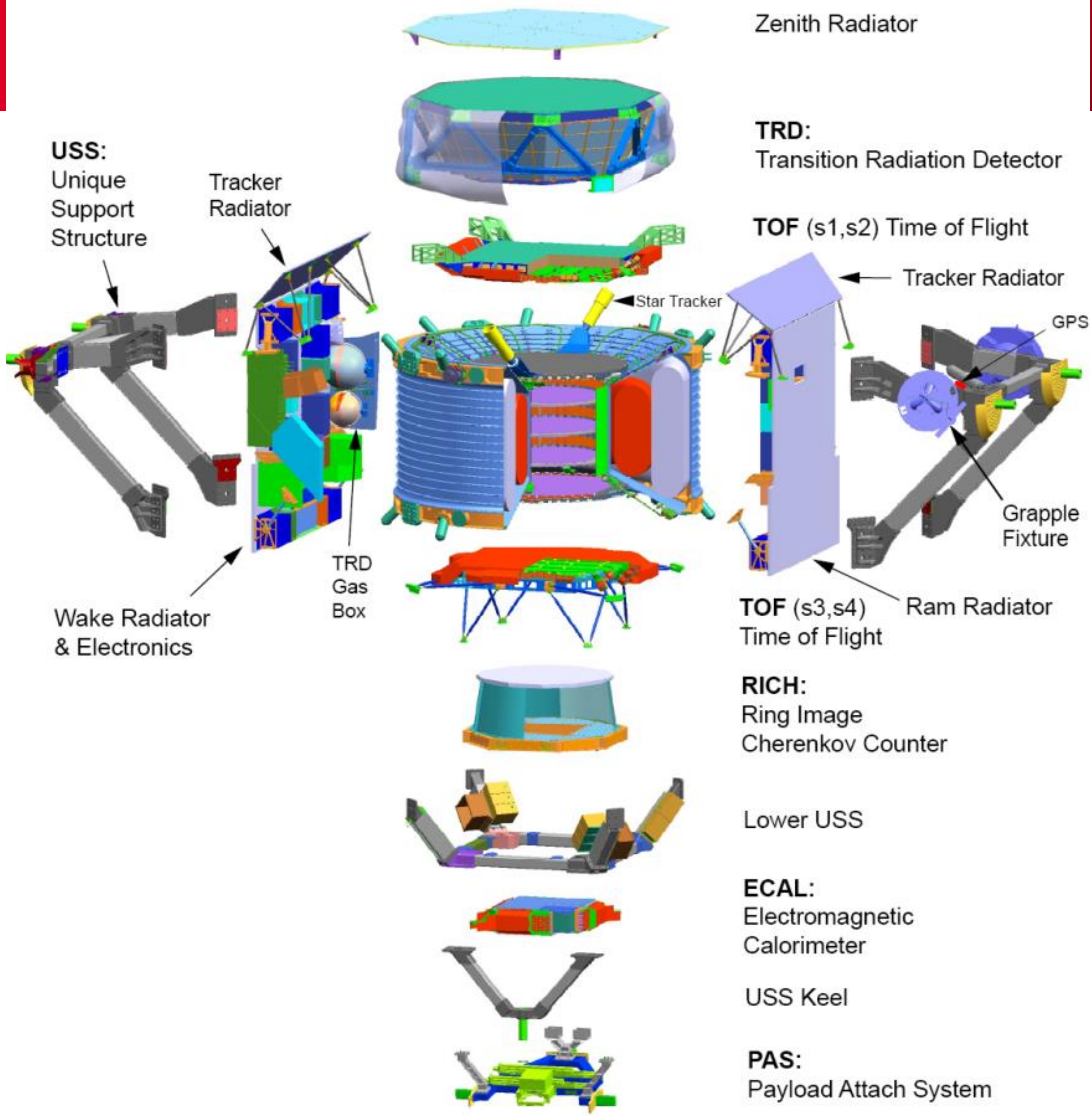
Zenith Radiator
TRD:
Transition Radiation Detector
USS:
Unique
Support
Structure
Tracker
Radiator
TOF (s1,s2) Time of Flight
Tracker Radiator
Star Tracker
GPS
Grapple
Fixture
TRD
Gas
Box
Wake Radiator
& Electronics
TOF (s3,s4)
Time of Flight
Ram Radiator
RICH:
Ring Image
Cherenkov Counter
Lower USS
ECAL:
Electromagnetic
Calorimeter
USS Keel
PAS:
Payload Attach System

GBAR at CERN

Schematic

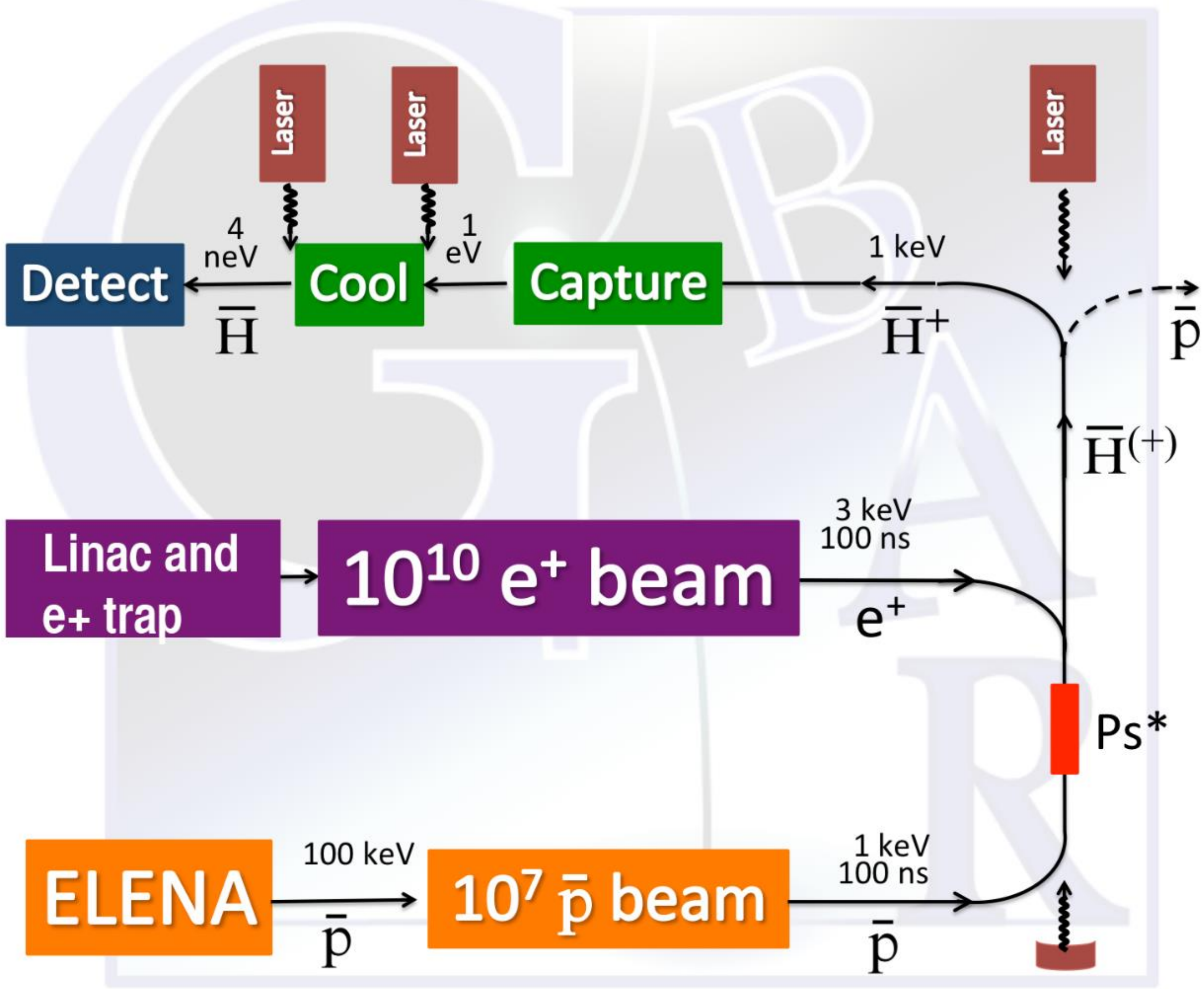

GBAR at CERN

Detection

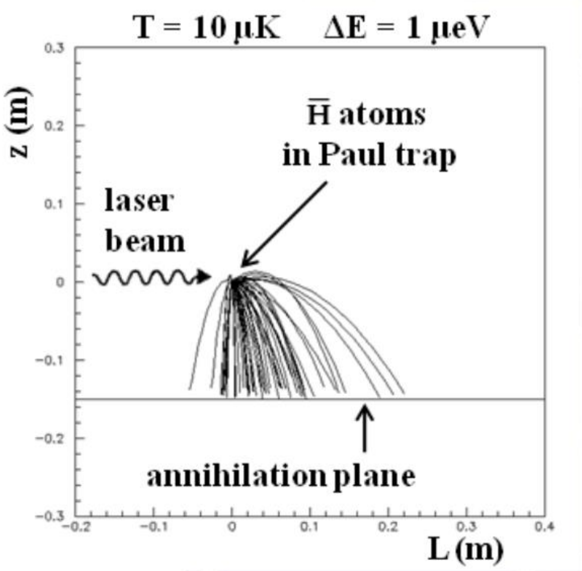

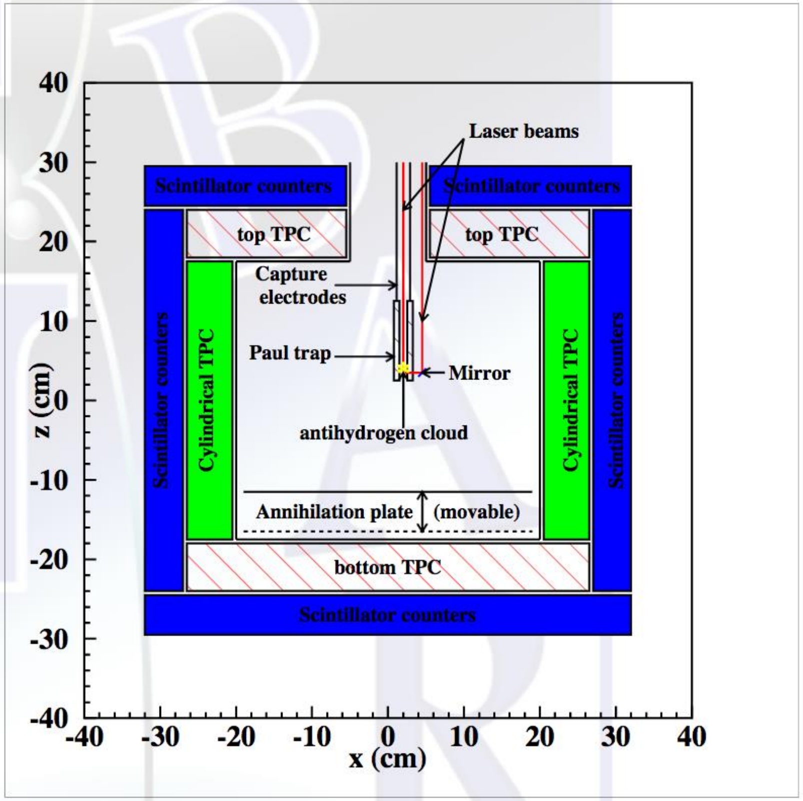

Detection requirement:

- TOF precision : 150 μs
- Annihilation vertex precision : 1 mm
- Background rejection through event topology

Scheme under design: TPC with micromegas chamber (as in T2K near detector)

$$\frac{\Delta \bar{g}}{\bar{g}} \approx 10^{-2}$$

PLAN DES COURS

Cours 1 : Généralités

-Introduction générale sur l'importance de la mesure
-Qu'est-ce qu'une expérience de physique subatomique ?
-Que veut-on observer à propos d'une particule?
-Architecture générale d'une expérience en physique subatomique

Cours 2 : Les détecteurs de particules

- Trajectographie :
  - Détecteurs Gazeux
  - Détecteurs au Silicium
- Calorimétrie
- Scintillation

Cours 3 : Exemple d'expériences

- Autour du Neutrino
- Nucléaire et Hadronique
- Rayons Cosmiques
- Antimatière

SOURCES

Basé sur les cours de Stefano Panebianco (CEA/IRFU) rencontre d'ete 2016

Le cours de Werner Riegler (CERN Summer Student Lecture Program 2009)

Particle Detectors , Second Edition, C. Grupen & B. Shwartz

DONUT

Detector for Observation of Tau Neutrino.

DONUT

Creating a Tau Neutrino Beam

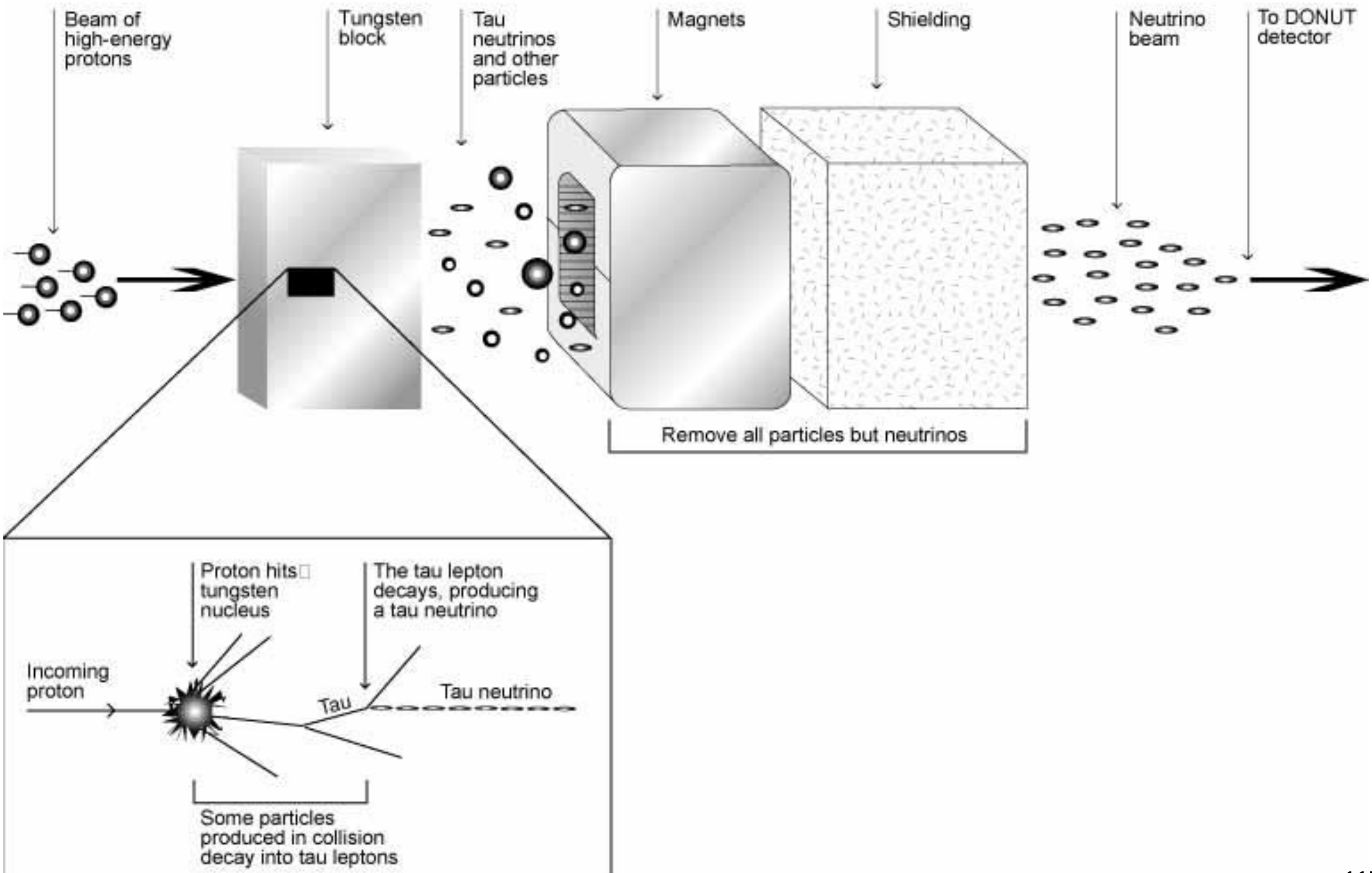

DONUT

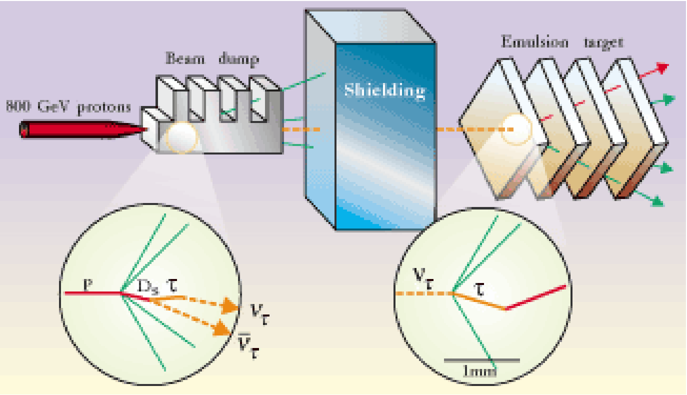
Beam dump
800 GeV protons
Shielding
Emulsion target
P
Ds
τ
ν_τ
$\bar{\nu}_\tau$
τ
1mm

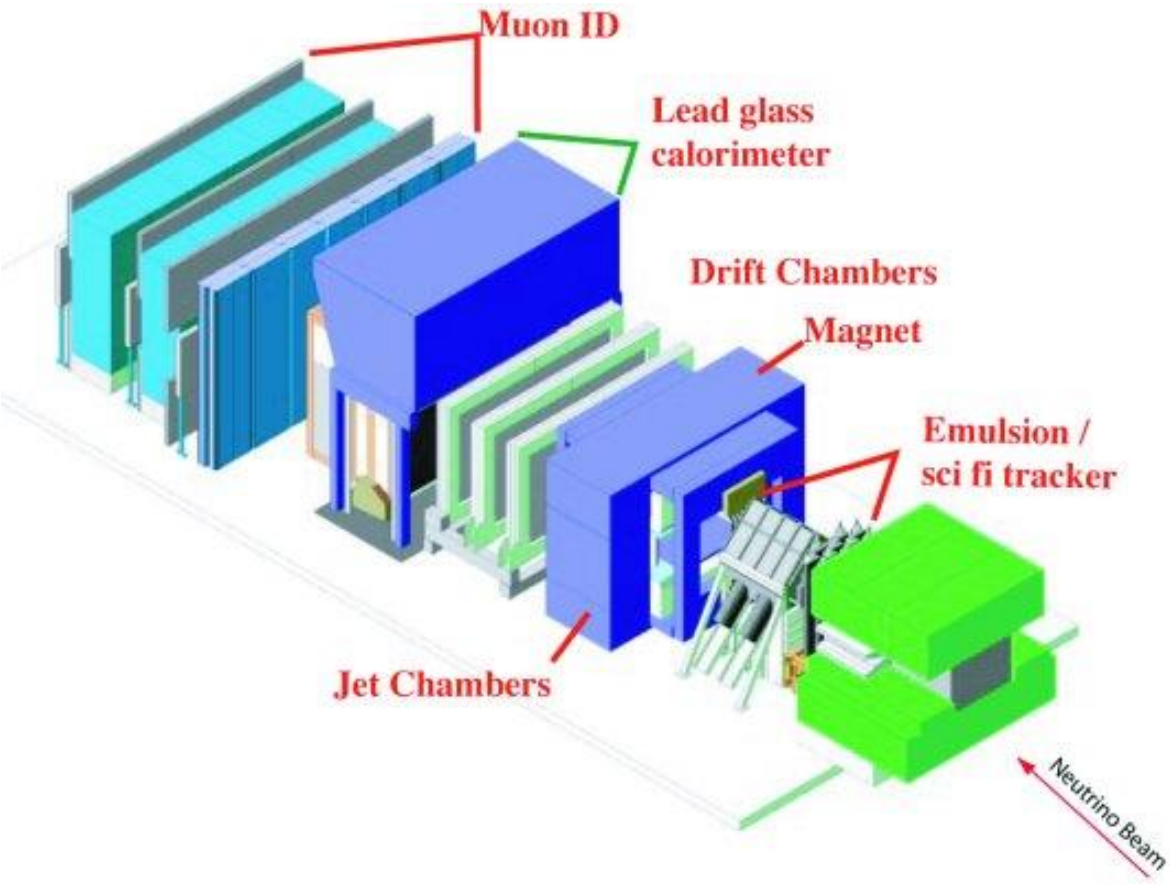
Muon ID
Lead glass calorimeter
Drift Chambers
Magnet
Emulsion / sci fi tracker
Jet Chambers
Neutrino Beam

Detecting a Tau Neutrino

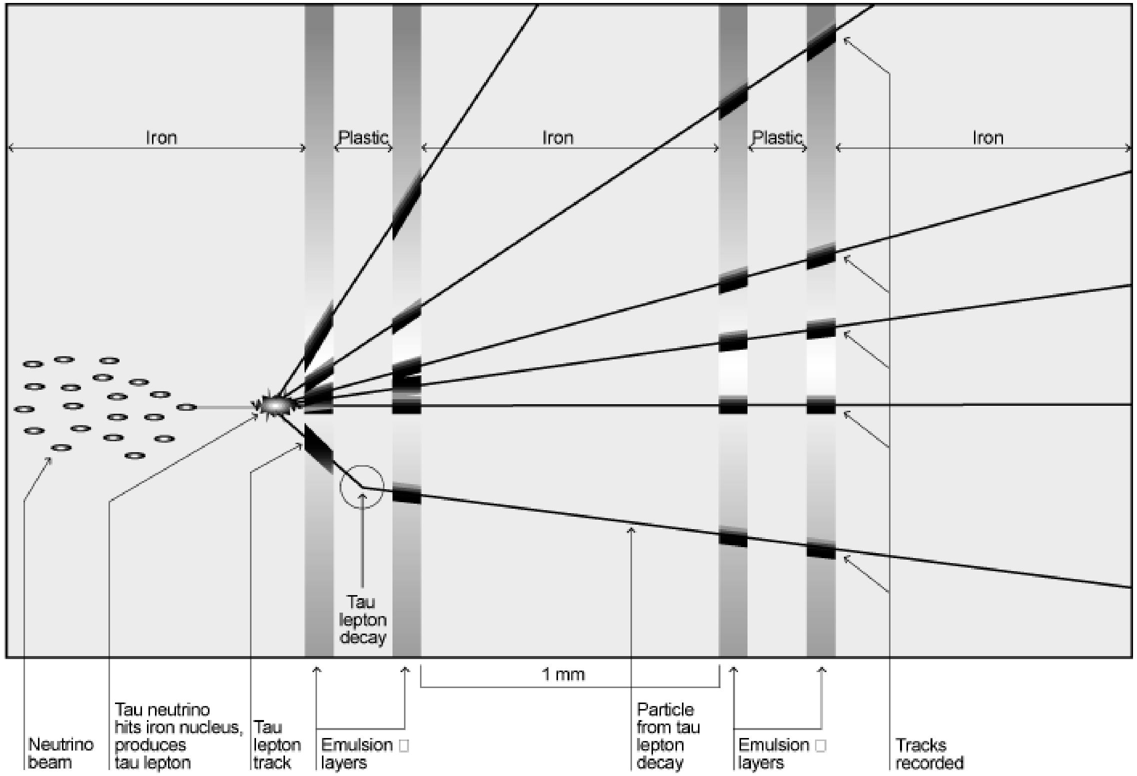

Of one million million tau neutrinos crossing the DONUT detector, scientists expect about one to interact with an iron nucleus.

Tau lepton has very short lifetime and is therefore identified by the characteristic 'kink' on the decay point.

DONUT

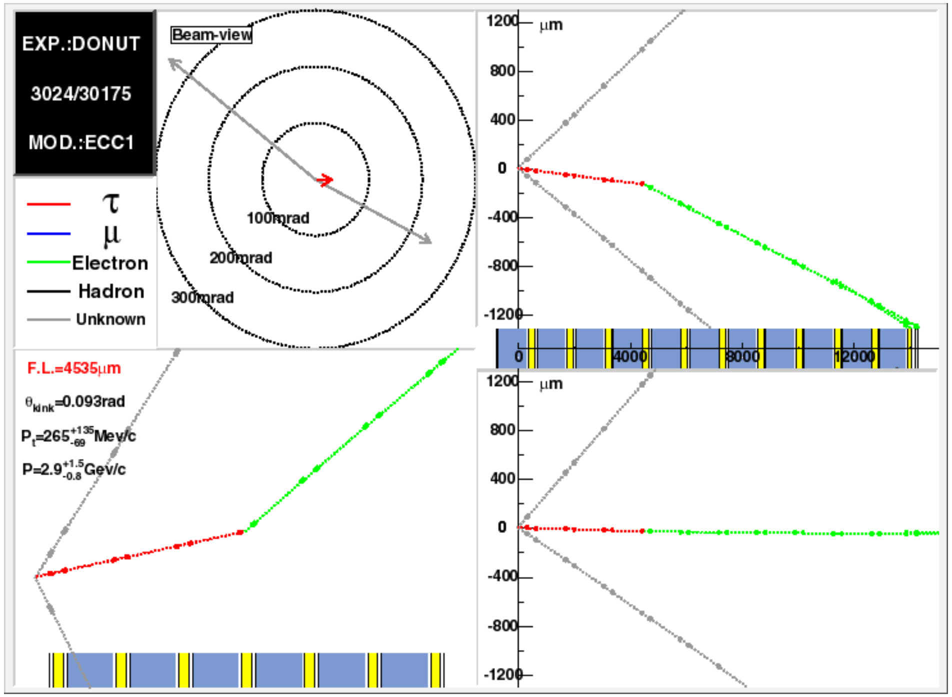

One of the 4 tau candidates.

Emulsion resolution 0.5um !

MICROMEGAS: INVENTION

Nuclear Instruments and Methods in Physics Research A 376 (1996) 29–35

ELSEVIER

Section A

MICROMEGAS: a high-granularity position-sensitive gaseous detector for high particle-flux environments

Y. Giomataris[a,*], Ph. Rebourgeard[a], J.P. Robert[a], G. Charpak[b]

[a] *CEA/DSM/DAPNIA/SED-C.E.-Saclay, 91191 Gif/Yvette, France*

[b] *Ecole Superieure de Physique et Chimie Industrielle de la ville de Paris, ESPECI, Paris, ESPCI, Paris, France and CERN/AT, Geneva, Switzerland*

Abstract

We describe a novel structure for a gaseous detector that is under development at Saclay. It consists of a two-stage parallel-plate avalanche chamber of small amplification gap (100 μm) combined with a conversion-drift space. It follows a fast removal of positive ions produced during the avalanche development. Fast signals (≤1 ns) are obtained during the collection of the electron avalanche on the anode microstrip plane. The positive ion signal has a duration of 100 ns. The fast evacuation of positive ions combined with the high granularity of the detector provide a high rate capability. Gas gains of up to 10^5 have been achieved.

1. Introduction

Multiwire proportional chambers have been originally designed for high-rate applications [1]. Their flux capability was mainly limited by the positive-ion space charge created because of the low ion drift velocity with a typical drift time of several tenths of microseconds. Their spatial resolution was limited by the wire spacing, which was of the order of 1 mm.

To overcome these limitations, a new technique, the microstrip gas chamber (MSGC), has been developed over the last eight years [2–4]. Wires are replaced by strips printed on an insulating support; a high electric field region, sufficient for electron multiplication, is created between the thin cathode and anode conductive strips. It is new class of gas detector relying on the microelectronics technology. The small inter-strip pitch allows a good spatial resolution, inferior to 100 μm and the fast collection of the charges offers the possibility to cope with higher counting rates. One limitation of the MSGC detector is the fact that the avalanche multiplication does not exceed 10^4, because of breakdown on the insulator surface. Positive ions created during the avalanche process and

the detector [5]. A lot of effort has been invested, during the last few years, resolve the charging-up problems by a careful choice of the resistivity of the substrate or a special treatment of its surface. Another type in this class of gas detectors, the micro-gap chamber [6], was recently developed aiming to resolve the charging-up problem and giving superior results in terms of rate capability and spatial resolution.

Another possible way out is the use of a special asymmetric configuration of the multiwire structure [7,8] with alternating anodes and field-shaping wires, mounted close to the cathode plane with engraved pick-up strips orthogonal to the wire direction. The performance of this structure equals that of the MSGC in terms of rate capability and spatial resolution. In addition it can achieve higher electron multiplication factors and it operates in a stable fashion for long irradiation periods. The drawback here is the use of delicate wires and the wire stretching force, which is proportional to the total number of wires acting in the wire frame; this therefore has to be of substantial thickness.

In this paper we present a new approach where the wire plane is replaced by a thin electroformed micromesh. The

avalanche chamber and it is called MICROMEGAS (MI-CRO-MEsh-GAseous Structure).

Voltaire
Micromégas
Texte intégral
+ dossier par Guillaume Peureux

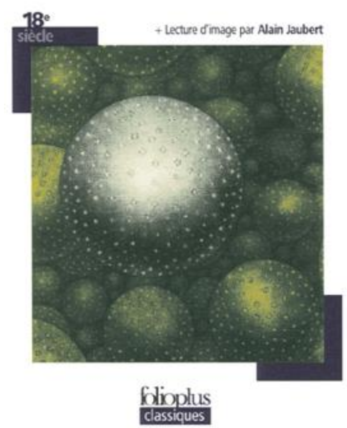

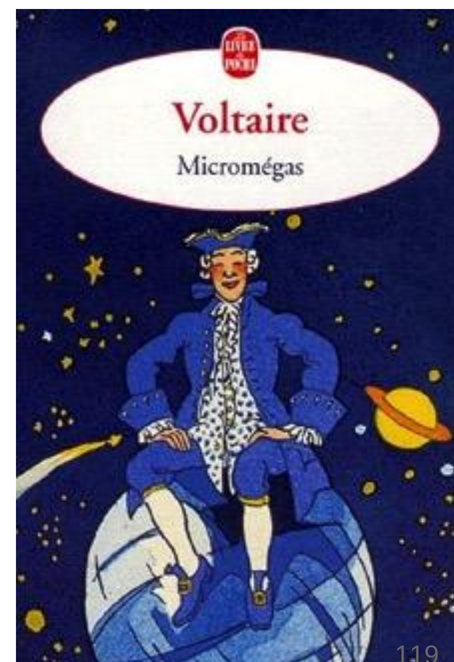

FONCTIONNEMENT DE MICROMEGAS

- Haut gain (>10^4)
- Bonne résolution en énergie (11% à 6kev)
- Bonne résolution temporelle (<1ns)
- Tenue à haut flux
- Bonne résolution spatiale (<50 µm)
- Remontée ionique réduite <1%
- Résistance aux radiations (10^{16} p/cm^2)

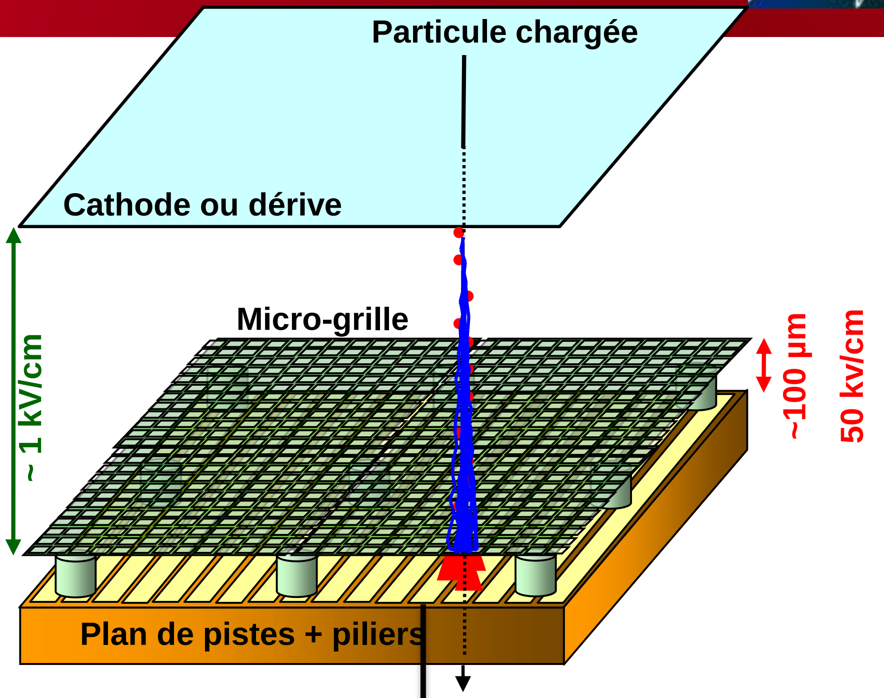

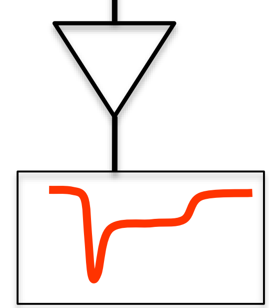

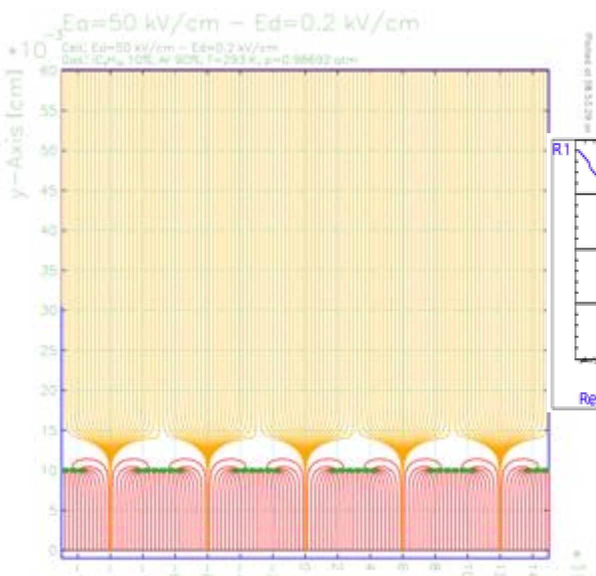

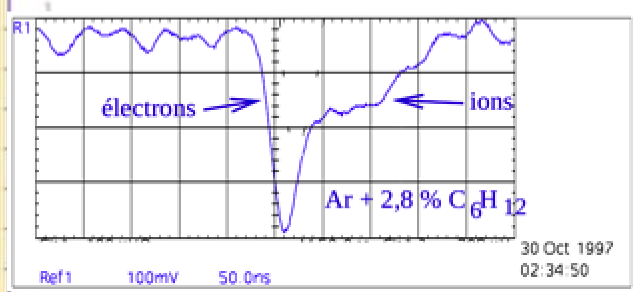

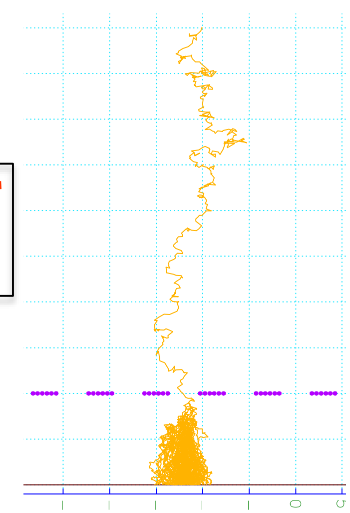

Collection rapide des ions → fonctionnement à haut flux

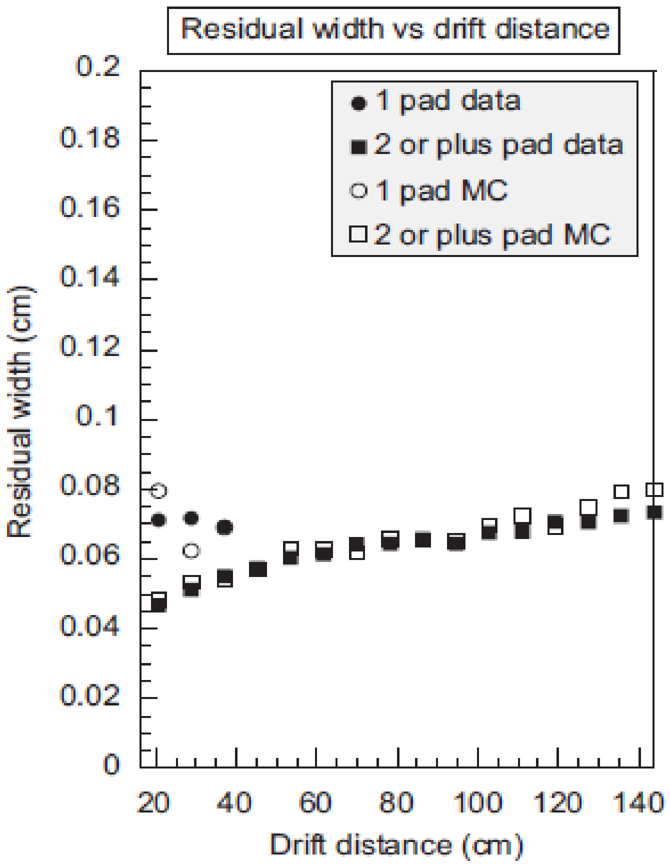

Résolution spatiale dans une TPC
(Chambre à projection temporelle)

Tenue à haut flux et vieillissement

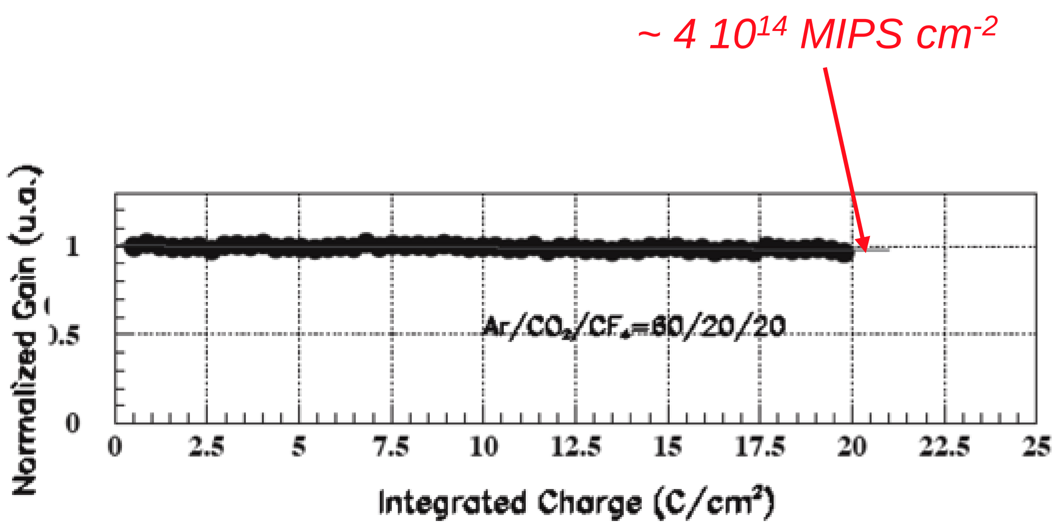

FABRICATION D'UN BULK

Premiers prototypes en 2004. Collaboration CERN/Irfu

La micro-grille tissée est laminée entre 2 couches photo-imageables

Mécanique réduite → diminution des zones mortes

Grandes surfaces

Robuste, procédé industriel (circuit imprimé)

Atelier BULK du SEDI


Lamination

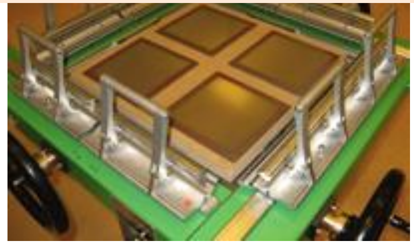
Intégration de la micro-grille


Insolation


Développement

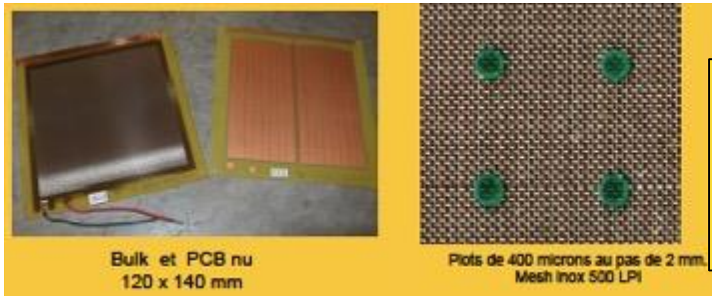

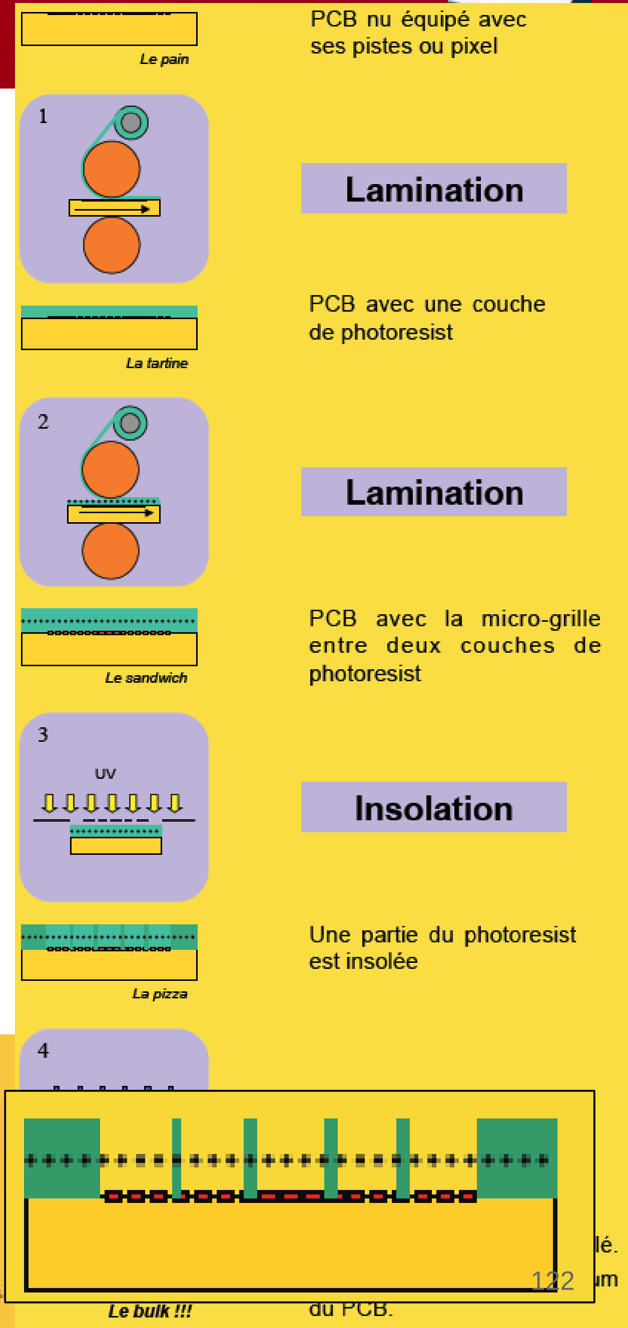

Historique des détecteurs gazeux

MWPC
Multi-Wire Proportional Chamber
G. Charpak et al., 1968

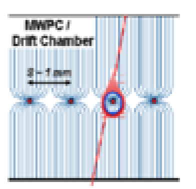

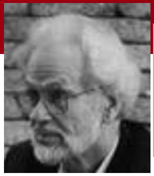

TPC
Time Projection Chamber
D. R. Nygren et al., 1974

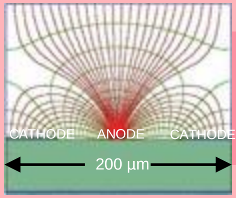

MSGC
Micro-Strip Gas Chamber
A. Oed, 1988

Micro Pattern Gaseous Detectors: MPGD

GEM
Gas Electron Multiplier
F. Sauli, 1997

MICROMEGAS
MICRO-MEsh GAseous Structure
I. Giomataris et al., 1996

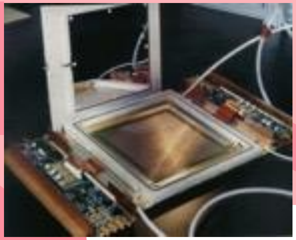

CLASSICAL
1996

BULK
2003

INGRID
2005

MICROBULK
2006

RESISTIVE ANODE
2005-2013

Les détecteurs Micromegas

	CLASSICAL 1996	BULK 2003	INGRID 2005	MICROBULK 2006
Mesh Readout plane	TWO mechanical entities	INTEGRATED: ONE single entity		
Type of mesh	Any type	30 µm Stainless steel	1 µm Aluminium	5 µm Copper
Advantages	Demontability Large Surface	Robust Industrial manufacturing process (PCB)	Excellent energy resolution Single electron efficiency	Intrinsically Flexible Low mass Radiopure

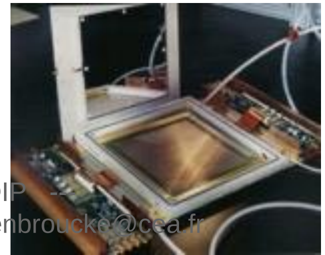

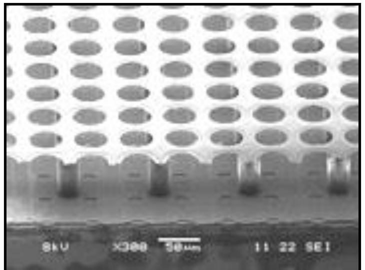

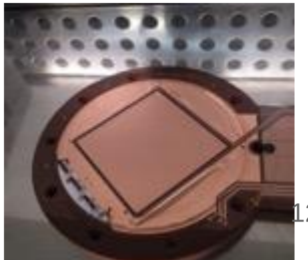

Si-Diode used as a Particle Detector !

At the p-n junction the charges are depleted and a zone free of charge carriers is established.

By applying a voltage, the depletion zone can be extended to the entire diode → highly insulating layer.

An ionizing particle produces free charge carriers in the diode, which drift in the electric field and induce an electrical signal on the metal electrodes.

As silicon is the most commonly used material in the electronics industry, it has one big advantage with respect to other materials, namely highly developed technology.

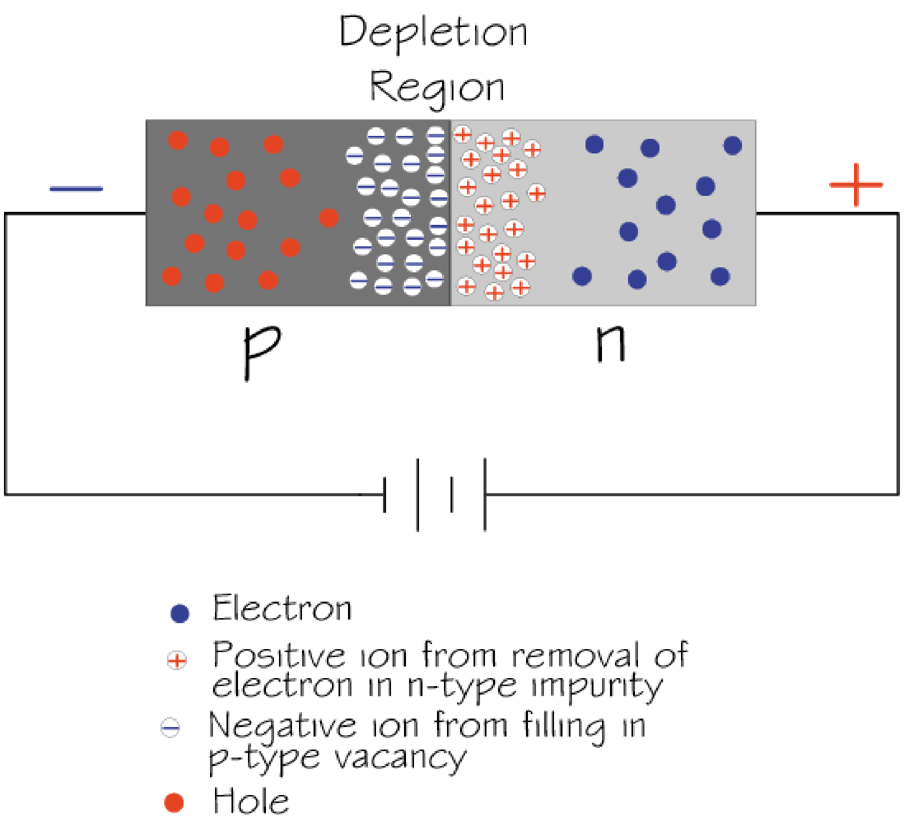

Doping of Silicon

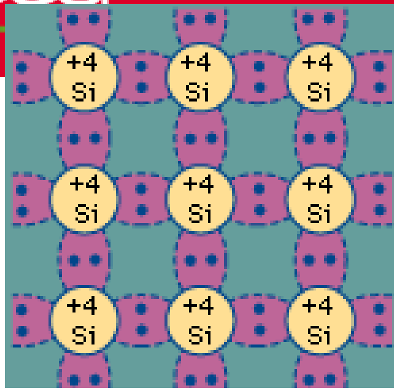

doping

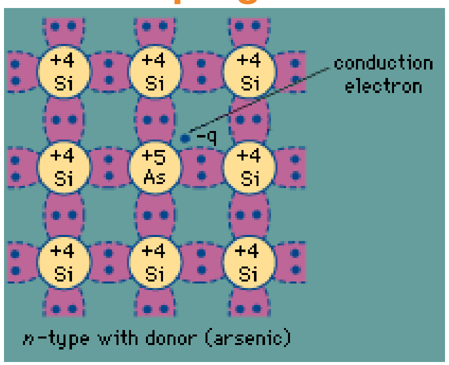

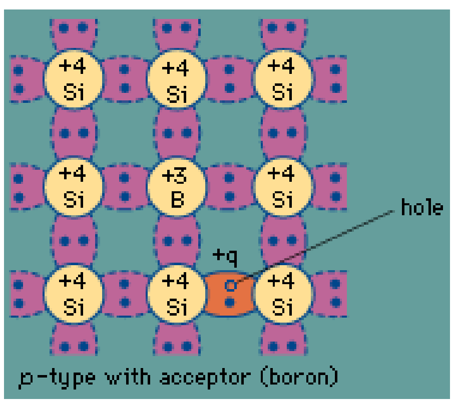

In a silicon crystal at a given temperature the number of electrons in the conduction band is equal to the number of holes in the valence band.

Doping Silicon with Arsen (+5) it becomes and n-type conductor (more electrons than holes).

Doping Silicon with Boron (+3) it becomes a p-type conductor (more holes than electrons).

Bringing p and n in contact makes a diode.